STARS

Electronic Theses and Dissertations, 2004-2019

2009

Molecular Dynamics Study Of Thermal Conductivity Enhancement Of Water Based Nanofluids

Parveen Sachdeva
University of Central Florida

Part of the Mechanical Engineering Commons

Find similar works at: https://stars.library.ucf.edu/etd

University of Central Florida Libraries http://library.ucf.edu

Showcase of Text, Archives, Research & Scholarship

MOLECULAR DYNAMICS STUDY OF THERMAL CONDUCTIVITY
ENHANCEMENT OF WATER BASED NANOFLUIDS

by

PARVEEN SACHDEVA
B.Tech. Indian Institute of Technology Kanpur, 2003
M.S. University of Central Florida, 2006

A dissertation submitted in partial fulfillment of the requirements
for the degree of Doctor of Philosophy
in the Department of Mechanical, Materials and Aerospace Engineering
in the College of Engineering and Computer Science
at the University of Central Florida
Orlando, Florida

Fall Term
2009

Major Professor: Ranganathan Kumar

ABSTRACT

A systematic investigation using molecular dynamics (MD) simulation involving particle volume fraction, size, wettability and system temperature is performed and the effect of these parameters on the thermal conductivity of water based nanofluids is discussed. Nanofluids are a colloidal suspension of 10 -100 nm particles in base fluid. In the last decade, significant research has been done in nanofluids, and thermal conductivity increases in double digits were reported in the literature. This anomalous increase in thermal conductivity cannot be explained by classical theories like Maxwell's model and Hamilton-Crosser model for nanoparticle suspensions. Various mechanisms responsible for thermal conductivity enhancement in nanofluids have been proposed and later refuted. MD simulation allows one to predict the static and dynamic properties of solids and liquids, and observe the interactions between solid and liquid atoms.

In this work MD simulation is used to calculate the thermal conductivity of water based nanofluid and explore possible mechanisms causing the enhancement. While most recent MD simulations have considered Lennard Jones (LJ) potential to model water molecule interactions, this work uses a flexible bipolar water molecule using the Flexible 3 Center (F3C) model. This model maintains the tetrahedral structure of the water molecule and allows the bond bending and bond stretching modes, thereby tracking the motion and interactions between real water molecules. The choice of the potential for solid nanoparticle reflects the need for economic but insightful analyses and reasonable accuracy. A simple two body LJ potential is used to model the solid nanoparticle. The

cross interaction between the solid and liquid atoms is also modeled by LJ potential and the Lorentz-Berthelot mixing rule is used to calculate the potential parameters.

The various atomic interactions show that there exist two regimes of thermal conductivity enhancement. It is also found that increasing particle size and decreasing particle wettability cause lower thermal conductivity enhancement. In contrast to the previous studies, it is observed that increasing system temperature does not enhance thermal conductivity significantly. Such enhancement with temperature is proportional to the conductivity enhancement of base fluid with temperature. This study demonstrates that the major cause of thermal conductivity enhancement is the formation of ordered liquid layer at the solid-liquid interface. The enhanced motion of the liquid molecules in the presence of solid particles is captured by comparing the mean square displacement (MSD) of liquid molecules in the nanofluid to that of the base fluid molecules. The thermal conductivity is decomposed into three modes that make up the microscopic heat flux vector, namely kinetic, potential and collision modes. It was observed by this decomposition analyses that most of the thermal conductivity enhancement is obtained from the collision mode and not from either the kinetic or potential mode. This finding also supports the observation made by comparing the MSD of liquid molecules with the base fluid that the interaction between solid and liquid molecules is important for the enhancement in thermal transport properties in nanofluids.

These findings are important for the future research in nanofluids, because they suggest that if smaller, functional nanoparticles which have higher wettability compared to the base fluid can be produced, they will provide higher thermal conductivity compared to the regular nanoparticles.

Dedicated to my mother Mrs. Asha Sachdeva & Nirankari Baba Hardev Singh Ji

ACKNOWLEDGMENTS

This work and my stay at UCF has been a great learning experience for me. I would like to take this opportunity to express gratitude to my advisor Dr. R. Kumar for his constant support, advice and guidance throughout my stay at UCF. It was a rewarding experience working with him. I also acknowledge and offer thanks to my committee members Dr. J. Kapat, Dr. Q. Chen, Dr. S. Basu and Dr. A. Masunov for their valuable comments and guidance. I also acknowledge the support of the College of Engineering & Computer Science and the I^{2}Lab at the University of Central Florida for the research presented here.

I would also like to thank my friends at UCF for making my stay memorable. I thank the UCF Indian student association, *Sangam* for their help when I first came to USA.

None of this would have been possible without the blessings of Nirankari Baba Hardev Singh Ji and the constant support and encouragement of my family members.

TABLE OF CONTENTS

LIST OF FIGURES

x

LIST OF TABLES

CHAPTER ONE: INTRODUCTION

With ever increasing need of high temperature applications in the area of microelectronics, lasers, space, transportation and power industries, there is a growing demand for more efficient heat exchange processes. Due to the shrinking sizes of microelectronic devices, and need for higher power outputs the thermal loads on these devices keep rising and thermal management to maintain them at optimal operating conditions is becoming a challenging issue for the technical community. It is well known that the thermal management of these microelectronic devices including integrated circuits and light emitting diodes plays a critical role in their performance. According to Moore's Law, the processing speed and memory capacity of computer hardware, which is proportional to the number of transistors that can be placed on an integrated circuit, doubles every two years. Their increasing processing speeds and reducing sizes cause the power density in these devices to double every three years. The temperature of these micro devices as well as macro devices (e.g. in internal combustion engines) is reaching at levels which will prevent optimal operation of these devices. So there is a growing demand for new enhanced thermal management processes. There is also a need to improve existing heat transfer processes, for example in the transportation industry, where improved heat transfer in automobiles could lead to a smaller cooling system, thereby reducing the overall weight of the vehicle.

The heat flow in a convective heat transfer process is given by:

$$Q = hA\Delta T \tag{1.1}$$

Here, Q is the heat flow, h is the heat transfer coefficient, A is the surface area where heat transfer is taking place, and ΔT is the temperature difference causing the heat flow. For an

efficient thermal management system, we would like to increase the heat flow from the device. As seen from equation (1.1) the heat flow increase can be achieved by: (1) increasing ΔT, (2) increasing A, or (3) increasing h.

Increasing the temperature difference between the cooling fluid and the device can lead to higher heat flow, but often these two temperature limits are set by environmental and material constraints. The temperature of the cooling fluid is often set at atmospheric conditions, and the device temperature is governed by the maximum temperature the material can take, for example in a power generation turbine, the highest temperature is decided by the blade material used in the first stage of the turbine. Increasing ΔT to enhance the heat flow is not an easy option, as in most processes these two temperatures have already been taken to their limits.

Another method to increase heat transfer rates in any application is to increase the heat transfer surface area, A. Conventionally the surface area is increased by using extended surfaces, such as fins, which exchange heat with the heat transfer fluid. Unfortunately, this method to increase heat transfer requires an increase in the size of the thermal management system. However, when dealing with microelectronic devices or high speed lasers, the surface area can not be increased at will. Increasing the surface area would mean a larger and heavier device, which is essentially going against the trend of reducing the size of devices.

The last method to improve the heat flow in an application is to increase the heat transfer coefficient, h. The heat transfer coefficient depends on the heat transfer process used, and on the properties of the heat transfer fluid, for example the heat transfer coefficient is higher for forced convection compared to natural convection, and it is also

higher for a turbulent flow compared to laminar flow. Since most of these thermal management processes already use forced convection heat transfer, the alternative to increase h, is to improve the thermal properties of the heat transfer fluid. Water, ethylene glycol and engine oil are the most common heat transfer fluids used in most industrial applications, like transportation, space applications, manufacturing and even microelectronics. Heat transport characteristics of these fluids are vital in designing and developing high efficiency heat transfer equipments. Unfortunately, these fluids have very low thermal conductivity (less than 1.0 $Wm^{-1}°K^{-1}$), so the inherently poor thermophysical properties of these cooling fluids greatly limit the performance of thermal management systems. Thermal conductivity of these fluids plays an important role in the development of thermal management systems. Low thermal conductivity of these fluids hinders high effectiveness and compactness of heat exchangers and other devices.

Additives are often added to heat transfer fluids, to improve their thermophysical properties, for example in automobiles, glycols (alcohols) are often added to water as antifreeze, to reduce its freezing point. Solids can also be added to the heat transfer fluids to enhance their thermophysical properties. As shown in Table 1.1 solids (metals, non-metals) have several orders of magnitude higher thermal conductivity compared to liquids. It can be seen that the thermal conductivity of copper is about 650 times greater than that of water, about 1500 times greater than that of ethylene glycol and about 3000 times that of engine oil. Therefore, it would be expected that adding these metallic or non-metallic solid particles would significantly enhance the thermophysical properties of conventional heat transfer fluids.

Table 1: Thermal conductivities of various materials at room temperature

Material	Thermal Conductivity ($Wm^{-1}{}^{\circ}K^{-1}$)	Specific Thermal Conductivity
Silver	429	700
Copper	401	654
Aluminum	237	387
Silicon	148	241
Alumina	40	65
Silica (α quartz)	8.2	13
Water	0.613	1
Ethylene glycol	0.253	0.41
Engine Oil	0.145	0.24

1.1 Colloids

Numerous theoretical and experimental studies on increasing the thermal conductivity of liquids by suspending solid particles have been performed in the past. Earlier studies on thermal conductivity measurement of solid-liquid colloidal suspensions were confined to millimeter and micrometer size particles. Ahuja [1975] studied suspension of micron size polystyrene particles suspended in ethylene glycol and observed that the heat transfer was increased by a factor of 3 under laminar flow conditions for particle volume fraction of up to 9%. No significant pressure drop was observed even for these high particle volume concentrations. Liu et al [1988] also found enhanced heat transfer in micron size particulate slurries.

Even with these promising high heat transfer rates and low rise in pressure drop by adding micron size particles to liquids, these suspensions were not used in any industrial application because of some problems associated with them. A major drawback of micron sized particles used in theses suspensions is that due to their weight, they tend to settle down quickly. The rapid settling of solid particles in flow situation can cause clogging of pipe or channel, resulting in high pressure drops. If the fluid is kept circulating to prevent settling of solid particles, these large particles can cause erosion to the channel walls. So the advantage of enhanced heat transfer in solid-liquid suspensions is hindered by the erosion and high pressure drop caused by particle settling. Even though the suspensions of these particles have higher thermal conductivity compared to their base fluids, they have little application in engineering systems due to above mentioned problems.

1.2 Nanofluids

With the advent of nanotechnology it has become possible to manufacture nano-sized particles from metals, oxides and carbides. Researchers have been able to manufacture nanometer sized particles using both, chemical and vapor deposition techniques. The most common method for the preparation of semiconductor nanoparticles is the synthesis from the starting reagents in solution by arresting the reaction at a definite moment of time. This is the so-called method of arrested precipitation. It is also possible to obtain semiconductor nanoparticles by sonication of colloidal solutions of large particles. The gas phase synthesis could also be used to manufacture nanoparticles. One method for the gas-phase synthesis of nanoparticles of various materials is based on the pulsed laser vaporization of metals in a chamber filled with a known amount of a reagent gas followed by controlled condensation of nanoparticles onto the support.

Nanofluids are a new class of solid-liquid suspensions which offer a promise in the development of energy-efficient heat transfer fluids. Application of solid nanoparticles provides an effective way of increasing thermal conductivity of fluids. Nanofluids are colloidal suspensions of metal or oxide particles, 1-100 nm in size, suspended in base fluids like water, ethylene glycol or oil. Nanofluids could positively impact the performance of heat exchangers or cooling devices, which are vital in many industries. For example the automotive and aerospace industry has been trying to reduce the weight of the thermal management systems to reduce the overall weight of the vehicle.

1.2.1 Benefits of Nanofluids

Nanofluids could increase the heat transfer in various applications involving coolants and lubricants and help reduce the system size and weight, which would also enhance the overall efficiency of the process. Due to their ultra small sizes, these nanoparticles have very high surface area to volume ratio and also high mobility. When these nanoparticles are properly dispersed in base fluid, they are expected to offer following benefits:

1)   Enhanced heat transfer - As seen from equation (1.1) the surface area at which heat transfer takes place is important in governing the overall heat flow rate. So the nanoparticle which have surface area to volume ratio much larger compared to microparticles, provide significantly more heat transfer at same volume fractions. Additionally, particles smaller than 20 nm have more than 20% of atoms on their surface [Choi et al 2004] making them instantaneously available for thermal interaction with fluid molecules. Due to their ultrafine size, these nanoparticles show high mobility and can flow even through tiny microchannels. These ultrafine nanoparticles flow with the base fluid and can increase the dispersion of heat in the fluid at faster rate.

2)   Stability – Again due to their small size, these particles weigh very less compared to microparticles. So gravity becomes less important in case of nanoparticles and chances of sedimentation of these particles in the suspension are very less. If proper chemical conditioning, e.g. dispersant, is used these nanoparticles can remain suspended in the base

fluid for weeks. This reduced settling of nanoparticles can overcome a major drawback because of which suspensions of microparticles were not used in many applications. The reduced sedimentation of nanoparticles makes them more stable.

3)   No clogging – Microchannels are used for cooling of MEMS devices and biotech devices like "lab on a chip". Due to their small sizes these nanoparticles can also be used in microchannel cooling applications. The combination of small nanoparticles with microchannel will provide for very high heat transfer surface area and due to their small size, these nanoparticles will not clog the small channels.

4)   Reduced erosion of channel walls – One other drawback of microparticles was that due to their larger size, they could wear the channel or pipe walls in which the microparticle-fluid suspension was flowing. But nanoparticles with their negligible mass would impart very less momentum to the channel wall and reduce the chances of erosion.

5)   Reduction in pumping power requirement – In a forced convection heat transfer process a ten fold increase in the pumping power is required to increase the heat transfer rate by a factor of two. Since the heat transfer rate is proportional to the thermal conduction of the fluid, if fluid thermal conductivity is increased by using nanoparticle suspensions, required increase in pumping power will be very less, unless the addition of nanoparticle causes sharp rise in fluid viscosity.

With all these benefits expected of nanofluids, the scientific community termed them as "next generation of heat transfer fluids" and significant research has undergone in measuring thermal transport properties of nanofluids. It has been shown that the nanofluids show these unique features:

1) Stability – It was expected that due to their small size the nanoparticle would not settle in the suspension for days. Nanofluids have been shown to be stable for over a month when proper dispersing agents were used [Lee et al 1999].

2) Small concentration requirement – Thermal conductivity increase of over 40% was observed at a mere 0.3% volume concentration of copper nanoparticles in ethylene glycol [Eastman et al 2001]. As discussed later in chapter 2, similar large increases in thermal conductivity have been observed for other nanofluids at very small nanoparticle volume concentration.

3) Anomalous increase in thermal conductivity – 160% increase in the thermal conductivity was observed when 1% multi-wall-carbon-nanotubes (MWCNT) were suspended in engine oil [Choi et al 2001]. As discussed later in chapter 2, other studies have also shown such anomalous increase in thermal conductivity of various nanofluids.

4) Particle size dependence – Early experiments with millimeter and micrometer size particles showed that the thermal conductivity increase depended only on the particle volume concentration, but in case of nanofluids, different thermal conductivity enhancements were observed

at same particle volume fraction [Masuda et al 1993, Lee et al 1999]. The difference in two cases was the size of the Al_2O_3 nanoparticles used. So for nanofluids, not only the particle concentration, but also the particle size affects the thermal conductivity enhancement.

5) Temperature dependence – In early experiments significantly higher enhancement in thermal conductivity of nanofluids was observed with increasing system temperature from 20 ˚C to 50 ˚C [Das et al 2003]. This is exciting as this could mean potential for use of nanofluids in many high temperature applications.

With these exciting benefits it is important to thoroughly study and understand various mechanisms causing these unique features in nanofluids. As discussed later in chapter 2, significant experimental and theoretical research has been conducted in the area of nanofluids in last decade, but till date no consensus has been reached on the possible mechanisms causing the thermal enhancement in nanofluids. The nanofluids experiments conducted by one group have not yet been reproduced by other groups. The anomalous increase in thermal conductivity of nanofluids could not be explained by classical theories like Maxwell's model [1881] and Hamilton-Crosser model [1962] for suspensions consisting of well dispersed particles. The inability of these models to predict the thermal conductivity enhancement of nanofluids was ascribed to the fact that they did not take important parameters like particle size, shape, system temperature, interaction between large number of surface atoms with fluid molecules, and modes of thermal transport at nanoscale into account.

Keblinski et al [2002] attribute the enhancement in thermal conductivity to four possible mechanisms, (1) Brownian motion of particles, (2) layering of liquid molecules around the particles, (3) ballistic nature of heat transport in nano-structures, and (4) nanoparticle clustering. Various other mechanisms including (a) collision between base fluid molecules, (b) thermal diffusion in nanoparticles in fluid, (c) collision between nanoparticles due to Brownian motion, (d) thermal interaction between nanoparticle and base fluid molecules [Jang & Choi 2004, Prasher et al 2005, Ren et al 2005] have been proposed. Particles move through liquid by Brownian motion and collide with each other, hence enabling direct solid-solid transport of heat from one to another. Some of these mechanisms have been later refuted [Gupta et al 2007, Eapen et al 2007], even by the groups that originally proposed them [Keblinski et al 2008]. Possible reason for all this is disconnect between experimental and theoretical understanding of thermal transport mechanisms at nanoscale. With macroscale experiments we can only measure thermal transport properties of nanofluids, but we can not explore the mechanisms causing the enhancement at the nanoscale.

1.3 Problem Description

A systematic study using computer simulation is required to determine the cause of thermal conductivity enhancement in nanofluids and to explore possible mechanisms at nanoscale. Due to the length and time scales involved in nanofluids, conventional macroscale computational techniques such as CFD and FEM can not be used to capture the properties. Molecular dynamics (MD) simulation, an atomic scale simulation technique has been proven to predict the static and dynamic properties of solids and

liquids. In this work, molecular dynamics simulation is used to calculate the thermal conductivity of water based nanofluids and study possible mechanisms contributing to significantly higher conductivity than proposed by traditional models such as Hamilton Crosser. Using MD, it is possible to observe the interactions between solid and liquid atoms occurring at the molecular level, which give rise to the macroscale transport properties. Accuracy of an MD model to simulate complex fluids such as nanoparticle suspensions depends on the potential functions used to model the interaction between various atoms in the system. Previous studies involving molecular dynamics simulation of nanofluids have considered simplistic Lennard-Jones (LJ) potential to model the interactions between both solid and liquid atoms [Keblinski et al 2002, Eapen et al 2007, Sarkar & Selvam 2007, Li et al 2008]. In this work liquid water is modeled as a flexible bipolar molecule using the Flexible 3 Center (F3C) model proposed by Levitt et al [1997]. This model maintains the tetrahedral structure of the water molecule and allows the H-O-H bond bending and O-H bond stretching modes, thereby mimicking the motion and interactions between real water molecules.

The choice of the potential for solid nanoparticle in this work reflects the need for economic but insightful analysis with reasonable accuracy. Since the complex surface chemical reactions between the solid nanoparticle and fluid atoms have not yet been identified by experiments, expensive quantum-chemistry based simulations would be required to identify them. In this work, a simple two body Lennard-Jones potential is used to model the solid nanoparticle. In addition, each atom in the nanoparticle is connected to its first neighbors by finite extensible nonlinear elastic (FENE) bonding potential [Vladkov & Barrat, 2006]. The atoms in this solid particle vibrate around their

mean position and simulate the phonon mode of heat transport as seen in solids. This model nanoparticle will closely simulate a non-metallic particle like oxides, where the thermal conductivity arises from the phonon mode and not from electrons as in the case of metals. The cross interaction between solid and liquid atoms is modeled by the Lennard-Jones potential and the Lorentz-Berthelot mixing rule [Allen & Tildesley, 1987] is used to calculate the potential parameters. Linear response theory is combined with the molecular dynamics simulation to calculate the thermal conductivity of the nanofluid system. A systematic investigation involving particle volume fraction, size, wettability and system temperature is undertaken using molecular dynamics simulation and the effect of these parameters on the thermal conductivity of nanofluids is studied.

The focus of this thesis is to study the possible mechanisms causing the enhanced thermal transport in nanofluids. The interaction between the solid and liquid atoms is examined by tracking the motion of these molecules. The study of these mechanisms is important as controversy still exists relating to the existence and nature of these mechanisms, and their role in enhancing the heat transfer characteristics in colloidal suspensions. The understanding of these mechanisms can help with the design of engineering devices that use these nanofluids as heat transfer fluids. In this dissertation, possible modes of thermal conduction in nanofluids are studied by decomposing the microscopic heat flux vector in to three modes, namely kinetic, potential and collision. Such a study of thermal transport in nanofluids would allow a practical engineer to engineer the nanofluids by understanding the nature and behavior of nanoparticles in the base fluids. The intellectual merit of this study is to understand the influence of the various atomic potentials in the different modes of heat transfer is immeasurable.

CHAPTER TWO: LITERATURE REVIEW

Increasing the thermal transport properties of liquids by mixing high conductivity solid particles is not a novel concept. As mentioned in chapter 1, Ahuja [1975] studied colloidal suspension of micron-size polystyrene particles in ethylene glycol. He observed heat transfer enhancement by a factor of 3 under laminar conditions at 9% particle volume fraction. Liu et al [1988] carried out turbulent pipe flow experiments using slurries containing micron sized high density polyethylene particles. They conducted experiments to study the effect of particle volume fraction, particle size and flow rate on the slurry pressure drop and heat transfer. They observed higher heat transfer in laminar and turbulent flow conditions using these particulate slurries.

2.1 Experimental Results for Nanofluids

Significant research work has been conducted in the past decade to measure thermal conductivity of nanofluids. Researchers have conducted experiments on nanofluids containing various types of nanoparticles (Ag, Au, Cu, Al_2O_3, CuO, SiO_2, TiO_2, CNT etc) dispersed in various base fluids (ethanol, ethylene glycol, oil, water, toluene etc). Nanoparticles of sizes ranging from 10 nm to 250 nm in diameter have been used in these studies. Researchers have looked at the effect of particle volume fraction, size and system temperature on the thermal conductivity of nanofluid. Table 2.1 gives a summary of experimental research work conducted in the last decade to measure thermal conductivity of nanofluids at room temperature.

Table 2.1: Experimental investigation of nanofluid thermal conductivity

Reference	Nanofluid used	Maximum observed $k_{nanofluid} / k_{Base\ fluid}$	Volume fraction
Masuda et al [1993]	Al_2O_3 – Water	1.33	4.3%
Xie et al [2002]	Al_2O_3 – Water	1.25	5%
Das et al [2003]	Al_2O_3 – Water	1.08	4%
Chon et al [2005]	Al_2O_3 – Water	2.1	4%
Li & Peterson [2006]	Al_2O_3 – Water	1.28	10%
Timofeeva et al [2007]	Al_2O_3 – Water	1.24	10%
Kim et al [2007]	Al_2O_3 – Water	1.08	3%
Zhang et al [2007]	Al_2O_3 – Water	1.3	40%
Wang et al [1999]	Al_2O_3 – EG	1.26	5%
Lee et al [1999]	Al_2O_3 – EG	1.12	5%
Xie et al [2002]	Al_2O_3 – EG	1.3	5%
Kim et al [2007]	Al_2O_3 – EG	1.11	3%
Timofeeva et al [2007]	Al_2O_3 – EG	1.28	10%
Wang et al [1999]	Al_2O_3 – Oil	1.26	5%
Xie et al [2002]	Al_2O_3 – Oil	1.38	5%
Venerus et al [2006]	Al_2O_3 – Oil	1.05	2.5%
Wang et al [1999]	CuO – Water	1.34	9.5%
Lee et al [1999]	CuO – Water	1.12	3.5%
Das et al [2003]	CuO – Water	1.13	4%

Reference	Nanofluid used	Maximum observed $k_{nanofluid} / k_{Base\ fluid}$	Volume fraction
Li & Peterson [2006]	CuO – Water	1.52	6%
Wang et al [1999]	CuO – EG	1.53	15%
Lee et al [1999]	CuO – EG	1.21	4%
Hwang et al [2006]	CuO – EG	1.05	1%
Kang et al [2006]	SiO_2 – Water	1.05	4%
Hwang et al [2006]	SiO_2 – Water	1.03	1%
Wang et al [2007]	SiO_2 – Water	1.03	1%
Wang et al [2007]	SiO_2 – EG	1.04	1%
Murshed et al [2005]	TiO_2 – Water	1.3	5%
Kim et al [2007]	TiO_2 – Water	1.11	3%
Zhang et al [2007]	TiO_2 – Water	1.07	3%
Murshed et al [2006]	TiO_2 – EG	1.18	5%
Kim et al [2007]	TiO_2 – EG	1.15	3%
Kang et al [2006]	Ag – Water	1.11	0.4%
Patel et al [2003]	Au – Water	1.05	0.01%
Kumar et al [2004]	Au – Water	1.2	0.01%
Putnam et al [2006]	Au – Ethanol	1.013	0.018%
Xuan & Li [2000]	Cu – Water	1.24	2%
Liu et al [2006]	Cu – Water	1.24	0.1%
Jana et al [2007]	Cu – Water	1.7	0.3%

Reference	Nanofluid used	Maximum observed $k_{nanofluid} / k_{Base\ fluid}$	Volume fraction
Eastman et al [2001]	Cu – EG	1.4	0.3%
Assael et al [2006]	Cu – EG	1.03	0.48%
Eastman et al [1999]	Cu – Oil	1.44	0.052%
Xuan & Li [2000]	Cu – Oil	1.45	0.05%
Xie et al [2003]	CNT – Water	1.07	1%
Assael et al [2006]	CNT – Water	1.39	0.6%
Hwang et al [2007]	CNT – Water	1.07	1%
Zhang et al [2007]	CNT – Water	1.4	0.09%
Xie et al [2003]	CNT – EG	1.12	1%
Choi et al [2001]	CNT – Oil	2.6	1%
Hwang et al [2007]	CNT – Oil	1.09	0.5%

It can be observed from Table 2.1 that nanofluids show significantly high thermal conductivity compared to the base fluid even at small volume fraction of nanoparticles. Some of the experimental data can be explained by models like Maxwell [1881] and Hamilton-Crosser [1962], but the thermal conductivity data shows significant variation. Different research groups have reported different enhancement in thermal conductivity even for same nanofluid suspensions. Some of the noticeable results from Table 2.1 are discussed here.

Masuda et al [1993] were the first group to do experiments with suspension of nanometer size particles and report enhanced heat transfer. They used Al_2O_3, SiO_2 and other oxide nanoparticle in water and reported 30% increase in thermal conductivity of base fluid suspended with Al_2O_3 nanoparticles at a volume fraction of 4.3%. They also observed that the friction factor of the suspension increased 4 times at same volume fraction. Choi [1995] was the first to use the term 'nanofluid' for the suspension of nanometer size particles in heat transfer fluids. He conducted experiments at the Argonne National Lab and reported a new class of engineered fluids consisting of nanometer sized copper particles suspended in ethylene glycol. He reported almost 100% increase in the thermal conductivity of base fluid at only 1% volume fraction of copper nanoparticles.

Eastman et al [1999] conducted experiments with Cu, Al_2O_3 and CuO nanoparticles suspended in HE-200 oil and water. They reported a 40% enhancement in conductivity of HE-200 oil at only 0.05% volume fraction of Cu nanoparticles. They observed 29% increase in the thermal conductivity for Al_2O_3-water nanofluid at 5% volume fraction and 60% increase in CuO-water nanofluid with 5% volume fraction of

35 nm CuO nanoparticles. They also reported a moderate 20% increase in the thermal conductivity of ethylene glycol suspended with CuO nanoparticle at 4% volume fraction.

Lee et al [1999] did experimental study using Al_2O_3 and CuO nanoparticles suspended in water and ethylene glycol and observed 15% enhancement in the thermal conductivity of Al_2O_3-water nanofluid at the same volume fraction as Masuda et al [1993]. The difference in their results was attributed to the size of nanoparticles used in the two experiments. Masuda et al [1993] used 13 nm Al_2O_3 nanoparticles while Lee et al [1999] used 33 nm nanoparticles. Wang et al [1999] measured the thermal conductivity of nanofluids consisting of Al_2O_3 and CuO nanoparticles suspended in water and ethylene glycol. They observed a maximum of 12% thermal conductivity enhancement for Al_2O_3 nanoparticles with a volume fraction of 3%.

Eastman et al [2001] reported a 40% thermal conductivity enhancement for Cu-ethylene glycol nanofluid at 0.3% volume concentration of 10 nm Cu nanoparticles. This high enhancement was observed when thioglycolic acid (1% volume concentration) was added to the nanofluid suspension to aid dispersion of nanoparticles. Same nanofluid suspension without the dispersant showed only 12% thermal conductivity enhancement. They also conducted experiments with Al_2O_3 and CuO nanoparticles dispersed in ethylene glycol and reported 18% enhancement for CuO-ethylene glycol nanofluid at 5% volume fraction and 22% enhancement for Al_2O_3-ethylene glycol nanofluid at 4% volume fraction.

Wang et al [2002] conducted experiments with several types of nanofluids. They prepared nanofluids using ethylene glycol as base fluid dispersed with CuO, Al_2O_3 and TiO_2 nanoparticles. They measured the thermal conductivity of nanofluids using steady-

state parallel plate method. They reported 18% increase in thermal conductivity for Al_2O_3-ethylene glycol nanofluid at 4% volume fraction. This is consistent with the enhancement showed by Eastman et al [2001]. In contrast, Xie et al [2002] reported 30% increase in thermal conductivity at 5% volume fraction for same nanofluid. However the Al_2O_3 nanoparticles used by Wang et al were 29 nm in diameter and that used by Xie et al were 60 nm in diameter. Xie et al [2002] also studied the effect of solution pH on the thermal conductivity and observed that the thermal conductivity decreased with increasing pH of the nanofluid. They concluded that among other parameters, the system chemistry also plays a role in determining the thermal conductivity of nanofluids.

Patel et al [2003] used Au and Ag nanoparticles dispersed in water and toluene to prepare nanofluid suspensions. They reported 4-7% increase in conductivity for Au-toluene nanofluid at a vanishingly small 0.005-0.011% volume fraction of silver nanoparticles. They also reported 3.2-5% increase in the conductivity of Ag-water nanofluid at a very small conductivity of 0.0013-0.026% volume fraction of gold nanoparticles. The same group later reported 20% increase in thermal conductivity of Au-water nanofluid at a mere 0.00013% volume fraction [Kumar et al 2004]. They attributed the anomalous increase in the thermal conductivity of nanofluids to very small size (4 nm) and very high thermal conductivity of the nanoparticles used. Putnam et al [2006] used the same nanoparticle and base fluid combination (4 nm Au nanoparticles with ethylene glycol) and reported only a moderate 1.3% ±0.8% increase in the thermal conductivity of nanofluid at 0.018% volume fraction. There results are in contrast to that reported by Patel et al [2003] and Kumar et al [2004] for same nanofluid.

Murshed et al [2005], Murshed et al [2006] and Leong et al [2006] conducted experiments with several types of nanofluids. They prepared nanofluids with water and ethylene glycol as base fluid, suspended with Al, Al_2O_3 and TiO_2 nanoparticles. They reported 32% increase in thermal conductivity for TiO_2–water nanofluid at 5% volume fraction, 18% increase in thermal conductivity for TiO_2–ethylene glycol nanofluid at same volume fraction, and a much higher 49% enhancement in thermal conductivity for Al–ethylene glycol nanofluid at the same volume fraction. They used cylindrical and spherical TiO_2 nanoparticles and observed higher enhancement for cylindrical nanoparticles compared to spherical ones. They observed that nanofluids consisting of higher conductivity nanoparticle (Al) showed higher thermal conductivity enhancement compared to the nanofluids consisting of lower thermal conductivity nanoparticle (TiO_2).

It is well known that carbon nanotubes (CNT) exhibit unusually high thermal conductivities [Berber et al, 2000]. Carbon nanotubes (CNT's) with their ultrafine size and very high thermal conductivity attracted researchers to use CNT's as the dispersed solid phase in the nanofluids. Choi et al [2001] used multi-wall-carbon nanotubes (MWCNT) in poly (α-olefin) oil and reported an astonishing 160% increase in thermal conductivity of poly (α-olefin) oil at only 1% volume fraction of MWCNT having 25 nm mean diameter and 50 μm length. They observed non-linear increase in thermal conductivity at very small volume fractions (< 1%). They attributed this huge enhancement in thermal conductivity of the nanofluid to the high thermal conductivity of nanotubes and interaction between carbon fiber and fluid molecules. Xie et al [2003] reported only 6% increase in thermal conductivity with MWCNT suspension in water at 1% volume fraction. Yang et al [2006] reported 200% increase in thermal conductivity of

poly (α-olefin) oil suspended with only 0.35% volume fraction of MWCNT. They also reported a 3 times increase in the viscosity of poly (α-olefin) oil at same volume fraction of MWCNT.

It was observed from experimental data that nanofluids consisting of nanoparticles with very high thermal conductivity show anomalously high enhancement. Hong et al [2005] conducted experiments with Fe–ethylene glycol based nanofluids and reported 18% increase in thermal conductivity at only 0.55% volume fraction of iron nanoparticles. They also observed that the sonication of the nanofluid suspension had a significant effect on the thermal conductivity. Zhu et al [2006] also reported a high 38% increase in thermal conductivity for Fe_3O_4–water based nanofluid at only 5% volume fraction of. They attributed this high enhancement to the nanoparticles forming clusters. These studies show that even nanofluids consisting of nanoparticles with relatively lower thermal conductivity (Fe, Fe_3O_4) can produce high thermal conductivity enhancement.

From the above mentioned literature survey it is clear that the thermal conductivity enhancement data shows a lot of scatter. Till date the data produced by one group has not been reproduced by another group. It has been observed that many parameters like nanoparticle-base fluid combination, particle volume fraction, size, shape, system temperature and the choice of dispersant used to stabilize the suspension affect the thermal conductivity of nanofluids. The effects of these parameters as reported by various groups are also contradictory. A clear consensus has not been reached yet among the scientific community on how each of these parameters affects the thermal conductivity of nanofluids. Now some experimental studies showing the effect of particle volume fraction, size and system temperature are discussed here.

2.1.1 Effect of Particle Volume Fraction

One point where the scientific community agrees about the thermal conductivity enhancement in nanofluids is that the thermal conductivity increases almost linearly with an increase in particle volume fraction. As shown in Figure 2.1, most of the experimental data in the literature shows a linear thermal conductivity increase with volume fraction. However, some exceptions have been reported to show non-linear increase in thermal conductivity at low volume fractions (< 1%) [Choi et al 2001, Murshed et al 2005, Hwang et al 2006]. Choi et al [2001] and Hwang et al [2006] used nanofluids consisting of MWCNT in oil and observed quadratic relationship between thermal conductivity of nanofluid with particle volume fraction at concentrations less than 1% as shown in Figure 2.2. Murshed et al [2005] in their experiments observed that the thermal conductivity versus particle volume fraction curve can be divided into two linear regimes. The transition typically occurred at volume fraction of around 1% as shown in Figure 2.3. Zhu et al [2006] also observed the same behavior, but they observed the transition at around 2% volume fraction. While some researchers have reported anomalous thermal conductivity enhancements at particle volume fractions less than 1% for metallic nanoparticles [Eastman et al 2001, Patel et al 2003, Kumar et al 2004, Jana et al 2007], other have reported conductivity enhancement that can be explained by classical models [Wang et al 2002, Xie et al 2002, Putnam et al 2006, Zhu et al 2006].
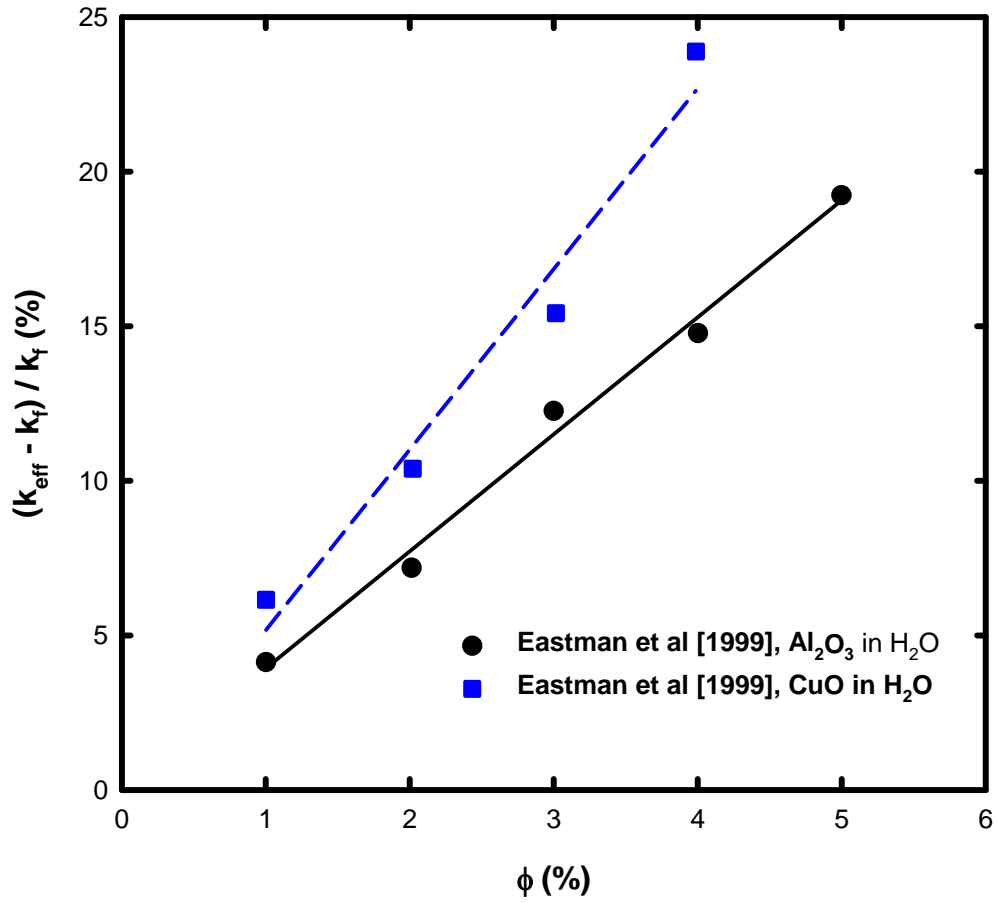
Figure 2.1: Thermal conductivity of aqueous nanofluids as measured by Eastman et al

[1999]. The straight lines represent linear fit to the data.
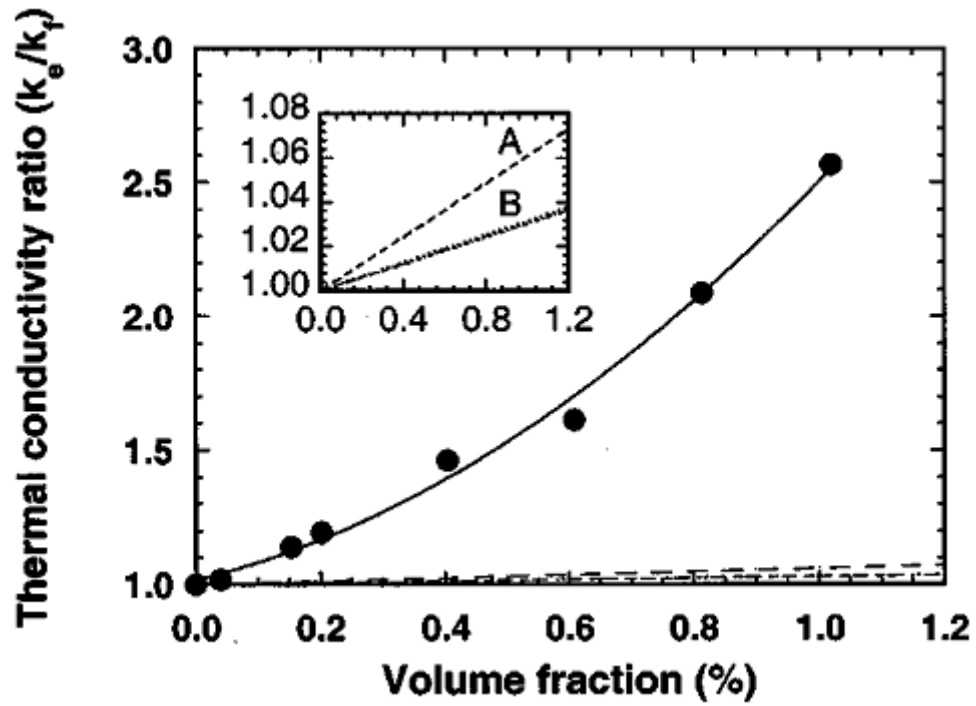
Figure 2.2: Relative thermal conductivity of oil-MWCNT suspension as measured by Choi et al [2001], showing the quadratic relationship between conductivity and volume fraction. In the inset, line A represents the Hamilton-Crosser model and B represents the Maxwell's model
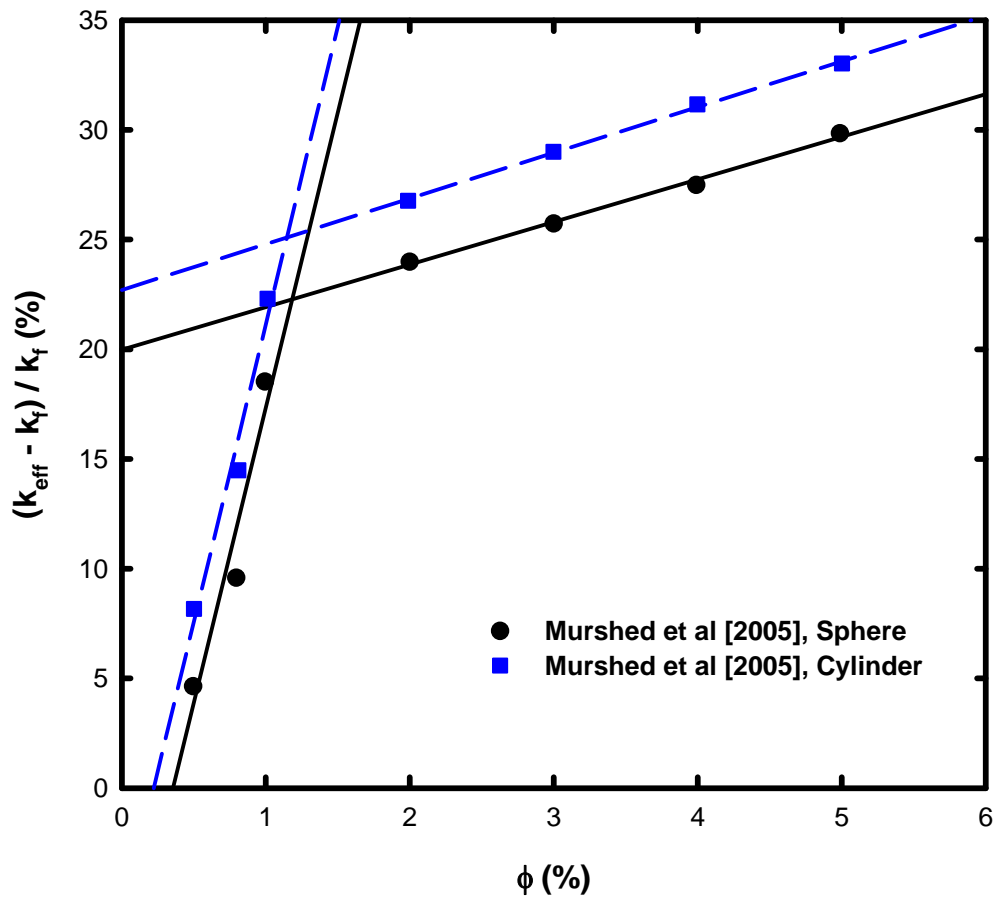
Figure 2.3: Thermal conductivity enhancement of nanofluids consisting of TiO_2 in water as measured by Murshed et al [2005], showing the two regimes of conductivity enhancement with volume fraction. The lines represent linear fit to the data.

2.1.2 Effect of Particle Size

Xie et al [2002] were the first group to report thermal conductivity of nanofluids containing different sizes of nanoparticles. They used Al_2O_3 nanoparticles ranging from 12 nm to 304 nm in diameter suspended in water. They observed that the thermal conductivity of the nanofluid increased with increasing particle size, except for the largest particles for which thermal conductivity showed a decline. They concluded that there is an optimal nanoparticle size, which will yield the highest thermal conductivity enhancement for a given nanoparticle–base fluid combination. Chon and Kihm [2005] used 11 nm, 47 nm and 150 nm Al_2O_3 nanoparticles suspended in water and reported that the smaller particles yielded higher increase in thermal conductivity contrary to what was observed by Xie et al [2002]. Li and Peterson [2007] also used 36 nm and 47 nm Al_2O_3 nanoparticles and observed that the 36 nm particle suspension showed 8% higher increase in conductivity compared to 47 nm particle suspension. Kim et al [2007] also observed the same trend of higher thermal conductivity for smaller particles in their nanofluid suspensions consisting of ZnO and TiO_2 nanoparticles in water and ethylene glycol. Beck et al [2009] used Al_2O_3 nanoparticles ranging from 8 nm to 282 nm in diameter suspended in water and observed that the thermal conductivity of nanofluid increased for with nanoparticle diameter up to 50 nm and then showed a saturation behavior for larger particles. On the contrary theoretical evidence [Keblinski et al 2002, Yu & Choi 2003, Jang & Choi 2004, Leong et al 2006] indicates that decreasing particle size causes increase in thermal conductivity of nanofluid. Figure 2.4 shows the effect of particle size on nanofluid thermal conductivity as reported in the literature by various groups.

27
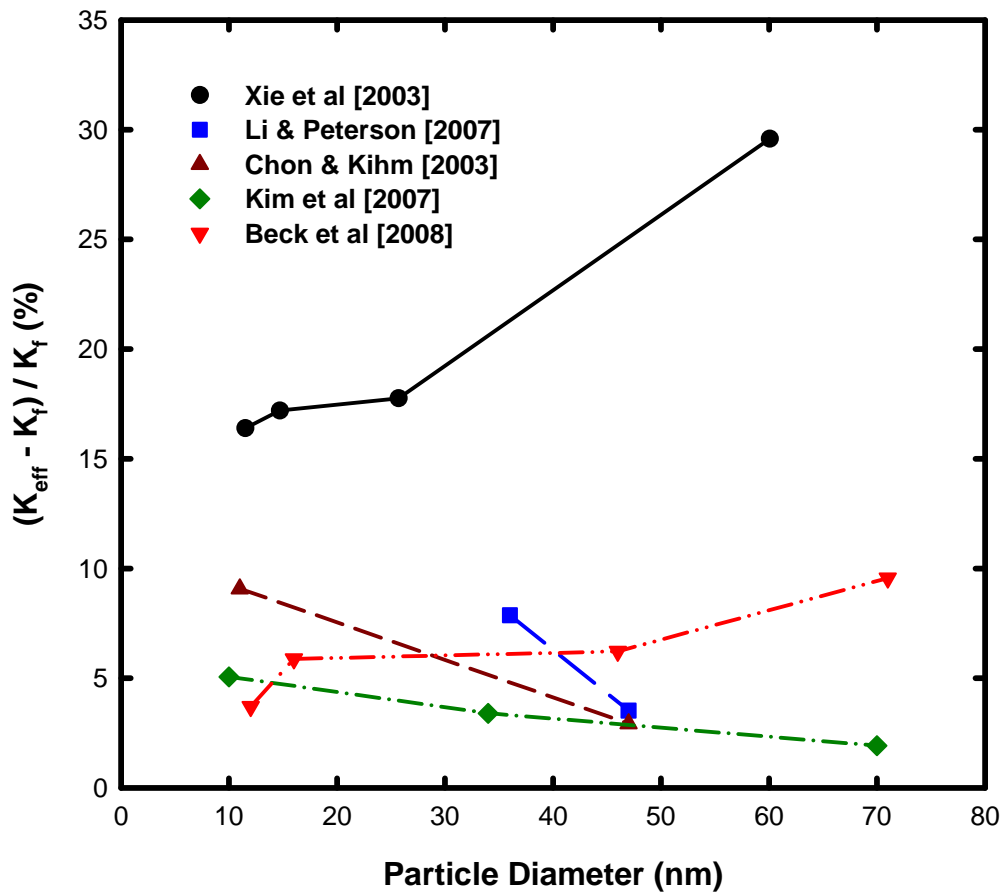
Figure 2.4: Thermal conductivity enhancement of nanofluids as a function of particle

size, as measured by various groups

2.1.3 Effect of System Temperature

Nanofluids have been proposed to be used in a wide variety of engineering applications due to their promising thermal transport properties. Some of these applications may involve high temperatures, which could play an important role in the thermal conductivity enhancement of nanofluids. Das et al [2003] experimentally studied nanofluids consisting of Al_2O_3 and CuO nanoparticles suspended in water at elevated temperatures. They reported that the thermal conductivity of Al_2O_3–water nanofluid increased from 16-25% and for CuO–water nanofluid increased from 22-30% as the suspension temperature was increased from 21-51˚C. The same group later used Au–water nanofluid [Patel et al 2003] and reported thermal conductivity increase from 5-21% at 0.026% volume fraction as the temperature was increased from 30-60˚C. They suggested that this strong temperature dependence on thermal conductivity of nanofluids was due to the Brownian motion of nanoparticles. They also speculated that this temperature dependence will remain the same even at higher fluid temperatures. Chon and Kihm [2005] also used Al_2O_3–water nanofluid and reported a moderate increase of 6-11% in thermal conductivity as the nanofluid temperature was raised from 31-51˚C. Murshed et al [2006] also reported a moderate increase in thermal conductivity by 9% for Al_2O_3–water nanofluid as the system temperature was increased from 30-60˚C. Li & Peterson [2007] also used Al_2O_3–water nanofluid and reported thermal conductivity enhancement from 7-23% at 2% volume fraction as the system temperature was increased from 27-36˚C.

Beck et al [2007] conducted experiments with Al_2O_3–ethylene glycol over a wide temperature range of 25-135˚C and reported a moderate increase in thermal conductivity of nanofluid with temperature. They observed that the nanofluid exhibit maximum thermal conductivity at the same temperature as the base fluid, and the thermal conductivity enhancement behavior of nanofluid with temperature mimicked that of the base fluid. Figure 2.5 shows the thermal conductivity enhancement with temperature as reported in the literature. So it can be seen from Figures 2.4 and 2.5 that as with the effect of particle size, no agreement has been found on the effect of system temperature on the thermal conductivity of nanofluid.
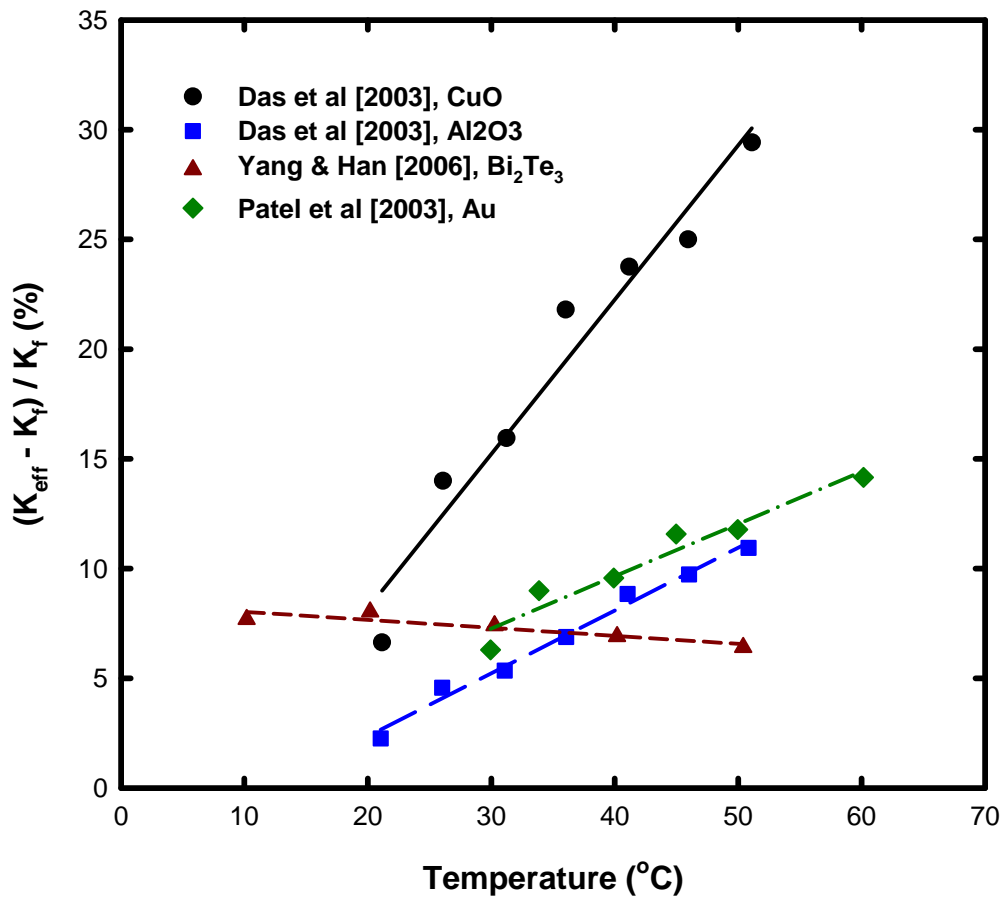
Figure 2.5: Thermal conductivity enhancement of nanofluids as a function of temperature as measured by various groups

2.2 Modeling of Nanofluids

It is evident that a significant experimental research has been conducted in determining the heat transport characteristics of the nanofluids in last decade, but still many questions remain unanswered. The data produced by one group is not reproducible by another and no concrete theory has been established to predict the thermal conductivity of nanofluids and explain the anomalous enhancement. Researchers have proposed many theories to explain the anomalous behavior observed in nanofluids. The early attempts to explain the enhanced transport characteristics of nanofluids were made with the classical theory of Maxwell [1881] for composite materials. This theory was developed to calculate the electrical or thermal conductivity of dilute solid–liquid suspension of spherical particles at low volume fractions. It is applicable to homogeneous isotropic solution of uniformly sized solid particles randomly dispersed in a fluid.

$$\frac{k_e}{k_f} = \frac{k_p + 2k_f + 2\phi(k_p - k_f)}{k_p + 2k_f - \phi(k_p - k_f)}$$

(2.1)

Here k_e is the effective thermal conductivity of the suspension, k_f is the thermal conductivity of the base fluid, k_p is the thermal conductivity of nanoparticle, ϕ is the volume fraction. This theory is also appropriate for predicting properties such as dielectric constant and magnetic permeability of composite materials. When compared with experimental data Maxwell's theory matched well for low particle concentrations with spherical particles of millimeter or micrometer size, but it did not conform well to particles of nanometer size and non-spherical shapes.

Hamilton and Crosser [1962] (HC) extended Maxwell's model and generalized it for non-spherical particles. They came up with an expression for effective thermal conductivity of a colloidal suspension as:

$$\frac{k_e}{k_f} = \frac{k_p + (n-1)k_f + (n-1)\phi(k_p - k_f)}{k_p + (n-1)k_f - \phi(k_p - k_f)} \tag{2.2}$$

Here, n is the non-spherical shape factor given as:

$$n = \frac{3}{\psi} \tag{2.3}$$

Here, ψ is the sphericity, defined as the ratio of the surface area of a sphere with volume equal to that of the particle to the surface area of the particle. For $n=3$ HC model reduces to Maxwell model for spherical particles. The HC theory was used by Xuan & Li [2000] to obtain rough estimation of thermal conductivity of nanofluids for different volume fraction and shape factor. They showed that for $\psi=0.7$ the HC model predicts results close to their experimental results. Lee et al [1999] showed that HC model predicted the right trend for oxide particles, but when used for very fine metallic particles [Eastman et al, 2001] it under-predicted the effective thermal conductivity by over an order of magnitude. Classical models like Maxwell and HC model can not explain or predict the nanofluid thermal conductivity data because they do not include the effect of particle size, shape, interfacial layer at the solid-liquid interface, system temperature and the Brownian motion of the particles, which have been found to affect the thermal conductivity of nanofluids. It was not surprising that both Maxwell's model and HC model were not able to predict the enhancement in thermal conductivity of nanofluids because they did not take into account various important parameters affecting the heat transport in nanofluids and modes of thermal transport in nanostructures.

Many theoretical studies have been conducted in recent past to explain and predict the anomalous thermal conductivity increase in nanofluids. Several theoretical models have been proposed which include the effect of various parameters like the particle size, system temperature and liquid layer at the solid-liquid interface. Keblinski et al [2002] attribute the enhancement in thermal conductivity to four possible mechanisms, Brownian motion of particles, layering of liquid molecules around the particles, ballistic nature of heat transport in nano-structures and nanoparticle clustering. Particles move through liquid by Brownian motion and collide with each other, hence enabling direct solid-solid transport of heat from one to another.

Yu & Choi [2003, 2004] considered the effect of ordered liquid layer and modified the Maxwell's model and HC model. They replaced the nanoparticle thermal conductivity and volume fraction with effective thermal conductivity (k_{pe}) and volume fraction of an equivalent nanoparticle, which is the nanoparticle surrounded by the ordered liquid layer.

$$\frac{k_e}{k_f} = \frac{k_{pe} + 2k_f + 2\phi(k_{pe} - k_f)(1+\beta)^3}{k_{pe} + 2k_f - \phi(k_{pe} - k_f)(1+\beta)} \tag{2.4}$$

Here, k_e is the effective thermal conductivity of nanofluid, k_{pe} is the equivalent thermal conductivity of equivalent nanoparticles, k_l is the thermal conductivity of fluid, and β is the ratio of the nano-layer thickness to the original particle radius. They concluded that the ordered liquid layer around the nanoparticles effectively increases the particle volume fraction and hence the effective thermal conductivity of the nanofluid. They assumed the effective thermal conductivity of the equivalent nanoparticle to be same as that of the original nanoparticle. This assumption is not realistic, since the ordered liquid layer is made of liquid atoms and not solid. So the thermal conductivity of

this ordered liquid layer at the solid-liquid interface would be in between the thermal conductivity of the liquid and the solid. Another unknown in their model was the thickness of this ordered liquid layer.

Xue et al [2003] proposed a model based on Maxwell's theory and average polarization theory, which also includes the effect of the ordered liquid layer. To validate their model with experimental data from Choi et al [2001], they used 2 incorrect parameters. Later when they used the corrected parameters Yu & Choi [2003] showed that this model predicted thermal conductivity of the nanofluid to be 32 times that of the base fluid. So this model has not been validated and its accuracy is yet to be established.

Wang et al [2003] modified Maxwell's model to include the effect of nanoparticle clustering and polarization. To predict the thermal conductivity of the nanofluid their model requires effective thermal conductivity and radius distribution of the nanoparticle cluster, which have to be determined numerically. This model is also yet to be validated with experimental data.

Other models have also been proposed by Jang & Choi [2004], Kumar et al [2004], Prasher et al [2005], Ren et al [2005], and Leong et al [2006]. Each of these models is based on one or more of the following thermal conduction mechanism in nanofluids (a) collision between base fluid molecules, (b) thermal diffusion in nanoparticles in fluid, (c) collision between nanoparticles due to Brownian motion, (d) thermal interaction between nanoparticle and base fluid molecules, (e) ordered liquid layer at the solid-liquid interface, or (f) nanoparticle clustering. These mechanisms have been proposed to be the origin of enhanced thermal properties of nanofluids. Since all these mechanisms involve interaction occurring at nano-scale, there is no direct way to

verify the presence of any of these mechanisms by macro-scale experiments like Transient Hot Wire, Oscillating Parallel Plate, or Optical Beam Deflection methods which have been used to measure the thermal conductivity in nanofluids. Some modeling method that can simulate the interaction between the solid nanoparticles and fluid molecules at nano-scale is required to validate the presence of these mechanisms.

2.3 Computer Simulations of Nanofluids

Several attempts have been made to study the nanofluids using simulation methods that can capture the complex thermal transport phenomenon occurring in nanofluids at the nanoscale. Molecular dynamics simulation, an atomic-scale simulation technique that can track the motion of solid and liquid atoms at molecular level has been used in these simulation studies. A list of molecular simulation studies performed on nanofluids is presented in Table 2.2 and some of the notable simulation studies on nanofluids are discussed here.

Table 2.2: Molecular dynamics simulation studies of nanofluid (*SS, LL, SL refer to solid-solid, liquid-liquid, and solid-liquid respectively)

Reference	Potential used	Volume Concentration	Conductivity Enhancement
Keblinski et al [2002]	LJ for SS, LL, SL	10%	-
Evans et al [2006]	LJ-FENE for SS, LJ for LL, SL	3.3%	2.5%
Eapen et al [2007]	LJ for SS, LL, SL (Xe-Pt)	0.8%	35%
Sarkar & Selvam [2007]	LJ for SS, LL, SL (Ar-Cu)	8%	52%
Lu & Fan [2008]	LJ for SS, LL, SL	5%	90%
Teng et al [2008]	LJ for SS, LL, SL (Ar-Cu)	0.688%	300 times
Li et al [2008]	LJ for SS, LL, SL (Ar-Cu)	1.5%	-
Vladkov & Barrat [2008]	LJ-FENE for SS, LJ for LL, SL	-	-

Keblinski et al [2002] used equilibrium molecular dynamics simulation to qualitatively study a model nanofluid system. Their simulation domain consisted of a single 2 nm diameter solid nanoparticle surrounded by fluid molecules in a cubic box of length 3.5 nm with 10% particle volume fraction. Lennard-Jones potential was used to simulate the interactions between all atoms pairs, solid-solid, liquid-liquid and solid-liquid. The Lennard-Jones energy parameter (ε_{ss}) for solid atoms was 10 times that used for the liquid atoms (ε_{ll}). By comparing the heat current autocorrelation function (HCAF) between solid and liquid atoms, they observed that the HCAF for liquid atoms decayed monotonically, while that for solid atoms decayed in an oscillatory manner. By this comparison they concluded that heat moves in a ballistic manner inside the solid nanoparticle and the particle-liquid interface plays a key role in translating fast thermal transport in solid particles into high overall thermal conductivity of the nanofluid. No quantitative information on the extent of heat transfer enhancement was provided in this study.

Wu and Kumar [2004] used non-equilibrium molecular dynamics (NEMD) simulation to calculate the thermal conductivity of nanofluid. A brief description of the NEMD method is given in the next section. They considered all the interactions, fluid-fluid, particle-particle and fluid-particle possible in a nanofluid suspension. They used a Lennard-Jones like potential to simulate the fluid-fluid and particle-fluid interactions and another inter-atomic potential was used for particle-particle interactions. The particle-particle potential takes into account the size of the particles also. They used perfectly elastic collisions between particles to simulate the non-agglomerated case and perfectly inelastic collision method to simulate to agglomeration between nanoparticles. The

results for non-agglomerated system match fairly well with the experimental results for nanofluid consisting of 10 nm copper nanoparticles with water. The random Brownian motion of particles show a strong dependence on temperature and the frequency of collision between fluid molecules and nanoparticle increases with temperature, therefore the effective thermal conductivity of the suspension also increases. It was also observed that the agglomeration between nanoparticles decreases the heat transfer enhancement, particularly at low concentration, since the agglomerated particles tend to settle down in liquid and also reduce the number density of particles, which creates large regions of particle-free liquid. It was also shown that the effective thermal conductivity of nanofluid decreases as the number of agglomerated nanoparticles increases. Although this work used simple potential functions to simulate the interactions, but it gives good insight into the difference between agglomerated and non-agglomerated system and the results also match well with experiments.

Bhattacharya et al [2004] carried out Brownian dynamics simulation with equilibrium Green-Kubo method to calculate effective thermal conductivity of nanofluid and found good agreement with experimental results, but their results depend on the correlated parameters, which were used to match with their experimental data and are difficult to apply in other nanofluid data as there is no systematic way to find these parameters. Although initial calculations showed significant increases in thermal conductivity from Brownian motion of particles, interaction parameters based on appropriate Debye length increased the conductivity by less than 2% [Gupta et al, 2007]. Eapen et al [2007] did an order of magnitude analysis between thermal diffusion and Brownian diffusion and showed that even for extremely small particles thermal diffusion

is much faster than Brownian diffusion, so they concluded that Brownian effects are small in heat transport in nanofluids.

Evans et al [2006] performed NEMD simulation of a single solid nanoparticle surrounded by liquid atoms. The interactions between the atoms in the solid nanoparticle and between fluid atoms were simulated using Lennard-Jones potential. The atoms in the solid nanoparticle were connected with their nearest neighbor using finite extension non-linear elastic (FENE) bonding potential. They observed a modest 2.5% increase in the thermal conductivity of nanofluid at 3.3% particle volume fraction. This enhancement is lower compared to that observed in any experimental study but is close to that predicted by effective medium (EM) theory [Putnam et al 2003] for well-dispersed thermal conductive nanoparticles.

Eapen et al [2007] conducted equilibrium molecular dynamics (EMD) simulation of a model nanofluid using Lennard-Jones potential to simulate the solid-solid, liquid-liquid and solid-liquid interaction. They used sub-nanometer size nanoparticles consisting of 10 atoms surrounded by liquid atoms in a cubic simulation domain. They used a repulsive potential between the nanoparticles to stop them from agglomerating. The number of nanoparticles was varied to study the effect of particle volume fraction on thermal conductivity. They used the Lennard-Jones energy (ε) and length parameter (σ) of Xe for liquid atoms and Pt for solid atoms. The parameters for solid-liquid interactions were calculated using the classical Lorentz-Berthelot mixing rule [Allen & Tildesley, 1987]. Green-Kubo correlation was used to calculate the thermal conductivity of the nanofluid. They observed a maximum of 35% increase in thermal conductivity at 0.8% particle volume fraction. They decomposed the heat current in to 3 constituents, namely

(a) Kinetic, (b) Potential, and (c) Collision modes and found that highest contribution to the thermal conductivity came from the collision mode, which represents the interactions between various atoms, but the enhancement in conductivity came mainly from the potential energy mode. They concluded that the enhancements arise from the strong solid-fluid attraction through the self correlation of the potential flux and that enhancement was primarily a surface phenomenon. The interfacial fluid atoms form a dynamic layer around the nanoparticle where potential energy is cooperatively exchanged between solid and fluid atoms causing the enhanced thermal transport in nanofluids.

Sarkar & Selvam [2007] also used Lennard-Jones potential to model solid and liquid atoms in their study of nanofluid system using molecular dynamic simulation. They used the Lennard-Jones energy (ε) and length parameter (σ) of Ar [Allen & Tildesley, 1987] for liquid atoms and Cu [Yu & Amar, 2002] for solid atoms. The parameters for solid-liquid interactions were calculated using the classical Lorentz-Berthelot mixing rule. Green-Kubo correlation was used to calculate the thermal conductivity of the nanofluid. They observed an increasing thermal conductivity with increasing particle volume fraction and reported a maximum enhancement of 52% at 8% particle volume fraction. They observed two regimes of conductivity enhancement as observed in the experiments by Murshed et al [2006]. The conductivity rose faster at small volume fractions and showed a saturation behavior at larger volume concentration. They studied the effect of particle volume fraction on thermal conductivity by varying the size of solid particle and keeping the number of liquid atoms constant at 2048. As it has been observed in the experiments that the particle volume fraction and size both affect the thermal conductivity of nanofluid, this approach of varying particle size to study the

effect of volume fraction will not be able to distinguish between the parameters causing the actual thermal enhancement. They compared the mean square displacement (MSD) of liquid atoms in the nanofluid to that with the liquid atoms in the base fluid and found that MSD was higher for nanofluid with higher volume concentration of solid. They concluded that the thermal enhancement in nanofluids is caused by the enhanced motion of the liquid atoms due to the presence of the solid nanoparticles.

Teng et al [2008] also used the same approach as used by Sarkar & Selvam [2007] with same Lennard-Jones parameters for solid and liquid molecules. They studied the effect of particle size at constant volume fraction and reported an increase in thermal conductivity with increasing particle size. They reported an astonishing 300 times increase in the thermal conductivity of nanofluid at a volume concentration of 0.688%. In their words "*This tremendous increase in thermal conductivity is amazing and needs to be verified, or modified with discussion.*" So their quantitative results on thermal conductivity need to be verified. They decomposed the heat current used in Green-Kubo correlation in convective and interatomic terms, and observed that the contribution of the convective mode is higher compared to diffusion mode or the interatomic mode. This finding is in contrast to previous findings by Eapen et al [2007] and Sarkar & Selvam [2007].

Li et al [2008] also used a model nanofluid system with Lennard-Jones potential to simulate interactions between all atom pairs. They also used Lennard-Jones parameters of Ar for liquid and Cu for solid atoms. They did not report any quantitative results for thermal conductivity but showed the presence of a layer of liquid molecules at the solid-liquid interface. They compared the number density of liquid atoms in concentric shells

outside the solid nanoparticle to that with the number density of liquid atoms in base fluid. They observed that the thickness of this ordered liquid layer was about 0.5 nm and concluded that this ordered liquid layer is an important phenomenon causing the thermal enhancement in nanofluids.

Although significant work has gone in experimentally measuring the thermal conductivity of nanofluids, not much work has been performed in studying various mechanisms of heat transport in nanofluids using computer simulations. As seen by the few simplistic studies done on nanofluids using molecular dynamic simulation, it is clear that this method shows promise in finding and confirming various nanoscale heat transport mechanisms occurring in nanofluids. All the molecular dynamic studies conducted till date have used the simplistic Lennard-Jones potential to model the solid-solid, solid-liquid and liquid-liquid interactions. As discussed later in chapter 3 the choice of interaction potential used in a molecular dynamic simulation determines the accuracy and closeness to real experiment. There is a need to systematically study the various mechanisms postulated by researchers using more realistic interaction potentials to understand the phenomenon occurring at nano-scale in the nanofluids. A small literature review of the molecular dynamic simulation technique and two ways of calculating thermal conductivity using the same are discussed in the next section.

2.4 Literature Review on Molecular Dynamics Simulation

Molecular dynamics is a very powerful computer simulation technique where the time evolution of a set of interacting atoms is studied by numerically integrating their equations of motion. Molecular dynamics essentially involves solving a classical many-

body problem in the context of the study of matter at the atomic scale. It allows predicting the static and dynamic properties of the system under consideration. For complex systems which are modeled poorly by continuum or analytical methods, Molecular dynamics simulation lends itself as a very good computational tool. Molecular dynamics has been used to support research in the areas of physics, chemistry, biology and materials science. Alder & Wainwright [1959] were amongst the first ones to do molecular dynamics simulation in 1959 at the Lawrence Livermore National Laboratory. They used a "hard sphere" model to study the molecules in liquid which interact as "billiard balls". They were able to simulate 32 and 108 molecules in computations requiring 10 to 30 hours with the fastest computers at that time, an IBM 704. Rahman [1964] studied many properties of liquid argon using Lennard-Jones potential on a system containing 864 atoms. Verlet [1967] calculated the phase diagram of argon using Lennard-Jones potential and computed correlation functions to test theories of liquid state. Most of the systems studied at that time contained a very small number of atoms but now with improvements in computer architecture it is possible to simulate millions of particles but the computations continue to be demanding.

2.4.1 Thermal Conductivity Calculation using Molecular Dynamics Simulation

Experimentally, thermal conductivity (λ) is typically calculated by measuring the temperature gradient that results from the application of a heat current. The thermal conductivity relates the heat current to the temperature gradient via Fourier's law as:

$$J_\mu = -\sum_v \lambda_{\mu v} \frac{\partial T}{\partial x_v} \qquad (2.5)$$

Here J_μ is a component of the thermal current, $\lambda_{\mu\nu}$ is an element of the thermal conductivity tensor, and $\partial T / \partial x_\nu$ is the gradient of the temperature. In molecular dynamics simulations the thermal conductivity can be computed either using the non-equilibrium molecular dynamic (NEMD) [Müller-Plathe, 1997] or equilibrium molecular dynamic (EMD) simulations [Vogelsang et al, 1987]. The two most commonly applied methods in molecular dynamics are the 'direct method' and the Green-Kubo method. The direct method is an NEMD method in which a temperature gradient is applied across the simulation cell, essentially mimicking the experimental situation. On the other hand, in the EMD method we use the Green-Kubo correlation, which uses the heat current fluctuations to compute the thermal conductivity via the fluctuation-dissipation theorem in the linear response of the system.

As mentioned above the NEMD or direct method of computing the thermal conductivity is analogous to the experimental measurement. Wu and Kumar [2004] used NEMD method to calculate the thermal conductivity of suspension of copper nanoparticles in water. Figure 2.6 shows a schematic representation of the simulation domain used in this study to compute the thermal conductivity by Wu and Kumar [2004].
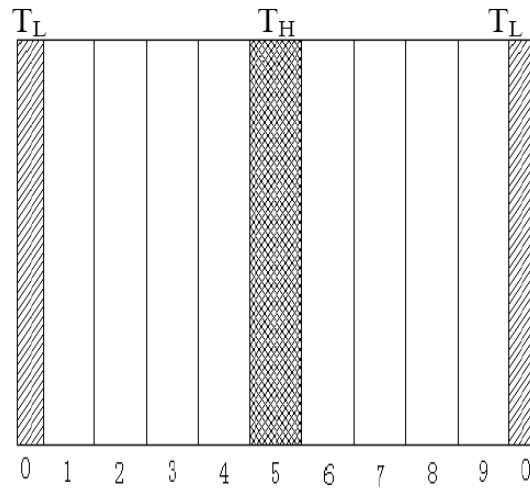
Figure 2.6: Schematic of the simulation domain used in NEMD simulation by Wu & Kumar [2004]

The simulation domain was divided into 10 layers with each layer having identical thickness and volume. Layer *0* was further divided into 2 equidistant parts to be consistent with the periodic boundary condition. Layer 0 is defined as the "cold" layer and layer 5 as the "hot" layer (Figure 2.6). The initial temperature of whole system is maintained somewhere in between T_H and T_L.

By exchanging the particles (fluid molecules and nanoparticles) with highest velocity in the cold layer with the ones having lowest velocity in the hot layer, the heat flux is generated in the system. By exchanging the velocities, the temperature in the hot layer increases and in the cold layer decreases, setting a temperature gradient in the system. This temperature gradient leads to an energy transfer from the hot layer to the cold layer by heat conduction. Total momentum, kinetic energy and total energy are kept constant in this exchange process.

When the system reaches steady state, the heat flow due to velocity exchange of particles must equal the heat conduction from the hot layer to the cold layer in both directions. The energy balance can be written as:

$$\sum_{i=0,1} \sum_{transfer} \frac{m_i}{2}(v_{i,h}^2 - v_{i,c}^2) = -2\lambda t A_{yz} \frac{\partial T}{\partial x} \tag{2.6}$$

Here, m_i is the mass of the particle ($i=0, 1$ refer to the fluid molecule and nanoparticle respectively), v_h and v_c are the velocity of particles in hot and cold layers respectively, A_{yz} is the cross section area of calculated domain and t is the thickness of the layer. All the quantities in equation (2.4) are exactly known, except the temperature gradient. The temperature gradient has to be calculated using the kinetic theory of gases, which relates temperature with velocity of particles as follows:

$$T_k = \frac{1}{3n_i k_B} \sum_i \sum_{j=1}^{n} m_i v_{j,i}^2 \tag{2.7}$$

Here T_k is the instantaneous local temperature of layer k, n_i is the number of ith particle in layer k, $v_{j,i}$ is the velocity of ith particle in layer k, and k_B is the Boltzmann constant. Using the atomic velocities calculated at each molecular dynamic time step we can calculate the temperature of hot and cold layer from equation (2.7) and then calculate the temperature gradient. The left hand side of equation (2.6) is already known and by plugging in the temperature gradient we can calculate the thermal conductivity of the simulation domain.

As we observe in Figure 2.6, the application of hot and cold layer (source and sink) and application of periodic boundary condition only generates a heat current in the x-direction and with a single simulation thermal conductivity only along one particular direction can be calculated. To obtain λ along a different crystal lattice direction, an entirely new simulation domain with layers along the required lattice direction must be created and new simulation must be carried out. This limitation does not exist for the Green-Kubo method, where the entire thermal conductivity tensor is computed in just one simulation. For the direct method, it is important that a steady-state heat current flow has been achieved. This can be achieved by plotting a stationary temperature profile as a function of time, thus insuring that only steady-state currents are flowing and, hence thermal conductivity can be computed using equation (2.6).

In EMD simulation, Green-Kubo correlation of the heat current is used to compute the thermal conductivity. In EMD simulation there is no imposed driving force on the system, and hence the system is always in the linear-response regime. Since the simulation is done in equilibrium and the system response in the linear regime, according

to the fluctuation-dissipation theorem, the transport coefficients can be calculated using the Green-Kubo correlations [McQuarrie, 2000]. As mentioned earlier one major advantage of Green-Kubo method over the NEMD method is that complete anisotropic thermal conductivity of the system can be calculated in one simulation. While in the case of direct method or NEMD, 3 separate simulations need to be run to calculate conductivity in 3 directions. So in this work the EMD simulation with Green-Kubo correlation is used to calculate the thermal conductivity of nanofluids. Details of the linear response theory as used with EMD simulation are given in the next chapter.

CHAPTER THREE: METHODOLOGY

The basic assumption of continuum that the properties of material e.g. temperature does not change very fast with change in time and space breaks down at the nano-scale. At the nano-scale, properties of materials change at the atomic scale and so the continuum methods like computational fluid dynamics (CFD) and finite element methods (FEM) can not be used to simulate these systems. No conventional equations or correlations are available to analyze the systems at the micro and nano-scale. Experiments can be performed to measure macro-scale properties of these systems, but experiments may have to be repeated several times which would increase the cost. So the only feasible method to systematically study these phenomena occurring at molecular level is by way of numerical experiments.

Figure 3.1 [Smith G., 1999] shows different numerical methods that can be used at various length and time scales. At millimeter length scale the assumptions used to derive continuum level equations are valid so we can use Navier-Stokes equations for fluid flow at this scale. Conventional finite element modeling or computational fluid dynamics numerical methods can be used to simulate the fluid flow and heat transfer at this scale. When the dimensions are of the order of a few hundred micro-meters, these conventional methods may still be used with reasonable accuracy. As we move to sub-micrometer dimensions the assumptions used in the continuum models do not hold and we can not use these conventional methods to appropriately model the systems with sub-micrometer length scales. At this scale, Monte Carlo (MC) method or Lattice Boltzmann
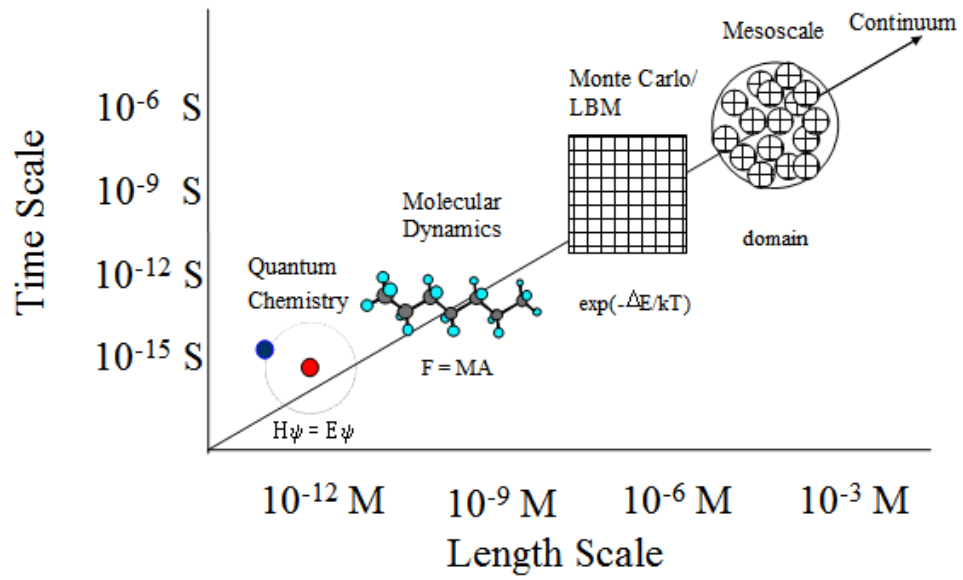
Figure 3.1: Simulation techniques for various length and time scales [Smith G., 1999]

Method (LBM) numerical techniques can be used to accurately simulate the fluid flow and heat transfer.

As we move to nano-scale length scales MC and LBM also can not be used to simulate the atomic scale system. At this scale, we should use a numerical technique which deals with individual atoms and molecules. Molecular dynamics simulation is an appropriate method to simulate the systems involving atomic size length scales. As the length scale decreases further and we deal with individual electrons quantum chemistry based methods e.g. quantum Molecular dynamics or density functional theory methods should be used to model the systems.

To analyze flows in nanochannels, conventional finite element modeling or computational fluid dynamics approach can not be used as these models break down at micro-scale when the mean free path and the system size become of same order. Molecular dynamics simulation is becoming a very widely used simulation technique for numerical simulation at molecular level. Molecular dynamics simulations have been used to simulate various atomic scale structures involving solids, liquids or gaseous systems. Molecular dynamics has shown great promise in its ability to accurately predict structural and thermodynamic properties of various systems. The basic premise for molecular dynamics comes from the real world behavior of solids or fluids at atomic scale. All materials, solids or liquids, consist of atoms and molecules, which are held together by weak van der Waals forces in noble gases with single atoms as its main constituting entity. In liquids or gases with molecules consisting of two or more atoms, the atoms are held together in the molecular structure with bonds and these molecules interact with each other via non-bonded interactions like van der Waals forces or coulombic forces. In

the solids all the atoms are bonded together in a crystal structure and interact with each other via various different forces. If a material consists of ions, they interact with each other by the coulombic forces. The inspiration to perform molecular dynamics simulation comes by observing the behavior of materials in real life. A molecular dynamics simulation consists of atoms constituting the material under consideration, e.g. for the noble gas argon, the simulation will consist of argon atoms. In real life these atoms interact with each other via the van der Waals forces.

Molecular dynamics is a computer simulation technique where the time evolution of a set of interacting atoms or molecules is followed by integrating their equations of motion. With this technique we can simulate the motion of molecules to gain deeper understanding of complex physical and chemical reactions, fluid flow, heat transfer, phase transformation and other physical phenomena that are driven by molecular interactions. Not only can we simulate motion of individual atoms or molecules in a fluid, but also the motion of a single large molecule consisting of many hundreds of atoms, e.g. protein or some other bio-molecules. Molecular dynamics is a very powerful simulation technique and does not require the use of empirical sub-models for each physical process. Accuracy of a molecular dynamics simulation depends on the interatomic potential used to simulate the interactions between various atoms and finite difference scheme used to integrate the equations of motion with time. For a detailed overview [Allen & Tildesley, 1987], Haile [1997] and Rapaport [2004] serve as excellent texts on the molecular simulation techniques.

3.1 Molecular Dynamics Simulation

In molecular dynamics we follow the laws of classical mechanics and numerically solve Newton's equation of motion for each particle at every time step. The classical equation of motion for a simple atomic system can be written as:

$$m_i \ddot{\vec{r}}_i = \vec{f}_i \tag{3.1}$$

$$\vec{f}_i = \sum_{\substack{j=1 \\ j \neq i}}^{N} \vec{f}_{i,j} \tag{3.2}$$

Where m_i is the mass and $\vec{r}_i$ is the position vector of ith atom, N is the total number of atoms in the simulation domain, $\vec{f}_{i,j}$ is the force applied on atom i by atom j, and $\vec{f}_i$ is the force vector acting on i^{th} atom due to interaction with other N-1 atoms in the simulation domain. So given an initial set of positions and velocities of all the particles in the simulation domain, the subsequent time evolution of the system can be completely determined. In more pictorial terms the atoms "move" in the simulation domain bumping into each other and using Newton's law we calculate the acceleration of each particle from the force acting on it by other atoms in the system. The acceleration of each particle is then integrated numerically to calculate its velocity and new position at each time step. All other properties of the system e.g. potential energy, kinetic energy, temperature etc are calculated from the velocity and position of each particle.
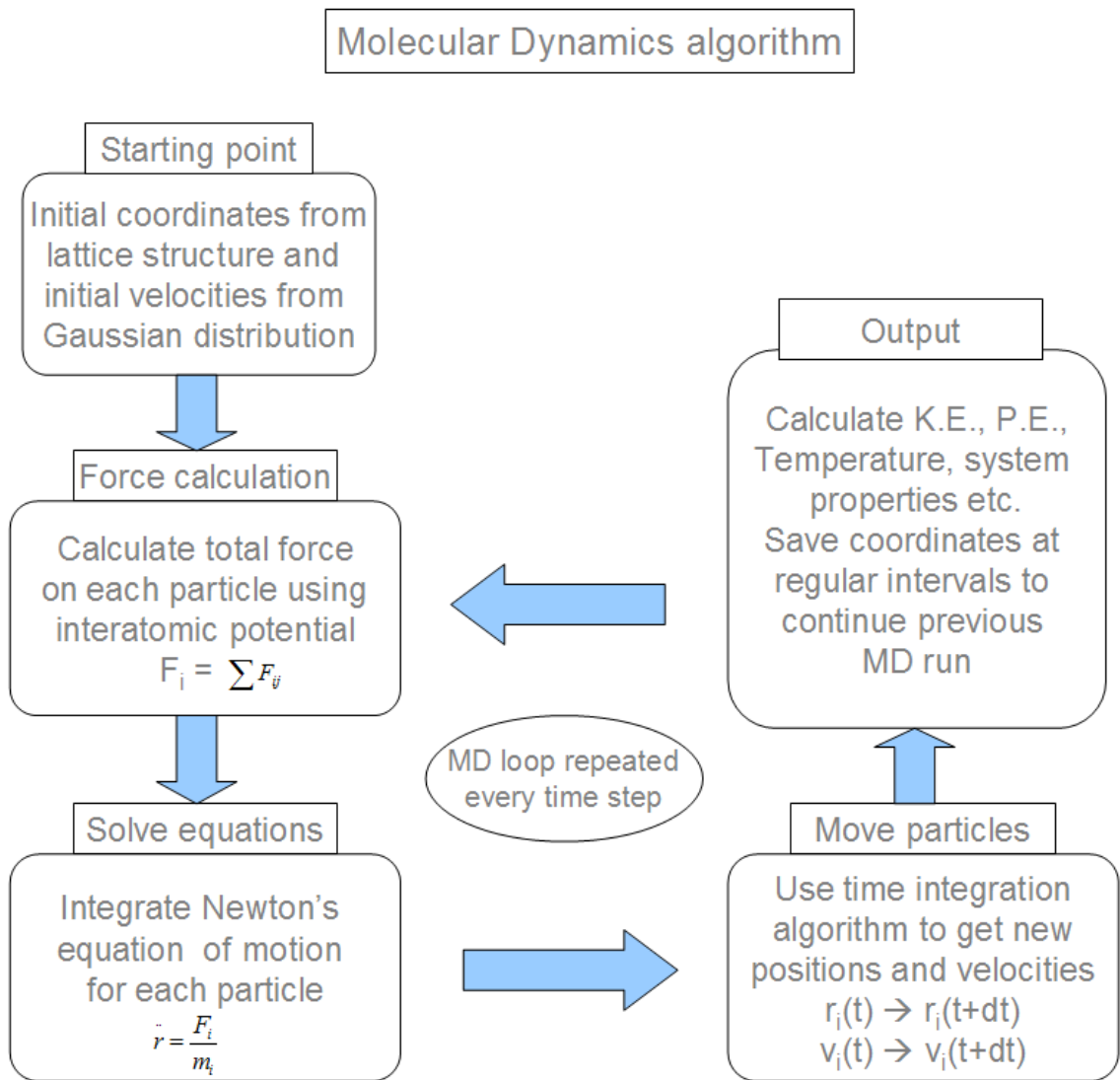
Figure 3.2: General flowchart of molecular dynamics simulation algorithm

Figure 3.2 shows a flowchart of molecular dynamics algorithm. Accuracy of a molecular dynamics simulation is greatly affected by the choice of potential function used to simulate the interaction between atoms. The potential is a function $\phi_{ij}(r_{ij})$ of the interatomic distance between atoms i and j, representing the potential energy of the system when the atoms are arranged in that specific configuration. This function is usually constructed from the relative positions of the atoms with respect to each other, rather than from the absolute positions. Forces on each atom are then derived as the gradient of the potential with respect to the atomic displacements:

$$\vec{f}_{ij} = -\vec{\nabla}_{r_{ij}} \phi_{ij}(r_{ij}) \tag{3.3}$$

Thus we can describe a model in terms of force or the potential energy. Since potential energy is a scalar quantity it is convenient to describe the model in terms of its potential energy. In this work a nanofluid system is simulated using molecular dynamics simulation. In this nanofluid system interaction between liquid-liquid, solid-solid and liquid-solid molecules are considered. These interactions occur between the liquid molecules, between the atoms of solid nanoparticle, and between the solid atoms and the liquid molecules. These interactions have been simulated with 3 different interatomic potentials, which are discussed later in this chapter. The electrostatic interaction between the charged atoms of water has also been taken into account.

3.1.1 Potential Functions

The interaction potential used in a molecular dynamics simulation can be bonded or non-bonded in nature. Most of non-bonded potentials are represented in terms of a pair

potential, which means the interactions between the atoms is considered as one pair at a time. The simplest and most widely used pair-potential in molecular dynamics simulation is Lennard-Jones [1924] or LJ potential. The molecular dynamics potential is a 12-6 potential which is attractive when the molecules are far apart and becomes strongly repulsive when they come close together. Lennard-Jones potential has a r^{-6} attractive term which represents the attractive van der Waals interaction between atom at large distances and a r^{-12} repulsive term which becomes dominant when atoms come close to each other this essentially represents the resistance to compression among atoms. For two atoms i and j the Lennard-Jones pair potential is represented as:

$$\phi_{LJ}(r) = 4\varepsilon \left[\left(\frac{\sigma}{r_{ij}} \right)^{12} - \left(\frac{\sigma}{r_{ij}} \right)^{6} \right] \tag{3.4}$$

Equation (3.4) gives the expression for the potential energy between an atom pair interacting via the Lennard-Jones potential. Here, ε is the energy parameter which gives the depth of the potential well, as shown in Figure 3.3, and σ is the length parameter, this represents the interatomic distance at which the curve crosses the zero potential line. These parameters are calculated by using quantum chemistry calculation or by curve-fitting the experimental data. The r^{-12} part of the potential is the repulsive part of the force and is dominant at small distances. As the two atoms come close to each other the repulsive force increases rapidly and does not allow the atoms to form a bond. The r^{-6} part of the potential is the attractive part of the force and is dominant at relatively larger interatomic distances. The resulting potential is shown in Figure 3.3.
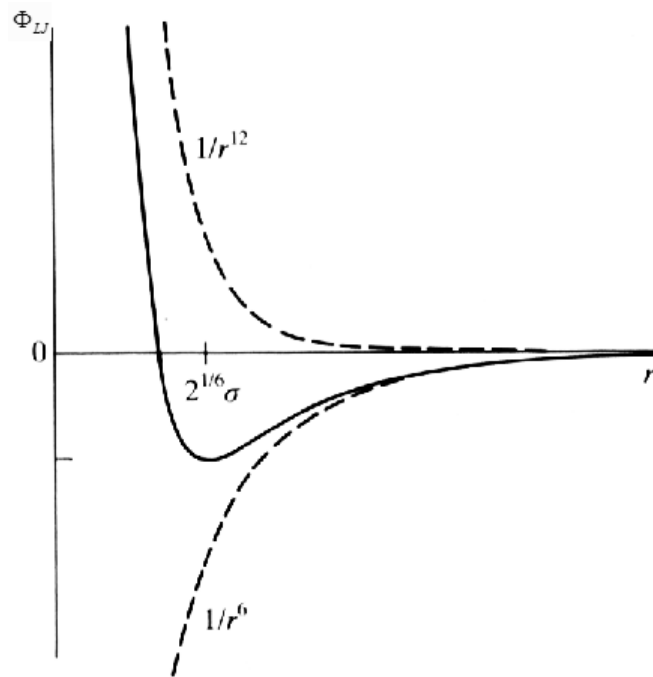
Figure 3.3: Potential energy of a particle in LJ model

3.1.2 Force Calculation

The interaction pair potential is then used to calculate the force between the pair of atoms and force on an atom i is then calculated by summing the interactions over all other atoms in the system. The force is calculated by taking a gradient of potential function as shown in equation (3.3). For Lennard-Jones potential the interatomic force between two atoms is given by:

$$\vec{f}_{LJ}(r) = \frac{\varepsilon}{r_{ij}} \left[48 \left(\frac{\sigma}{r_{ij}} \right)^{12} - 24 \left(\frac{\sigma}{r_{ij}} \right)^{6} \right] \hat{r}_{ij} \qquad (3.5)$$

3.1.3 Cut-off Radius

The force calculation is the most time consuming step in a molecular dynamics simulation since force on each atom i by all other N-1 atoms in the simulation domain is calculated. Moreover at each time step the force on each and every atom from all remaining atoms in the simulation domain has to be calculated. The force calculation grows as $O(N^2)$ in a molecular dynamics simulation of N atoms. In order to save some computation time, a cut-off radius $r_{cut\text{-}off}$ is used and for atom i the interaction by atoms which fall outside a sphere of radius $r_{cut\text{-}off}$ is neglected. Commonly used cut-off radius for Lennard-Jones potential is 2.5σ - 3.2σ [Allen & Tildesley, 1987]. The Lennard-Jones potential with implementation of cut-off radius is represented as:

$$\phi(r) = \phi_{LJ}(r) - \phi_{LJ}(r_c) \qquad \text{if } r \leq r_c \qquad (3.6)$$

$$\phi(r) = 0 \qquad \text{if } r > r_c$$

59

3.1.4 Verlet Neighbor List

As mentioned earlier, in a MD simulation the force calculation is the computationally most intensive step. Even after using the cut-off radius we do not save a lot on computation time since for each atom i we have to calculate r_{ij} for all other N-1 atoms in the simulation domain and check if atom j lies inside or outside the cut-off radius. Other efficient algorithm called the neighbor list has been developed by Verlet [1967] which significantly reduces the computation time spent in force calculation. The basic principle of this algorithm is that we create a neighbor list for each atom i and calculate the force on i by only the atoms which lie in this neighbor list. This algorithm saves lot of computation time because this neighbor list is not updated at every step but is updated after few time steps, namely 10. So now r_{ij} is calculated between all pairs, when new neighbors are checked in every 10 time steps.

Now in this interval of 10 or more time steps some of the atoms might move outside the cut-off radius or some new atoms might come in so in order to account for this movement, the neighbor list is generated using a slightly longer radius r_{list}. Where r_{list} = $r_{cut-off}$ + Δr. Figure 3.4 shows the effect of r_{list} while generating the neighbor list.
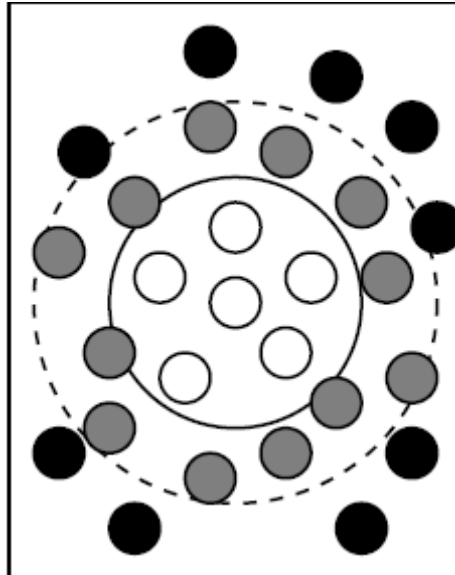
Figure 3.4: Neighbor-list construction with radius r_{list}

3.1.5 Integration of Equation of Motion

At every time step the force on every atom is calculated and then using Newton's law the acceleration of the particle is calculated. At each time step equation of motion for every atom is then integrated numerically to find their velocities. The velocities are used to advance the atoms and their new positions are calculated by numerically integrating the velocities. The choice of numerical integration scheme is important in molecular dynamics simulation, as it determines the stability of the system and also has an effect of the energy conservation for the whole system. Verlet [1967] and predictor-corrector [Allen & Tildesley, 1987] algorithms are commonly used for marching in time in a molecular dynamics simulation. The basic idea behind the velocity Verlet algorithm is to write one forward and one backward third-order Taylor series expansion of the position r(t):

$$r(t + \Delta t) = r(t) + v(t)\Delta t + (1/2)a(t)\Delta t^2 + (1/6)b(t)\Delta t^3 + O(\Delta t^4)$$

$$r(t - \Delta t) = r(t) - v(t)\Delta t + (1/2)a(t)\Delta t^2 - (1/6)b(t)\Delta t^3 + O(\Delta t^4) \tag{3.7}$$

Where v(t) is the velocity, a(t) is the acceleration and b(t) is the third derivative of r with respect to t. Adding the two expressions we get:

$$r(t + \Delta t) = 2r(t) - r(t - \Delta t) + a(t)\Delta t^2 + O(\Delta t^4) \tag{3.8}$$

This is the basic form of the Verlet algorithm, in which first we calculate r(t+Δt) from r(t), r(t-Δt) and a(t) and then use r(t+Δt) and r(t-Δt) to calculate v(t). Now we can calculate the velocities using the position as:

$$v(t) = \frac{r(t + \Delta t) - r(t - \Delta t)}{2\Delta t} \tag{3.9}$$

We neglect the $O(\Delta t^4)$ term in equation (3.8), so the truncation error associated with velocity Verlet is 4th order with respect to atomic position. However, the error associated with velocity is order 2nd order.

In this work a 5th order Gear predictor-corrector method was used to integrate the equations of motion. This method has two stages. First the predictor stage, which is applied at the start of each time step.

$$\begin{pmatrix} r_0^p(t+\delta t) \\ r_1^p(t+\delta t) \\ r_2^p(t+\delta t) \\ r_3^p(t+\delta t) \\ r_4^p(t+\delta t) \\ r_5^p(t+\delta t) \end{pmatrix} = \begin{pmatrix} 1 & 1 & 1 & 1 & 1 & 1 \\ 0 & 1 & 2 & 3 & 4 & 5 \\ 0 & 0 & 1 & 3 & 6 & 10 \\ 0 & 0 & 0 & 1 & 4 & 10 \\ 0 & 0 & 0 & 0 & 1 & 5 \\ 0 & 0 & 0 & 0 & 0 & 1 \end{pmatrix} \begin{pmatrix} r_0(t) \\ r_1(t) \\ r_2(t) \\ r_3(t) \\ r_4(t) \\ r_5(t) \end{pmatrix} \tag{3.10}$$

Here, $\vec{r}_i = \frac{1}{i!}\left(\frac{\partial^i \vec{r}}{\partial t^i}\right)\delta t^i$, is the ith derivative of position vector $\vec{r}$,

This predicts the positions and velocities for the new time step. These predicted positions are used to calculate the forces and potential energy at that step. The acceleration is calculated from the forces using the equation of motion, for each atom. This calculated acceleration is used in the corrector stage to correct the positions and velocities at that step. The correction term is given as:

$$\delta \vec{r}_2 = \vec{r}_2(t+\delta t) - \vec{r}_2^p(t+\delta t) \tag{3.11}$$

The equation for corrector stage is:

$$\vec{r}_n^c = \vec{r}_n^p + \alpha \delta \vec{r}_2 \tag{3.12}$$

Here, $\alpha = \begin{pmatrix} 3/16 \\ 251/360 \\ 1 \\ 11/18 \\ 1/6 \\ 1/60 \end{pmatrix}$

These constants for the corrector stage are given by Gear. The corrected velocities are used to calculate the kinetic energy, system temperature and other system properties. Main motivation for using the predictor-corrector integrator is that the Gear algorithm has very small energy fluctuations.

3.1.6 Periodic Boundary Condition

Periodic boundary condition (PBC) is used in almost all molecular dynamics simulations where a wall is not encountered. The periodic boundary condition acts in a way to simulate the bulk property of the system. In PBC each face of the cubic simulation domain acts as a mirror and there is a mirror system on the other side of the boundary. So every atom in the simulation domain actually represents infinite set of particles in the replicated systems. All these "image" particles move together but are represented by only a single atom in the actual simulation domain. Provided the interatomic forces are not long-range we can consider that an atom only interacts with its nearest atom or image in the periodic array. So every atom i in the simulation domain now interacts not only to the atoms j in the simulation domain but also to the images in the surrounding boxes. If an atom comes close to the boundary and then crosses it, it is re-inserted in the system from the opposite boundary with same velocity. So the periodic boundary condition actually makes sure that the number density of atoms in simulation domain and the momentum of

whole system is conserved. In molecular dynamics simulation, the periodic boundary condition is applied in the following way:

$$
\begin{array}{lll}
r_x = r_x & & r_x < l_x \\
r_x = r_x - l_x & \text{if} & r_x > l_x \\
r_x = r_x + l_x & & r_x < 0
\end{array}
\tag{3.13}
$$

Where r_x is the x-coordinate of the atom i, l_x is the length of the simulation domain in x-direction. It is assumed that one of the vertices of the simulation domain is the origin.

3.2 Molecular Simulation of Liquid Water

In this work the water molecules were modeled using molecular dynamics simulations. The water molecule consists of two hydrogen atoms and one oxygen atom in a tetrahedral bond structure. The angle between the two H-O bonds is 109.47°, as shown in Figure 3.5.

The water molecule has a bond length, $r_{H-O} = 0.1nm$ and the angle $\theta_{HOH} = 109.47°$ with charges directly on oxygen and hydrogen atoms. It takes charge on oxygen and hydrogen atoms equal to $\delta- = -0.820e$ and $\delta+ = +0.410e$, respectively. Here, *e*, is the electronic charge. There are various interactions that occur between the atoms in a water molecule and between a pair of water molecules. The H-O bond can stretch or the H-O-H bond angle can change causing bond bending in the molecule.
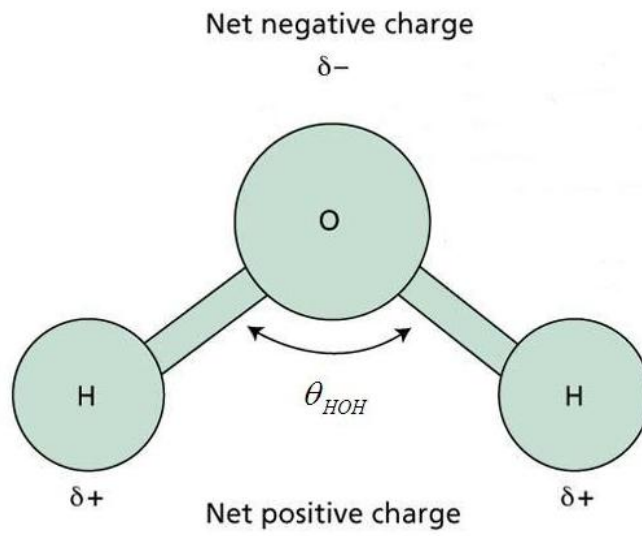
Figure 3.5: Structure of water molecule

In a pair of water molecules, the oxygen atoms belonging to two molecules can exert force on each other, or the hydrogen atom of one molecule can exert force on hydrogen atom of other molecule, or on the oxygen atom of other molecule. There can also be H^+ or O^{-2} ions in water, which will interact with each other via the coulombic interaction.

In earlier studies simplifications have been made and the complex water molecule has been replaced with a single "LJ atom" and the various interactions mentioned above have been modeled using the famous LJ potential, because of its simplicity and also because it required low computational resources. In this approach the bi-polar nature of the water molecules is lost and it interacts with another molecule via only the van der Waals forces. Although this approach is simple to implement and requires very low computational resources, this simplicity comes at the cost of accuracy of results. The LJ water model is not able to reproduce the properties like diffusion coefficient, radial distribution function, and thermal conductivity of water as measured in real experiments.

To accurately predict the structural and thermodynamic properties of water and compare them well with the experimental data, all the complicated bonded and non-bonded interactions have to be taken into account in the model. Several models for water molecule have been proposed in the past such as SPC (simple point charge) model [Berendsen et al, 1981], TIPS model [Jorgensen, 1981] and TIPS2 [Jorgensen, 1982]. Berendsen et al, [1987] reparametrized the SPC model to obtain correct energy and better matching density and called it SPC/E (simple point charge extended) model. These potentials model the water molecule as 3 site, 4 site or 5 site models. In the 3 site model, the charge on individual hydrogen and oxygen atoms are kept on the atoms itself. In the

67

4- and 5-site models, the charge is kept at a distance from the atoms' locations. These models predict the structural and thermodynamic properties of water with varying degree of accuracy. The SPC/E model has been tested and used by many researchers to model water molecules in the past. Although these potentials compare well with experiments, they model the H-O bonds as rigid bonds and restrict the 'bond-stretching' and 'bond-bending' mechanisms in a water molecule.

3.3 Potential Functions Used in This Work

In a conventional sense, molecular dynamics uses interatomic potentials derived based on *ab initio* calculations. From these potentials the interaction force between atoms, the kinetic and potential energies of atoms are calculated. As a result the accuracy and validity of the MD simulation are dependent on the potential functions used. In order to accurately simulate the nanofluid system under consideration all possible atomic interactions have been considered. In this simulation interaction between liquid-liquid, solid-solid and liquid-solid atoms along with the coulombic interaction between charged particles are taken into account. This chapter discusses all the potential functions used in this work.

3.3.1 Liquid-Liquid Interaction

Levitt et al [1997] proposed a model for water that consists of 3 atomic sites, corresponding to H, O, and H atoms, with flexible bonds to mimic the real behavior of the water molecule. This model is called the Flexible 3 Center (F3C) model. In this model the flexible nature of H-O bonds and the bi-polar nature of water molecule are

kept intact. The F3C model represents the H-O bond stretching and H-O-H bond bending in water molecule as spring forces. Various atomic pairs between two water molecules (H_1-H_2, H_1-O_2, O_1-O_2) interact with each other via a Lennard-Jones type 12-6 potential. Here, the subscripts represent water molecule 1 and 2. The ionic pairs between 2 molecules (H_1^+-H_2^+, H_1^+-O_2^{-2}, O_1^{-2}-O_2^{-2}) interact with each other via the coulombic or electrostatic interaction. The following expressions are used for the various interactions mentioned above:

- Interaction potential for H-O bond stretching:

$$\phi = \sum_i K_b \left(b_i - b_0 \right)^2 \qquad (3.14)$$

Here, b_0 is the original H-O bond length, and K_b is the spring constant for the H-O bond stretching.

- Interaction potential for H-O-H bond bending:

$$\phi = \sum_i K_\theta \left(\theta_i - \theta_0 \right)^2 \qquad (3.15)$$

Here, θ_0 is the original H-O-H bond angle, and K_θ is the spring constant for the H-O-H bond bending.

- Non-bonded interaction between a pair of atoms i, j:

$$\phi = \sum \left[\varepsilon \left(\frac{r_o}{r_{ij}} \right)^{12} - 2\varepsilon \left(\frac{r_o}{r_{ij}} \right)^6 - S_{vdw} \left(r_{ij} \right) \right] \qquad (3.16)$$

Here, ε is the energy parameter for the i, j atom pair, r_o is the length parameter for the i, j atom pair, and S_{vdw} is the first order truncation function.

- Non-bonded electrostatic interaction between a pair of atoms i, j:

$$\phi = \sum \left[\frac{1}{4\pi\varepsilon_o} \frac{q_i q_j}{r_{ij}} - S_{els} \right]$$
(3.17)

Here, ε_o is the electric constant, and q_i and q_j are the charges on the atoms i, and j and r_c is the cut-off radius.

For the LJ and coulombic potentials, only the atom pairs falling inside a specified cut-off distance are accounted for while calculating the forces. As seen in Figure 3.1 the potential energy for LJ potential almost goes to zero at a distance greater than *2.5σ*. So any atoms falling outside this distance will not contribute much towards the force and potential calculation. This cut-off approach reduces the number of force & potential energy calculations thereby reducing the computational load. The first order truncation shift function, *S(t)*, is used to implement the cut-off radius in the simulation. *S(t)* is given as:

$$S_f(r) = \begin{cases} f(r_c) + (r - r_c) \left[\dfrac{df(r_c)}{dr} \right] & for, \ r < r_c \\ \qquad\qquad 0 & for, \ r \geq r_c \end{cases}$$
(3.18)

So the cut-off part of LJ type potential S_{vdw} is given as:

$$S_{vdw}(r) = \left[\varepsilon \left(\frac{r_o}{r_c} \right)^{12} - 2\varepsilon \left(\frac{r_o}{r_c} \right)^6 \right] - \frac{12(r - r_c)}{r_c} \left[\varepsilon \left(\frac{r_o}{r_c} \right)^{12} - \varepsilon \left(\frac{r_o}{r_c} \right)^6 \right]$$
(3.19)

And, the cut-off part of the coulombic potential S_{ele} is given as:

$$S_{els}(r) = \frac{1}{4\pi\varepsilon_o} \left[\frac{q_i q_j}{r_c} - \frac{(r - r_c)}{r_c} \left(\frac{q_i q_j}{r_c} \right) \right]$$
(3.20)

Levitt et al [1997] calculated various structural and thermodynamic properties of water using the F3C model and compared them with properties calculated from other water models and with experimental data. They calculated the potential energy, specific

heat at constant volume (C_v), diffusion coefficient, mean-square distance between oxygen atoms, and the radial distribution function for water at 298 $\degree$K temperature. Good agreement was found when this data was compared with other models and experiments.

In this work the F3C model was used to simulate water and calculate its thermal conductivity. This work will also prove as a validation for further work in which water is used as a base fluid for a nanofluid system.

To start a molecular dynamics simulation, initial coordinates and velocities of each water molecule are required. The molecular dynamics simulation was started with tetrahedral, bi-polar, water molecules placed in a simple cubic lattice. This initial structure was chosen to keep symmetry in the system. The initial velocities were calculated using the kinetic theory of gases. According to the kinetic theory each atom has $\frac{1}{2}K_BT$ kinetic energy along each degree of freedom. Here, K_B is the Boltzmann constant, and T is the temperature of the system. For a monoatomic system there are 3 degrees of freedom from the translational motion. So, a system of N atoms will have total of $\frac{3}{2}NK_BT$ kinetic energy.

$$KE = \sum_{i=1}^{N} \frac{1}{2}m_i v_i^2 = \frac{3}{2}NK_BT \qquad (3.21)$$

In the flexible water molecule, since the bonds are not rigid, each atom can move independently in the x, y, and z directions (while still forming the bonds in the water molecule) and hence has 3 degrees of freedom. For 3 atoms total degrees of freedom in every water molecule then become 9. If we consider the motion of water molecule as a whole, it has 3 translational degrees of freedom, 3 rotational degrees of freedom, and 3 vibrational (2 bond-stretching and 1 bond-bending) degrees of freedom. So a total of 9

degrees of freedom are there in the water molecule. The flexible water model mimics the behavior of a real water molecule by letting each atom move individually. This flexible nature of the bonds also simulates the rotational motion of the water molecule.

In a rigid water model, e.g. SPC/E, the 3 vibration degrees of freedom are not accounted for. Also the rotation of molecules adds more complication to the computational procedure. The rotational motion is simplified in flexible water model as it comes out of the individual motion of the atoms in the molecules.

3.3.2 Interactions in Solid Nanoparticle

The choice of interaction potential for the solid nanoparticle in this work reflects the need for an economic, insightful analysis with reasonable accuracy. The complex chemical reactions between the surface atoms of a nanoparticle and the liquid molecules have not yet been identified in the experimental research. To identify these chemical reactions quantum-chemistry models like Carr-Parrinello Molecular Dynamics (CPMD) or Density Functional Theory (DFT) are required. In this work we wish to study general water based nanofluid system, rather than a specific nanofluid like alumina-water. So a simple two body Lennard-Jones potential is used to model the solid nanoparticle. The solid nanoparticle in this simulation consists of Lennard-Jones atoms in a FCC lattice. Each atom in the nanoparticle is connected to its first neighbors by finite extensible nonlinear elastic (FENE) bonding potential [Vladkov & Barrat, 2006] as shown in equation (3.22).

$$\phi_{FENE} = \frac{k}{2} R_o^2 \ln \left[1 - \left(\frac{r_{ij}}{R_o} \right)^2 \right], \quad r_{ij} < R_o$$

(3.22)

Here, $R_o = 1.5\sigma$, and $k = 30.0 \dfrac{\varepsilon}{\sigma^2}$.

The atoms in this solid particle vibrate around their mean position and simulate the phonon mode of heat transport as seen in solids. This model nanoparticle will closely simulate a non-metallic particle like oxides, where the thermal conductivity arises from the phonon mode and not from electrons as in the case of metals. The Lennard-Jones parameters for copper, as used by Sarkar & Selvam [2007] and Li et al [2008] are used for the solid nanoparticle. The primary focus this thesis is to predict the qualitative trends of thermal conductivity enhancement and study various mechanisms causing the higher thermal transport in nanofluids using molecular dynamic simulation and not to capture the complex chemical reactions between these atoms.

3.3.3 Interaction between Solid-Liquid Atoms

The third important potential to establish is the interfacial potential between the atoms in solid nanoparticle and the liquid molecules. The pairwise Lennard-Jones potential is used to model the interaction between atoms of solid nanoparticle and atoms in liquid water. To determine the parameters for the solid-liquid interaction, the Lorentz-Berthelot mixing rule [Allen & Tildesley, 1987] is used:

$$\sigma_{sl} = \frac{\sigma_{ss} + \sigma_{ll}}{2}$$

and

$$\varepsilon_{sl} = \sqrt{\varepsilon_{ss}\varepsilon_{ll}} \qquad\qquad\qquad (3.23)$$

Here, subscripts s and l refer to the solid and liquid respectively. A list of the potential

function parameters for solid and liquid atoms used in this work is presented in Table 3.1.

Parameter Units	Parameter Values
ε^{OO} (kcal mol^{-1})	0.1848
ε^{HH} (kcal mol^{-1})	0.0100
ε^{OH} (kcal mol^{-1})	0.0429
r_o^{OO} ($\overset{o}{A}$)	3.5532
r_o^{HH} ($\overset{o}{A}$)	0.9000
r_o^{OH} ($\overset{o}{A}$)	1.5932
q^{O} (e unit)	-0.820
q^{H} (e unit)	0.410
b_o^{OH} ($\overset{o}{A}$)	109.47
θ_o^{HOH} (deg)	1.0000
K_b^{OH} (kcal mol^{-1} $\overset{o}{A}^{-2}$)	250.0
K_θ^{HOH} (kcal mol^{-1} rad^{-2})	60.0
ε_{Cu} (kcal mol^{-1})	9.4453

σ_{Cu} ($\overset{o}{\text{Å}}$)	2.3377

Table 3.1: Potential function parameters used in this work

3.3.4 Coulombic Interaction

Till now various pair potential functions used in this simulation have been discussed here. These interactions are essentially short-ranged in nature, which means that the potential decreases quickly as the distance between a pair of atoms increases and we can use a cut-off radius to ignore the interactions with interatomic distance larger than the cut-off radius. Short-range interactions exclude a very important group of interactions involving electric charges and dipoles. In this system even though individual water molecules are electrically neutral but individual oxygen and hydrogen carry negative and positive charges respectively, similarly the silica nanoparticle as a whole does not carry any charge but oxygen and silicon atoms carry negative and positive charges respectively. The interactions between electric charges are long-ranged in nature, which means that the force between charges does not decay even at large distances, so it can not be truncated and the interactions over the whole simulation domain should be considered. The electronic interaction between charge-charge decays as r_{ij}^{-1} and the interaction between dipole-dipole decays as r_{ij}^{-3}. So these interactions do not decay fast even at large distances. A spherical truncation using a cut-off radius can not be done here because the resulting sphere around a given charge could be charged (i.e. sum of all charges in the spherical domain might not be zero). Also the charges moving in and out of this spherical domain would create artificial surface effects at $r=r_c$. The electronic interactions or coulombic interactions essentially require $O(N^2)$ computational time. Even with modern high speed computers this high computational cost is a serious problem in MD simulations with thousands of atoms.

In this simulation an approximate method called Wolf method [Wolf et al, 1999] is used to simulate the coulombic interactions between charged atoms. The Wolf method was conceptualized on the fact that ionic systems have a tendency to be locally charge neutral, i.e. the ions arrange themselves in such a way that each charge is surrounded by neighboring charges of opposite sign, thereby creating a locally charge neutral zone. This kind of behavior is called "screening" of ions and is observed in molten salts, ionic gases, ionic solutions and metallic conductors. It has been shown both theoretically [Evjen, 1932] and numerically [Clarke et al, 1984, Woodcock, 1975, Wolf 1992] that the effective coulombic interaction in condensed systems are actually short-ranged. It has also been suggested that at long range there is almost complete cancellation of coulombic effects. Based on these findings, Wolf et al [1999] proposed an exact method for simulation of coulombic system by spherically truncated, pairwise 1/r summation. Wolf method is suited for this simulation since there are no ions in the simulation domain, individual atoms carry certain charge but the molecules as a whole are locally charge neutral.

This method sums the total potential energy over all the atomic sites in the system and solves iteratively the self-consistent equations for the induced dipoles at each step of the molecular dynamics. Since we are using a truncated potential the following term is added to the total potential energy of the system to consider the effect of interaction between charges which are at an interatomic distance greater than the cut-off radius.

$$U_{pol} = -\frac{1}{2} \sum_k \mu_k E_k \qquad (3.24)$$

Where, E_k is the electric field at the location of site k due to all the fixed charges in the system and μ_k is the induced dipole moment vector at location k. The induced dipoles are determined by iteratively solving the equation:

$$\mu_k = \alpha_k \left[E_k - \sum_{k \neq l} T_{kl} \cdot \mu_l \right] \qquad (3.25)$$

Here α_k is the atomic polarizability assigned to site k, and T_{kl} is the dipole–dipole tensor. In the above approach, one needs to readjust the positions of the charges for each atom, and to assign atomic polarizability to each atom without changing the form of each potential expression. The electrostatic interactions between charges q_i and q_j are then modeled using the following approximation:

$$\frac{q_i q_j}{r_{i,j}} = \frac{q_i q_j \times erf(\alpha r_{i,j})}{r_{i,j}} \qquad (3.26)$$

The advantage of the Wolf method over the traditional Ewald sum method [Allen & Tildesley, 1987] is that it can significantly reduce the required computational time. The Wolf method is essentially equivalent to ignoring the long range electrostatic interactions in the Ewald sum method. Even though Wolf method ignores the long-range interaction but it is successful because it forces the net charge to be zero in the spherical volume confined by the cut-off radius. The parameter α in Eq. (3.19) provides the damping necessary to make the electrostatic interaction short range. Demontis et al [2001] propose a value of *4/L* for α, where *L* is the length of simulation domain. They also show that this value gives good agreement with the Ewald sum method. For the current simulation, two constant values of 0.25 and 0.07 are chosen for silica and water respectively.

3.3 Generation of Nanoparticle

In order to establish a reliable molecular dynamics model initial coordinates of the atoms in the solid nanoparticle are required. A crystallographic-based coordinate system is necessary to get the position of each atom in the nanoparticle. Before building a lattice structure, the primitive vector should be obtained and a unit cell of the crystal is created. The unit cell is then replicated in x, y, and z directions to create a bulk crystal structure. For this work the solid nanoparticle was prepared by creating the bulk copper crystal in a FCC arrangement and then carving out a spherical nanoparticle of desired diameter from this bulk crystal. The atoms within the sphere were linked to their first neighbors by the FENE bond. Figure 3.6 shows the FCC unit cell, 1 nm and 2 nm nanoparticle structure used in the simulation.
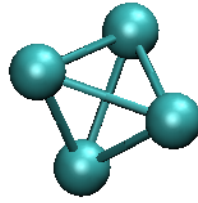
(a)
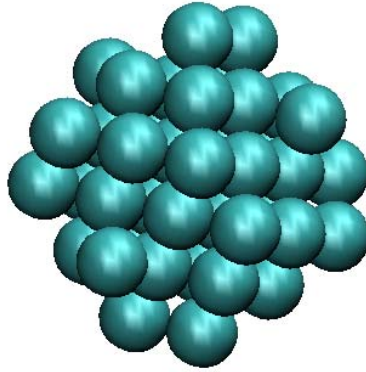
(b)
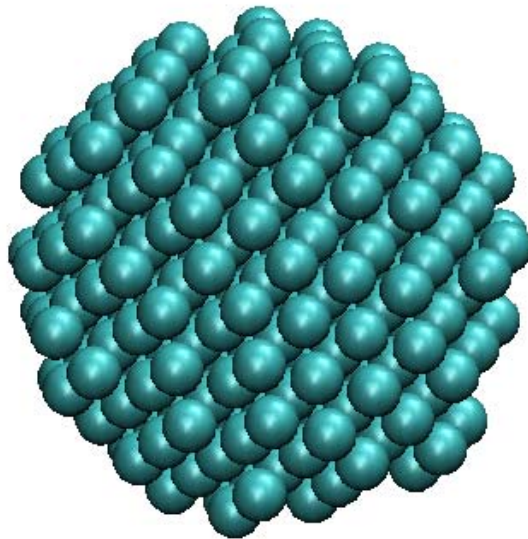
(c)

Figure: 3.6: (a) FCC unit cell (b) 1 nm solid nanoparticle (c) 2 nm solid nanoparticle

3.4 Molecular dynamics simulation of Thermal Conductivity

As mentioned in Chapter 2, thermal conductivity is obtained from molecular dynamics using either equilibrium (EMD) simulations (Green-Kubo equations) or from steady-state non-equilibrium (NEMD) simulations [Young et al, 1991, Muller-Plathe, 1997, Florain, 1997]. At equilibrium the net flow of heat in a solid given by the heat current vector *q*, fluctuates about zero. In the Green-Kubo method, the thermal conductivity is related to how long it takes for these fluctuations to dissipate. In the range of linear response, thermal conductivity is related to the time autocorrelation function of the heat-flux operator according to the fluctuation-dissipation theorem. This relationship between correlation functions and transport coefficients are known as Green-Kubo relationships and for thermal conductivity it is given as follows:

$$\lambda = \frac{1}{3k_B V T^2} \int_0^\infty \left\langle \vec{q}(0).\vec{q}(t) \right\rangle dt \tag{3.21}$$

Here λ is the thermal conductivity, V the system volume, T the system temperature, $\vec{q}(t)$ is the heat current vector at time t, k_B is the Boltzmann constant, and the angular brackets denote an ensemble average, or, in the case of MD simulation it denotes an average over all atoms in the simulation domain. In equation (3.21) $\left\langle \vec{q}(0).\vec{q}(t) \right\rangle$ is the heat current autocorrelation function (HCACF) and the thermal conductivity is proportional to the rate of decay of the HCACF. In materials where the fluctuations in heat current are short lived, like in liquids or amorphous solids, the HCACF decays quickly, leading to a small integral and hence low thermal conductivity. In materials where the fluctuations are long

lived, the HCACF decays slowly, leading to a larger integral and hence higher thermal conductivity.

The instantaneous heat current vector $\vec{q}(t)$ is defines as [Hoheisel, 1987]:

$$\vec{q}(t) = \frac{d}{dt}\sum_i \vec{r}_i(t)E_i(t) - \sum_i \vec{v}_i h \tag{3.22}$$

Here $\vec{r}_i(t)$ is the position vector of atom i at time t and $E_i(t)$ is the total energy of atom i. The second term on the right hand side consisting of the mean (instantaneous) enthalpy (**h**) arises because of the definition of the heat current in a binary system, where heat and mass are coupled. The mean enthalpy (**h**) is calculated as the sum of average potential energy, average kinetic energy and average virial terms per particle of each species. Total energy for each atom i is defined as:

$$E_i(t) = \frac{1}{2}m_i v_i^2 + \frac{1}{2}\sum_j \phi_{ij}(r_{ij}) \tag{3.23}$$

Here the first term is the kinetic energy and second term is the potential energy of atom i, and $\phi_{ij}(r_{ij})$ is the pair-wise interaction. Plugging equation (2.10) in (2.9) the expression for heat current becomes:

$$\vec{q}(t) = \sum_j \vec{v}_j \left(\frac{1}{2}m_i v_i^2 + \frac{1}{2}\sum_i \phi_{ij}(r_{ij}) \right) + \frac{1}{2}\sum_{ij, i \neq j} \vec{r}_{ij}(\vec{f}_{ij} \cdot \vec{v}_i) - \sum_j \vec{v}_j h \tag{3.24}$$

Here **v** is the velocity vector of an atom, and f_{ij} is the force on atom i due to its neighboring atoms j calculated using the pair potentials. The first term in equation (2.11) represents the contribution from the convective transport and second term represents the contribution from atomic interactions.

As mentioned earlier one major advantage of Green-Kubo method over the NEMD method is that complete anisotropic thermal conductivity of the system can be calculated in one simulation. While in the case of direct method or NEMD, 3 separate simulations need to be run to calculate conductivity in 3 directions. In the NEMD simulation, extreme temperature gradients (10^{10} $^{\circ}K/m$) are encountered, due to the small simulation domain size, which can adversely affect the dynamics at the solid-liquid interface. So in this work the equilibrium molecular dynamic simulation with Green-Kubo correlation is used to calculate the thermal conductivity of nanofluids. The Green-Kubo approach has been used to calculate thermal conductivity of LJ argon [Vogelsang et al 1987, Kaburaki et al 1999], diamond [Che et al 2000], silicon [Volz & Chen 2000] and nanofluids [Keblinski et al 2002, Eapen et al 2007, Sarkar & Selvam 2007].

CHAPTER FOUR: VALIDATION OF THE MD CODE

In any computer simulation work it is necessary to validate the model with some well known experimental results or with other simulation work published in the literature. In this work two main potential functions, (1) Lennard-Jones potential, and (2) F3C model for water, were used with the Green-Kubo correlation to calculate the thermal conductivity of the nanofluid system. Before presenting the results for the nanofluid system, it is necessary to validate the code for both of these models. The molecular dynamics code developed in this work is separately validated for the Lennard-Jones potential and F3C model.

4.1 Validation of Lennard-Jones based MD code

Lennard-Jones potential was first developed to model rare gases like Argon etc. [Rahman, 1964]. Lennard-Jones potential has been proven to be reliable in predicting the static and dynamic properties of both solid and liquid Argon [Vogelsang et al 1987, Kaburaki et al 1999, Tretiakov & Scandolo 2004]. The Lennard-Jones potential parameters that best reproduce the thermodynamics of Argon are $\varepsilon = 1.67 \, x \, 10^{-21} \, J$, and $\sigma = 3.405 \, Angstrom$ [Allen & Tildesley, 1987]. To validate the molecular dynamics code and the application of Green-Kubo correlation, the thermal conductivity of liquid Argon is calculated and compared with the thermal conductivity calculated by Vogelsang et al [1987]. The thermal conductivity was calculated for state point 1, defined in Vogelsang et al [1987] by the dimensionless temperature and number density as $T^* = 0.73$ and $\rho^* = 0.8442$. The dimensionless temperature and density are given as:

$$T^* = \frac{Tk_B}{\varepsilon}$$

$$\rho^* = \frac{N}{V}\sigma^3 \tag{4.1}$$

Here, N is the number of atoms, V is system volume, T is system temperature, k_B is Boltzmann constant, and ε & σ are Lennard-Jones potential parameters.

Number of Argon atoms in the simulation domain was varied from 108 to 1372 atoms to study the effect of system size on the thermal conductivity. The system was initialized with Argon atoms placed in a face centered cubic (FCC) lattice and the velocities were initialized in a Gaussian distribution according to the given temperature. The length of the FCC unit cell was *5.719 Angstrom* to maintain given number density. Each FCC unit cells contains 4 atoms as shown in Figure 4.1. The sub-lattice of the four shaded atoms (Figure 4.1) can be used to generate a full lattice. The FCC unit cell of Argon was replicated in *x, y* and *z* directions and the number of unit cells was varied from 3 to 7 to get desired number of atoms in the simulation domain. Figure 4.2 shows the initial system configuration for the Argon system with 256 atoms.
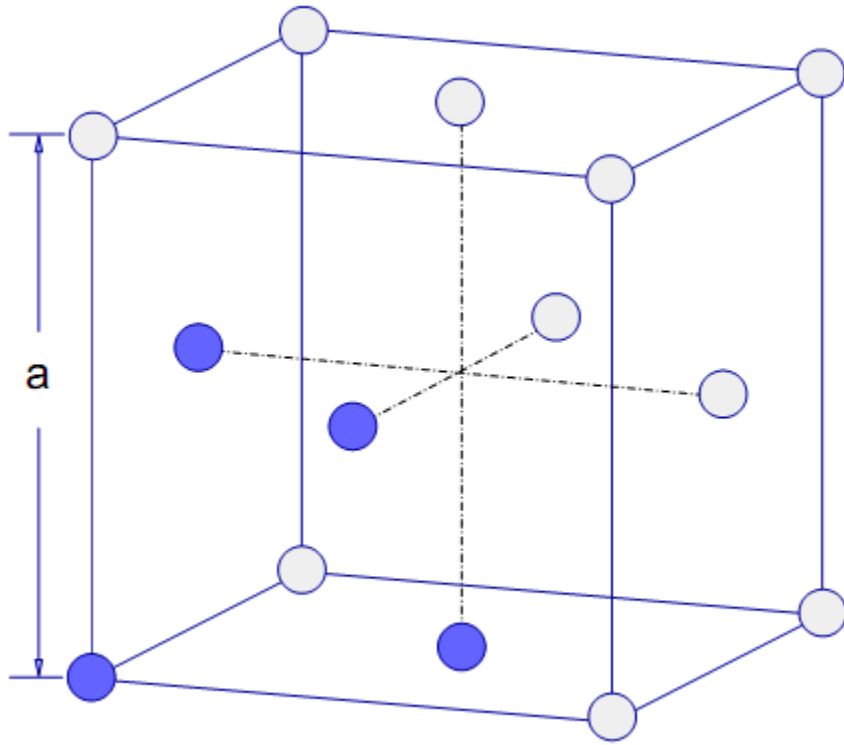
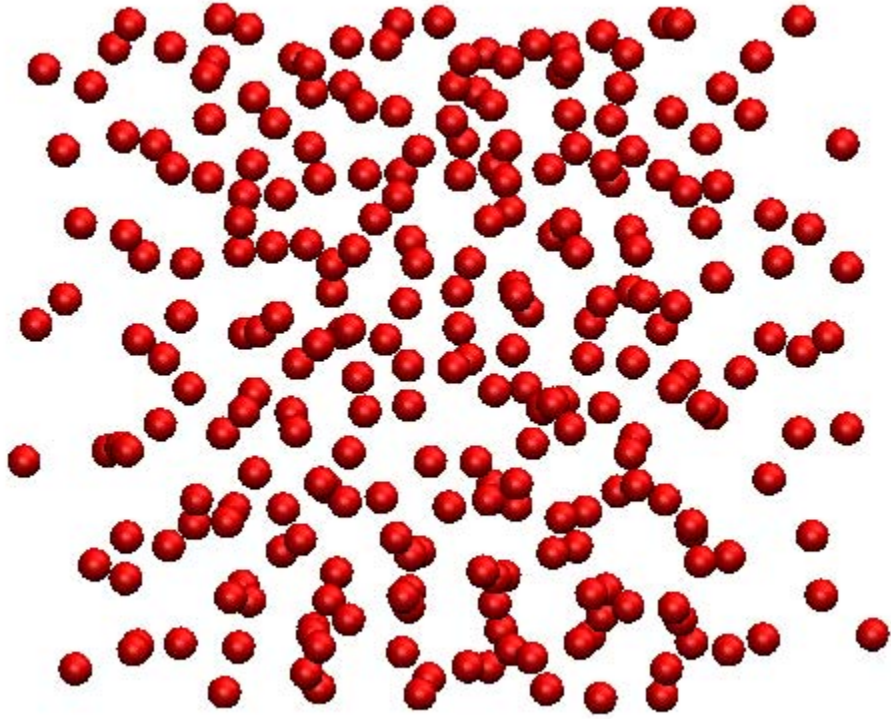Figure 4.1: Face centered cubic (FCC) unit cell structure

Figure 4.2: Initial system configuration for a 256 atoms Argon system

After initializing the system in FCC lattice and with a Gaussian velocity distribution corresponding to the given temperature the system was equilibrated in NVT ensemble for 5×10^5 time steps. In the NVT ensemble, number of atoms, volume of the simulation domain and the system temperature are kept constant. Velocity scaling method was used to keep the temperature constant in the equilibration period. A time step of *0.01 picoseconds* was used for the simulation and was found to be sufficient to resolve the phenomenon under consideration. Velocity verlet [Verlet, 1968] algorithm was used to integrate the equations of motion. Atomic interactions were truncated and shifted at a cut-off radius of *2.5σ*. After first 5×10^5 steps equilibration period was over, temperature constraint from the system was removed and the system was allowed to evolve in the NVE ensemble for 10^6 time steps. The heat current was calculated in this period and Green-Kubo correlation with a correlation length of 5×10^4 time steps was used to calculate the integral of the heat current autocorrelation function. Thermal conductivity of various systems was calculated and is compared with the values published by Vogelsang et al [1987] in Table 4.1 and Figure 4.3. It is observed that the thermal conductivity value calculated by our molecular dynamics code is in good agreement with the values published in the literature for the given temperature and density.
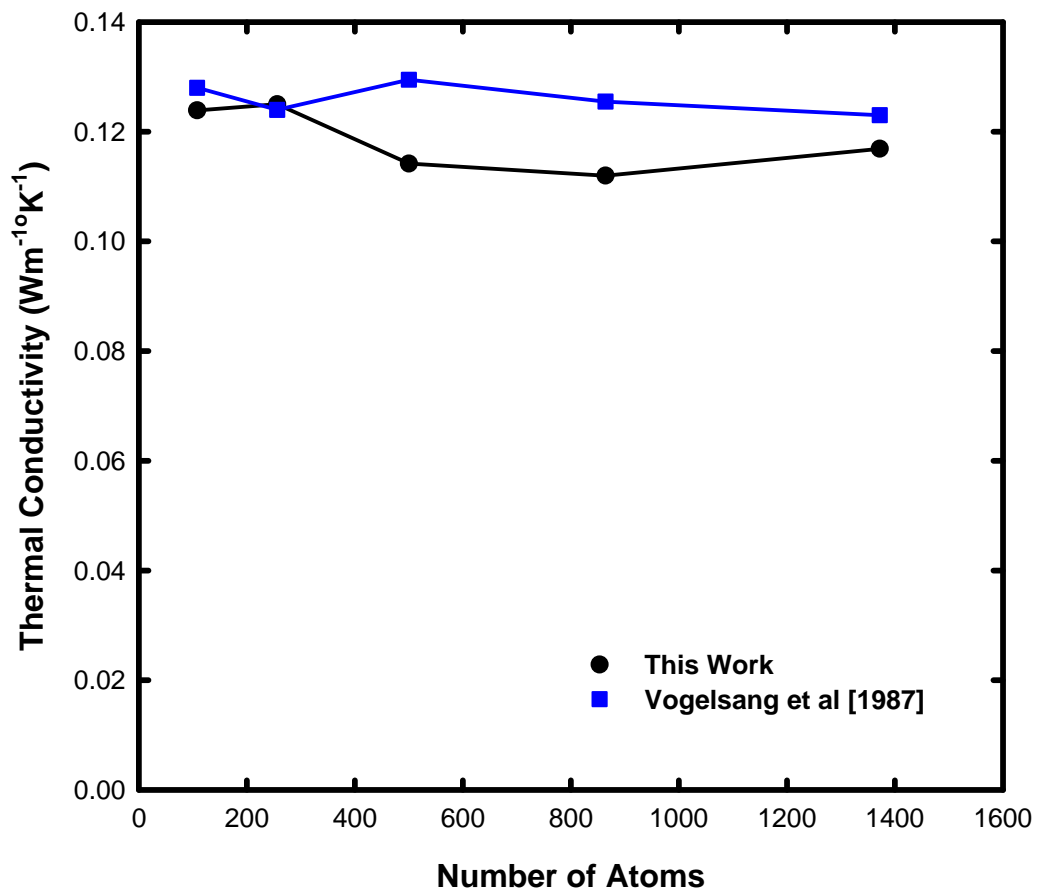
Figure 4.3: Thermal conductivity of the liquid argon at $T^* = 0.73$ and $\rho^* = 0.8442$

Table 4.1: Thermal conductivity of liquid argon with varying system size

Number of Argon Atoms	Thermal Conductivity $(Wm^{-1}{}^{\circ}K^{-1})$ This Work	Thermal Conductivity $(Wm^{-1}{}^{\circ}K^{-1})$ Vogelsang et al [1987]
108	0.124	0.128
256	0.125	0.124
500	0.114	0.130
864	0.112	0.126
1372	0.117	0.123

4.1 Validation of F3C water model

A molecular dynamics code implementing the F3C (flexible 3 center) model for water was developed for this work. The F3C model has been proven to predict various thermodynamic properties of water like potential energy and specific heat at constant volume, kinetic properties like the diffusion coefficient and structural properties like the radial distribution function of oxygen in water [Levitt et al 1997]. But this model has never been used to calculate the thermal conductivity of water, so it is even more important to validate the model before using it to calculate the thermal conductivity of the nanofluid system. Number of water molecules was varied to study the effect of simulation domain size (or the number of water molecules) on the thermal conductivity of water. 216, 343, 512, 729 and 1000 water molecules were used in a series of simulation at 300 °K temperature and 1 atm. pressure. Simulation domain size was changed from 18.62 *Angstrom* to 31.03 *Angstrom* in order to keep the density of water constant at 1 *gm/cm³*. Water molecules were initialized in a simple cubic lattice to avoid overlap of molecular positions which could happen in a random placement of molecules. The size of the simulation domain was increased with the number of simple cubic unit cells in all three directions form 6 to 10 unit cells. The size of the unit cell to maintain a density of 1 *gm/cm³* was 3.1036 *Angstrom*. A time step of 0.1 *fs* was used in all simulations. The system was equilibrated in the NVT ensemble for $5x10^5$ time steps. In the equilibration period the system temperature was kept constant using the velocity scaling method. After the equilibration period, the temperature constraint was removed and system was allowed to evolve in the NVE ensemble. The heat current was calculated

and the Green-Kubo correlation was used to calculate the thermal conductivity of the water only system.

Figure 4.4 shows the initial system configuration for a 500 molecule water system. Figure 4.5 shows the thermal conductivity values for various cases, the values are also presented in Table 4.2. It was observed that the calculated thermal conductivity of the F3C water system fluctuates around the experimentally measured value of 0.61 $Wm^{-1}{}^{\circ}K^{-1}$ at 300 ˚K and 1 atm. pressure.
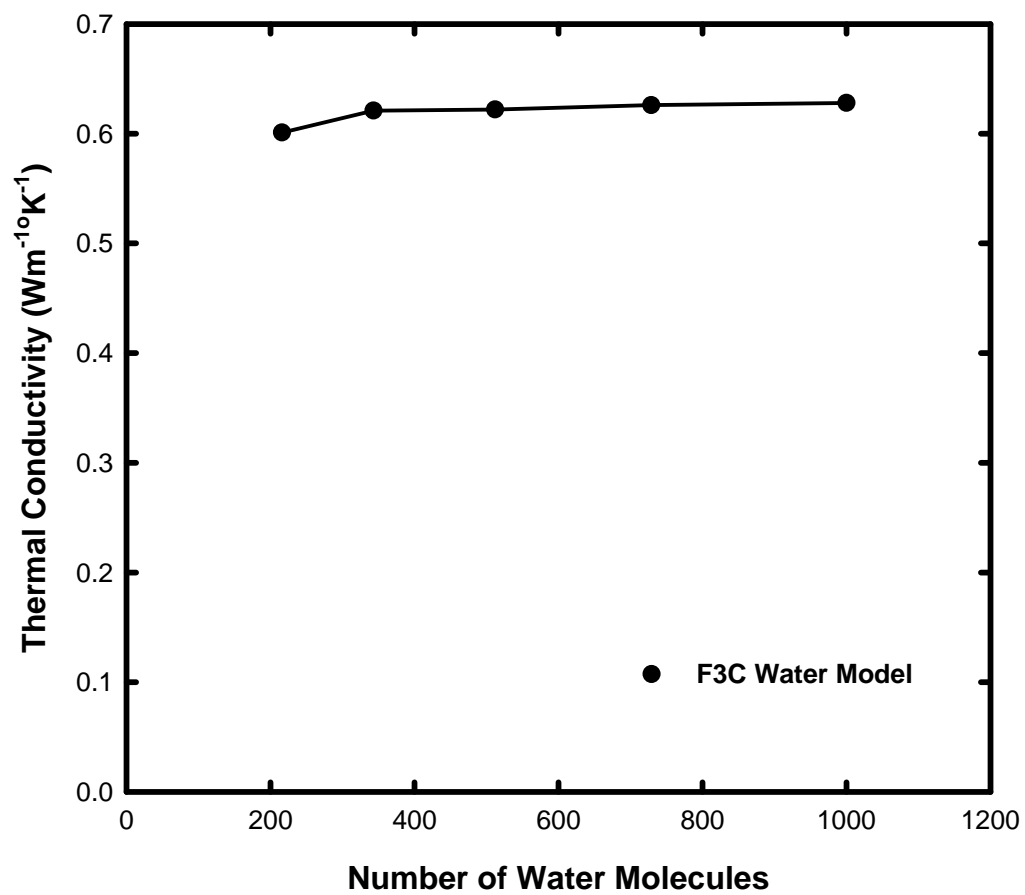
Figure 4.5: Thermal conductivity of water with varying simulation domain size

Table 4.2: Thermal conductivity of water with varying system size

Number of Water Molecules	Thermal Conductivity ($Wm^{-1}{}^{\circ}K^{-1}$)
216	0.601
343	0.621
512	0.622
729	0.626
1000	0.628

Although the calculated thermal conductivity is approximately 3% higher compared to experimental value of 0.61 W/m-K, it is well within the acceptable numerical error range of 5%, which could arise from truncation error or from the model potential function itself.

Figure 4.6, shows the variation of thermal conductivity vs. correlation length as calculated from the Green-Kubo correlation for 512 and 1000 molecule runs. The correlation length is the number of time steps used in the Green-Kubo correlation to compute the integral of heat current autocorrelation function with time.
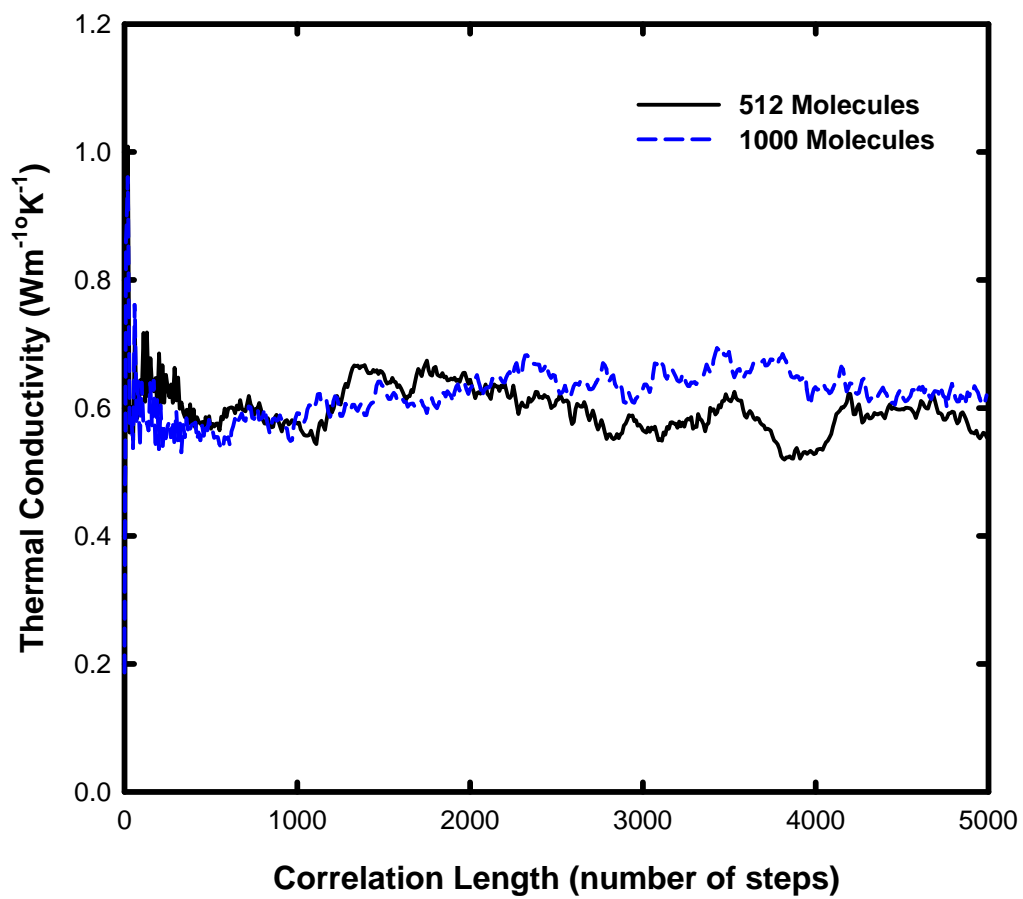
Figure 4.6: Thermal conductivity of water vs. the Green-Kubo correlation length

This work validates the molecular dynamic simulation code and the Green-Kubo formulation for calculating the thermal conductivity using the Lennard-Jones potential and the F3C model. This work was extended to calculate the thermal conductivity of the nanofluid system with water as the base fluid surrounding the solid nanoparticle. The results for the nanofluids system are presented in Chapter 5.

CHAPTER FIVE: RESULTS & DISCUSSION

Details of various computational experiments conducted in this study are presented in this chapter. The focus of this work was to calculate the thermal conductivity of water based nanofluids using equilibrium molecular dynamics (EMD) and Green-Kubo (GK) formulation. For all the cases discussed in this chapter a MD time step of 0.1 *fs* was used, predictor-corrector method was used to numerically integrate the equations of motion. The nanoparticle was generated as described in section 3.3 and water molecules were placed in a simple cubic arrangement around the nanoparticle. Figure 5.1(a) shows the initial configuration of a typical nanofluid simulation run considered in this work and Figure 5.1(b) shows how the periodic boundary condition used in molecular dynamic simulation simulates a colloidal suspension with multiple particles, even though there is only a single particle in the simulation domain. The simulations for varying volume concentration, varying particle size and particle wettability were run at a system temperature of 300 $°K$ and pressure of 1 *atm*, and the simulation domain size was varied with the number of water molecules to maintain a density of 1 gm/cm^3. The system was first equilibrated in the NVT ensemble for $5x10^5$ time steps. In the equilibration period the system temperature was kept constant using the velocity scaling method. After the equilibration period, the temperature constraint was removed and system was allowed to evolve in the NVE ensemble for 10^6 time steps. In this period, the heat current was calculated and the Green-Kubo correlation was used to calculate the thermal conductivity of the nanofluid system. Results of various particle size, volume

concentration, particle wettability and system temperature are presented and discussed in this chapter.
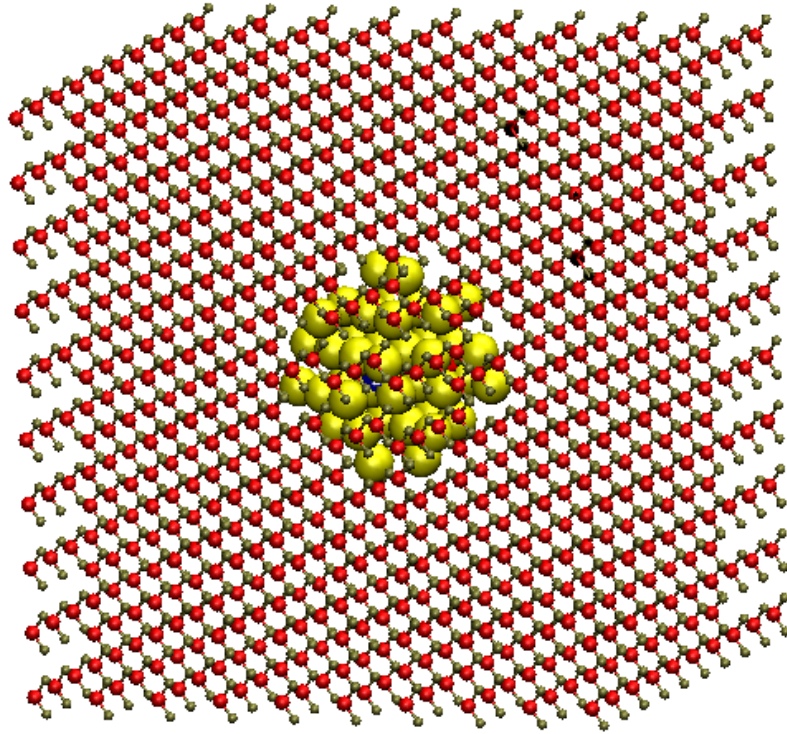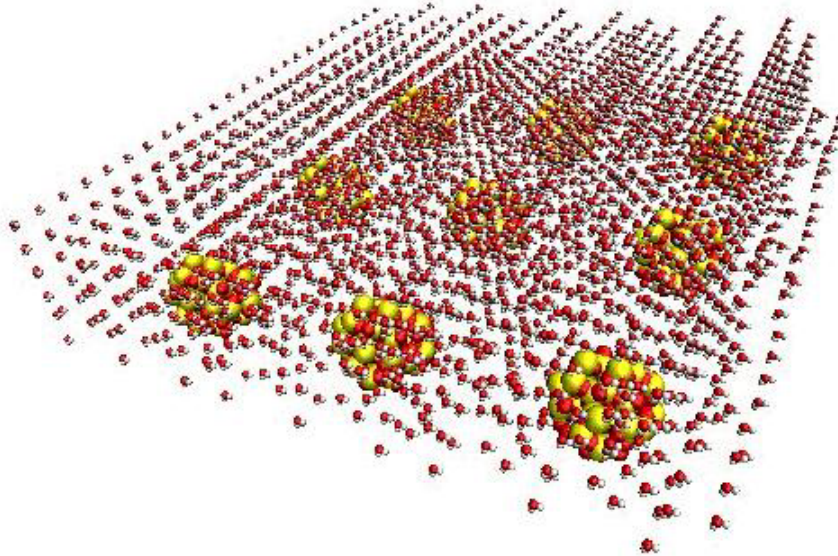
(a)

Figure 5.1: (a) Initial configuration of a 1 nm nanofluid at 1.8% volume concentration,

(b) Nanofluid system with periodic boundary condition applied in *x* and y planes

5.1. Effect of Particle Volume Fraction

The effect of nanoparticle volume fraction on the thermal conductivity of nanofluids has been studied previously in detail in the literature. Both experimental [Wang et al 1999, Eastman et al 2001, Patel et al 2003, Murshed et al 2008] as well as computational [Sarkar & Selvam 2007, Eapen et al 2007, Teng et al 2008] studies have been conducted to measure the effect of particle volume fraction on transport properties of nanofluids. Therefore, a comparison study of the thermal conductivity vs. volume concentration with the previous studies can be done for validation purposes. In the previous studies, almost a linear increase in the thermal conductivity has been observed with increasing the volume fraction of the particles. However the slope of this linear increase in thermal conductivity enhancement with increasing particle volume fraction was different in different studies [Eastman et al 2001, Xie et al 2003, Eapen et al 2007, Beck et al 2009]. This linear slope not only depends on the particle volume fraction, but also depends on the choice of the base fluid and particle type, size of the nanoparticles and also on the experimental conditions like the system temperature. As mentioned in chapter 2, thermal conductivity increase of up to 40% was observed by Eastman et al [2001] for ethylene glycol and copper nanofluid at a mere 0.3% volume concentration and increase of up to 250% was observed by Choi et al [2001] for carbon nanotube and oil nanofluid at 1% particle volume fraction. In a molecular dynamic study by Sarkar & Selvam [2007], thermal conductivity enhancement in model Ar-Cu nanofluid thermal conductivity enhancement from 14% up to 52% was observed when the particle volume fraction was increased from 0.5% to 8%. This study showed a steeper increase in thermal

conductivity for lower volume fraction of particle and a saturation behavior at higher volume fractions. Eapen et al [2007] also observed a similar behavior in their molecular dynamic study of Xe-Pt nanofluid. Once again, it needs to be pointed out that LJ potential was used for base fluid in these studies.

In this work, a nanofluid system consisting of single nanoparticle surrounded by water molecules was modeled using the molecular dynamics simulation. Number of water molecules surrounding the nanoparticle was varied to model nanofluid with varying volume concentration and to study its effect on the thermal conductivity. A system containing a 1 nm diameter particle surrounded by 316 to 1696 water molecules was studied. The volume concentration in various cases considered here varied from 1% in the lowest case to 5.1% in the highest case. Table 5.1 shows the number of water molecules and the corresponding volume concentration for 1 nm diameter particle case. System temperature of 300 °K and pressure of 1 atm. was considered in all the cases. Size of the cubic simulation domain was varied from 2.17 nm for 5.1% volume concentration to 3.73 nm for 1% volume concentration case to keep the density of water constant at 995 kg/m^3.

Thermal conductivity values for the cases considered in Table 5.1 are presented in Table 5.2 and Figure 5.2. As observed in previous studies the nanofluid thermal conductivity increases almost linearly from 0.833 W/m.K to 1.346 W/m.K as the particle volume concentration is increased from 1% to 5.1% for 1 nm particle diameter case. Thermal conductivity results for 2 nm particle diameter at varying volume concentration are presented in Table 5.3 and Figure 5.3. As observed in the 1 nm particle case, the data for 2 nm particle also shows an almost linear increase in thermal conductivity from 0.964

W/m.K to 1.588 W/m.K with increase in particle volume concentration from 3.4% to 10.5%.
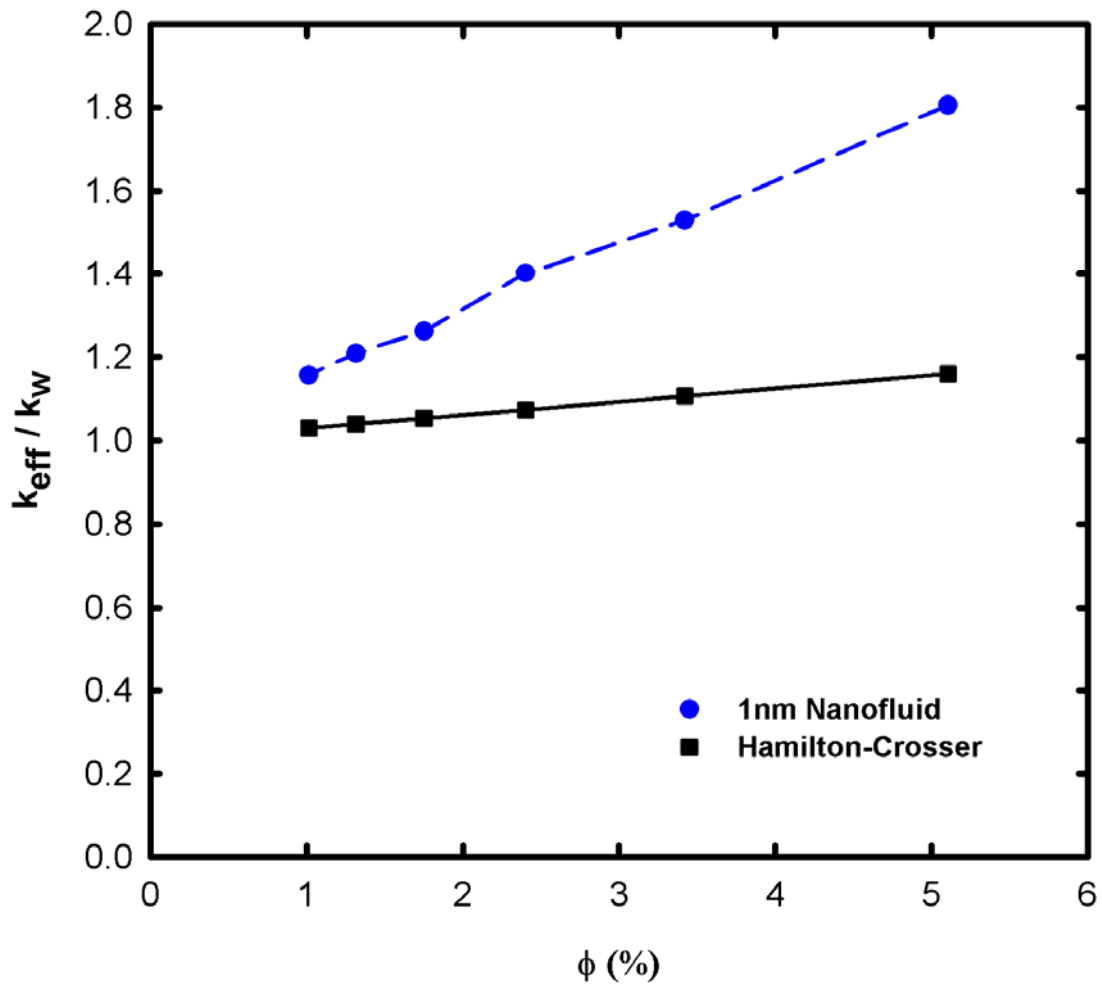
Figure 5.2: Thermal conductivity vs. volume concentration for 1 nm particle

Figure 5.3: Thermal conductivity vs. volume concentration for 2 nm particle

Table 5.1: Volume concentration of various cases considered for 1 nm nanoparticle

Number of Water Molecules	Simulation Domain Volume (*nm3*)	Volume Concentration (*%*)
316	10.25	5.1
480	15.30	3.4
702	21.79	2.4
968	29.89	1.8
1304	39.79	1.3
1696	51.65	1.0

Table 5.2: Thermal conductivity of various cases considered for 1 nm nanoparticle

Volume Concentration	Thermal Conductivity $(Wm^{-1}{}^{\circ}K^{-1})$	$k_{nanofluid}/k_{water}$	k_{HC}/k_{water}
5.1			1.16
3.4			1.11
2.4			1.07
1.8			1.05
1.3			1.04
1.0			1.03

Table 5.3: Thermal conductivity of various cases considered for 2 nm nanoparticle

Volume Concentration	Thermal Conductivity $(Wm^{-1}{}^{\circ}K^{-1})$	$k_{nanofluid}/k_{water}$	k_{HC}/k_{water}
10.5			1.35
8.1			1.26
6.4			1.20
5.1			1.16
4.2			1.13
3.4			1.11

The data presented in Table 5.2 and 5.3 qualitatively shows the same trend as observed by previous molecular dynamics studies of nanofluids [Sarkar & Selvam 2007, Eapen et al 2007]. Thermal conductivity increase is steeper for lower volume concentration (up to 2%) and a saturation behavior is observed for higher particle volume concentration (greater than 2%) where the thermal conductivity increases slowly compared to that at smaller volume concentrations. Since the nanoparticle considered in this study is a Lennard-Jones solid, the thermal conductivity data can not be quantitatively compared with any experimental study, it can only be qualitatively compared. The thermal conductivity enhancement in this study is higher compared to that reported by some experimental studies for different nanoparticles at low volume concentrations and compared to theoretical models as Maxwell model and Hamilton-Crosser model for various nanoparticles at same volume concentration, but other molecular dynamic studies [Sarkar & Selvam 2007, Eapen et al 2007, Teng et al 2008, Wen-Qiang & Qing-Mei 2008] have also observed high thermal conductivity compared to Maxwell and Hamilton-Crosser models. A discussion on possible reasons for this behavior is provided later in this chapter.

5.2. Effect of Particle Size

As mentioned in chapter 2, the effect of nanoparticle size on the thermal conductivity of nanofluid is debatable. Researchers have observed both increasing and decreasing thermal conductivity of nanofluid with increasing the nanoparticle size. To shed some light on this matter, the effect of particle size is systematically studied in this work. Nanoparticles of diameter 1 nm, 2 nm, and 3 nm were simulated at the same volume fraction, system temperature and pressure conditions. Volume fraction of 5.1% and system temperature and pressure of respectively 300 ˚K and 1 atm. were considered. The number of water molecules was varied for different nanoparticle diameters to keep the volume fraction of the nanofluid same. The results of the simulation are presented in Table 5.4 and Figure 5.4. It is observed that the nanofluid thermal conductivity decreases with increasing particle diameter. This trend of increasing thermal conductivity with decreasing particle size has been observed by researchers in the literature [Kang et al 2006, Kim et al 2007, Jang and Choi 2007, Feng et al 2007].

Figure 5.4: Thermal conductivity vs. particle size

Table 5.4: Thermal conductivity for variable particle size at 5.1% volume concentration

Particle Size (nm)	Thermal Conductivity $(Wm^{-1}°K^{-1})$	$k_{nanofluid}/k_{water}$
1.0		
2.0		
3.0		

5.3. Effect of System Temperature

Nanofluids have been termed as 'futuristic coolants' because of their enhanced transport properties. They have heat exchanger applications, including some applications at high temperature like high temperature lasers, nuclear power plants, space applications and also in automobile industry. Although the current simulation can not reach very high temperatures, the trend in the thermal conductivity can be studied with slight rising temperatures in the system. While most experimental studies have focused on measuring thermal conductivity or heat transfer coefficient of nanofluids at room temperature, some researchers have conducted experiments at elevated temperatures as well and reported contradictory trends of thermal conductivity with increasing temperature. Das et al [2003] showed a steep increase in thermal conductivity for water based Al_2O_3 and CuO nanofluids when the system temperature was increased from 295 °K to 320 °K, while Beck et al [2007] have shown a moderate increase in thermal conductivity for aqueous alumina nanofluids over a temperature range of 290 °K to 420 °K.

To study the effect of system temperature on the thermal conductivity of water based nanofluids, molecular dynamics simulations were performed for nanofluid consisting of 1 nm nanoparticle at 5.1% volume concentration for temperature ranging from 300 °K to 340 °K. As the temperature of the nanofluid is increased, the density of water decreases, or the volume increases with little change in the density or volume of the solid nanoparticle. Hence the particle volume fraction of the nanofluid suspension decreases with increase in temperature. But it was found that over the range of temperature considered in this study, the particle volume fraction changed very little. So

the volume concentration of various cases considered here are the volume concentrations of nanofluid at room temperature. The calculated thermal conductivity with varying temperature is reported in Table 5.5 and Figure 5.5 Thermal conductivity of water-only cases with varying temperature is also reported in Table 5.5 and Figure 5.6.

As seen in Figure 5.5 relatively low increase in the thermal conductivity is observed with temperature as compared to that observed by Das et al [2003]. In addition, the increase in the nanofluid thermal conductivity is almost similar to the increase in the thermal conductivity of the base fluid for the temperature range considered in this study.

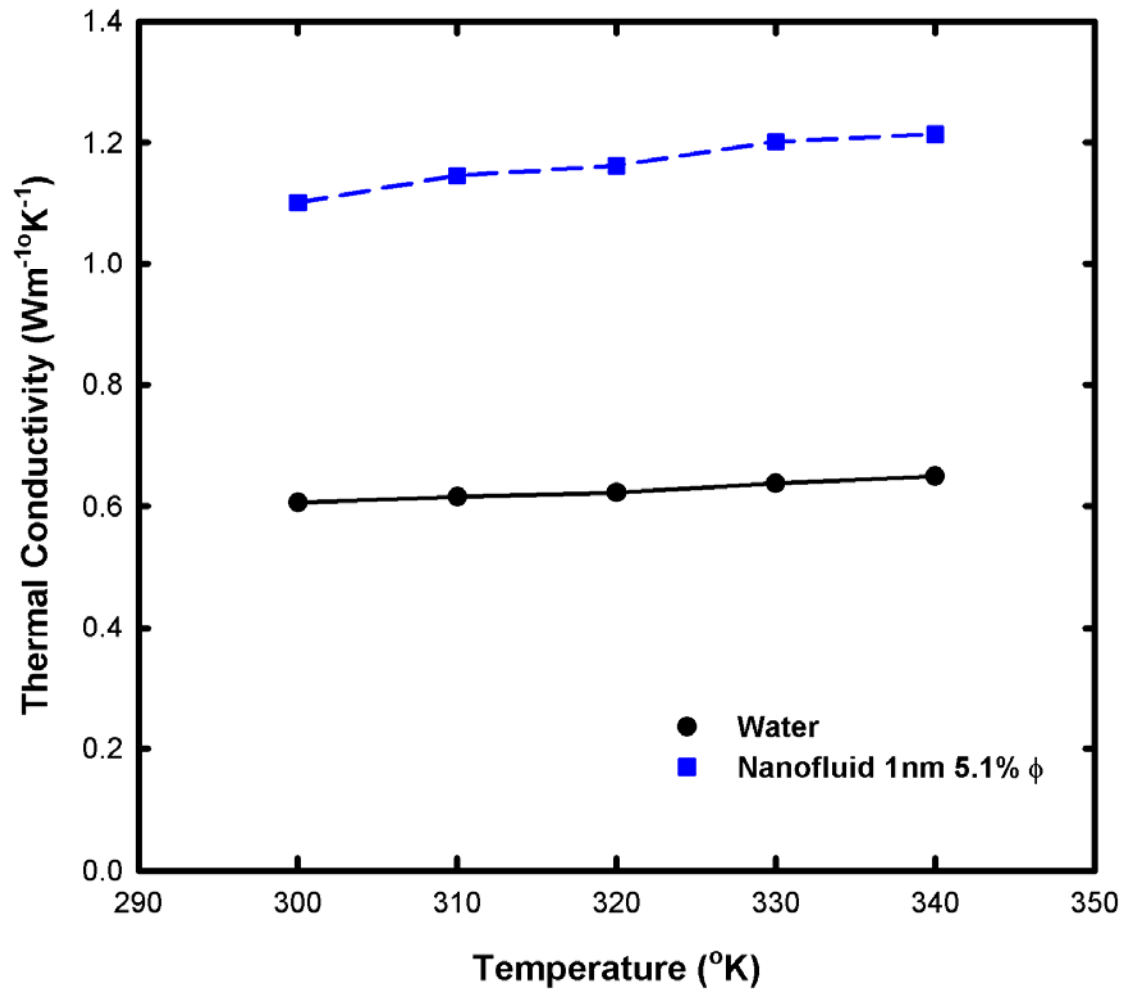Figure 5.5: Thermal conductivity vs. system temperature

Table 5.5: Thermal conductivity at various system temperatures for 1 nm particle case

System Temperature ($^{\bullet}$K)	Nanofluid Thermal Conductivity ($Wm^{-1}{}^{\circ}K^{-1}$)	Water Thermal Conductivity ($Wm^{-1}{}^{\circ}K^{-1}$)
300		0.606
310		0.615
320		0.623
330		0.638
340		0.649

5.4. Effect of Particle Wettability

Most common base fluids considered in nanofluids applications like water and ethylene glycol are polar in nature and the nanoparticles used in these nanofluids like oxides (Al_2O_3, CrO_2, SiO_2) are chemically reactive. It has been shown that these nanoparticles (especially Cerium based) may have oxygen vacancies, which can lead to oxidization in optimal conditions. It has also been reported that the pH of the nanofluid suspension affects its stability and also transport properties Xie et al [2002]. Various surfactants are added to stabilize the nanofluid suspension. The presence of surfactants in these nanofluids also makes the case that the surface chemistry could be playing an important role in nanofluids. The chemical reactions are not modeled in the current work. In order to model such interactions with classical molecular dynamics simulation, quantum molecular dynamics or other sub-atomic computations are required to simulate such reactions, which is beyond the scope of this work. However, in this work an attempt is made to study the effects of surface wettability of nanoparticle on the thermal conductivity of nanofluids. This objective is achieved by varying the strength of the attractive force between the solid and fluid atoms. The 6-12 Lennard-Jones potential is considered here as the interaction between the solid and fluid atoms. The r^{-6} term in the Lennard-Jones potential accounts for the attractive force between a pair of atoms. A modified Lennard-Jones potential as proposed by Vladkov & Barrat [2006], is used to model the solid-fluid interaction for this study. The r^{-6} term in the Lennard-Jones potential determines the attraction force between a pair of atoms. A constant 'c' is

multiplied to the r⁻⁶ term in the solid-liquid Lennard-Jones potential, as shown in equation (5.1), and varying this constant will vary the strength of solid-liquid attraction force.

$$u_{sf} = 4\varepsilon_{sf}\left[\left(\frac{\sigma}{r}\right)^{12} - c\left(\frac{\sigma}{r}\right)^{6}\right] \tag{5.1}$$

The strength of the cross-interaction between solid and liquid atoms can be varied by changing the parameter 'c' in equation 5.1. A low value of parameter 'c' would mean less attraction force between solid-liquid atoms and would model a non-wetting particle, while a high value of 'c' (>1) would mean higher attraction force between a pair of solid-liquid atoms and would model a highly wetting particle. The value of parameter 'c' is varied from 0.2 to 1.25 in this study to model a range of wetting properties. In their study, Vladkov & Barrat [2006] varied the parameter 'c' to simulate varying Kapitza resistance at the solid-liquid interface. A higher value of parameter 'c' (>1, wetting) translates to lower Kapitza resistance and a lower value (<1, non-wetting) would model higher Kapitza resistance at the solid-liquid interface. Results for various cases are reported in Table 5.6 and Figure 5.6. It is observed that the thermal conductivity increases as the parameter 'c' is increased or in other words, the thermal conductivity is higher for a wetting particle when compared to a non-wetting particle. These results are important as they show that if some functionalized particles can be produced and used in these nanofluids which could improve the wetting nature of these particles, the thermal conductivity could be enhanced further compared to standard nanoparticles.
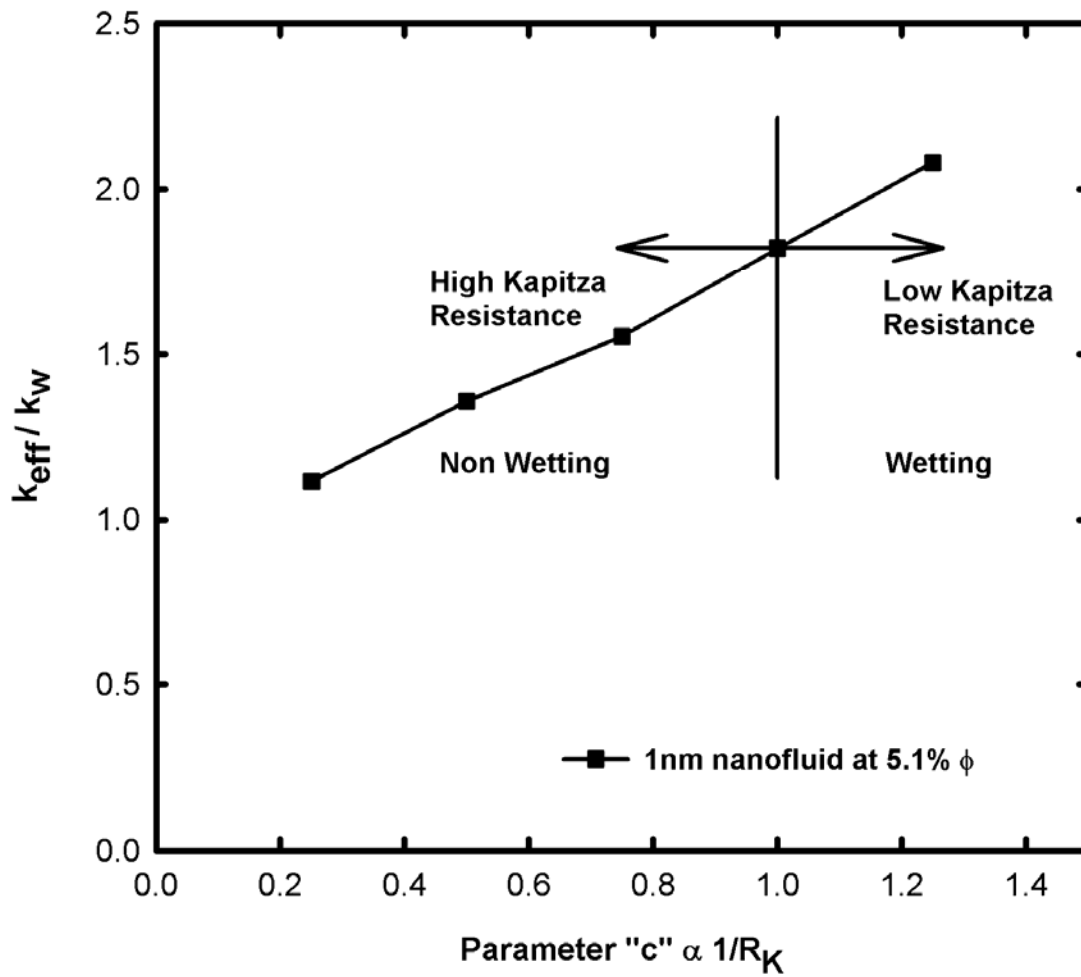
118

Figure 5.6 Thermal conductivity vs. particle wettability (increasing "c" means higher wettability)

Table 5.6: Thermal conductivity of nanofluid with varying wettability (increasing "c" means higher wettability)

Interaction Parameter (c)	Thermal Conductivity ($Wm^{-1}\,^{\circ}K^{-1}$)	$k_{nanofluid}/k_{water}$
0.20		
0.50		
1.00		
1.25		

5.5. Possible Mechanisms Enhancing Thermal Conductivity in Nanofluids

5.5.1. Hydration Layer Formation at the Solid-Liquid Interface

As discussed in chapter 2, various heat transfer mechanisms have been proposed in the past to explain the thermal conductivity enhancement in nanofluids. One of the mechanisms Keblinski et al [2002] proposed was the presence of solid like layer of liquid molecules or an ordered liquid layer around the solid nanoparticle. This layer of liquid molecules at the particle-fluid interface is also called ordered liquid layer, second layer or the hydration layer. Yu and Choi [2003] developed a modified Maxwell model for effective thermal conductivity of nanofluids. In this model, they assumed that a thin ordered layer of liquid molecules with higher thermal conductivity compared to the base fluid is present around the nanoparticle. They concluded that even a very thin liquid layer would increase the effective volume fraction in the nanofluid and subsequently enhance the thermal conductivity of nanofluid for particles smaller than 10 nm in diameter. Their work did not include an MD simulation. Leong et al [2006] also proposed a model and included the effect of an interfacial liquid layer in their model. They concluded that the liquid layer at the solid-liquid interface and nanoparticle size are the main parameters affecting the thermal conductivity of nanofluids. They used a liquid layer of 1 nm thickness in their model to explain their experimental data.

The interface between a solid and liquid or solid and solid is a study of great interest since the surface can either provide thermal barrier or thermal enhancement. The interfacial resistance, also called the Kapitza resistance, arises due to the difference in

phonon spectra between the two phases. Nanocrystalline materials with large Kapitza resistance and grain boundaries less than 40 nm can decrease the thermal conductivity and provide a thermal barrier [Eastman et al, 2006]. Quite the opposite application of enhancing thermal conductivity can be found in nanofluids. It is shown that the interfacial resistance from the collision correlation is not the limiting mechanism in nanofluids [Eapen et al 2007]. Domingues et al [2005] studied the heat transfer between two nanoparticles and reported that, as the two nanoparticles are brought closer, the heat transfer between them is found to be 2 to 3 orders of magnitude more efficient, before mechanical contact, than when the two nanoparticles are in contact. This means that the Kapitza resistance between the two nanoparticles before mechanical contact is expected to be order of magnitude lower as the inter-particle distance becomes smaller. They concluded that the traditional theories are no longer valid at these length scales. As shown in this work, when nanoparticles are suspended in water, a hydration layer is formed around each particle. When there is a strong interaction between the solid and liquid atoms at the interface, the Kapitza resistance is lower. The hydration layer scatters the incoming and the outgoing phonons, and influences the interface characteristics, and increases the nanofluid thermal conductivity. The strong cluster-fluid interaction creates a dynamic interface around the nanoparticle that facilitates the exchange of energy between solid and liquid atoms.

The presence of a liquid layer can not be examined easily by an experimental study. With the advancement of technology, it is possible to look at individual nanoparticles using Transmission Electron Microscopy (TEM) or Scanning Electron Microscopy (SEM), but only a small sample of the nanofluid can be put under the

scanner in a TEM or SEM. The presence of a liquid layer can only be postulated in experiments but it can not be confirmed. However in a molecular dynamic simulation all the details of the atomic trajectory can be captured. The position and velocities of liquid and solid atoms are recorded at every step. To check the presence of the liquid layer around the solid nanoparticle, the density distribution of liquid atoms around the nanoparticle can be examined using the trajectory data. Using the recorded positions of liquid and solid atoms during the simulation, the number of liquid molecules can be counted in a specified space around the nanoparticle in the simulation domain. So the simulation domain is divided in to multiple concentric spherical shells around the nanoparticle, as shown in Figure 5.7 [Teng et al, 2008], and the number density of liquid molecules is calculated in these spherical shells.

The number density is defined as number of atoms per unit volume.

$$n = \frac{\Delta n}{\Delta V} \qquad (5.2)$$

Here, Δn is the number of atoms in a specified volume ΔV. In this case the volume ΔV is the volume of each concentric spherical shell of thickness Δr_i as shown in Figure 5.7. The number of liquid molecules in each of these shells is counted at different time intervals to calculate the number density. Figure 5.8 shows the distribution of relative number density of liquid molecules around the nanoparticle at various times. Relative number density $\frac{n}{n_o}$ is defined as the number density of liquid molecules in the nanofluid at some time (t) during the simulation (n), divided by the number density of liquid (n_o) at time zero. It is observed from Figure 5.8 that the density of water is high near the surface of the nanoparticle and it decreases as the distance from the nanoparticle

surface increases. This observation confirms the presence of the interfacial liquid layer as postulated by researchers in the literature. It is also observed from Figure 5.8 that the thickness of the ordered liquid layer is about 0.5 nm, which is consistent with observation made by Li et al [2008]. They conducted an MD study and used the LJ potential to simulate interactions between all atom pairs of a model nanofluid system. They used the Lennard-Jones parameters of argon for liquid and copper for solid atoms. They did not report any quantitative results for thermal conductivity enhancement but showed the presence of a layer of liquid molecules at the solid-liquid interface of the order of 0.5 nanometer.

By tracking the movement of liquid atoms around the nanoparticle, the presence of a liquid layer at the solid-liquid interface is confirmed. This liquid layer is formed because of the stronger interatomic force between the solid-liquid atoms as compared to the interatomic force between the liquid atoms. This finding is important in understanding the heat transfer mechanisms in nanofluids. This finding confirms the contribution of ordered liquid layer to the enhancement of thermal conductivity as proposed by Jang and Choi [2004], "thermal interaction of nanoparticle with base fluid", and by Ren et al [2005], "enhancement by nanolayer" and by Keblinski et al [2002], "liquid layering at liquid-particle interface".
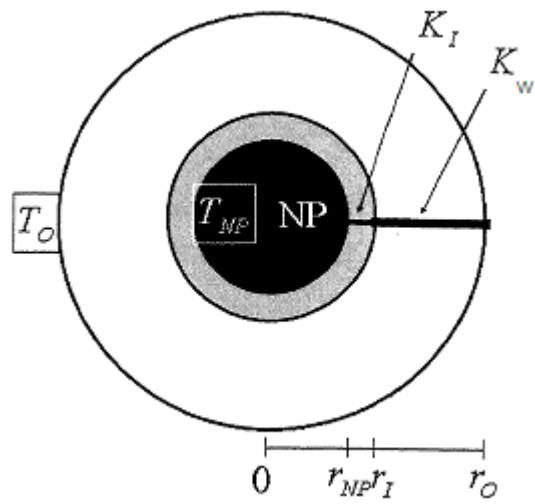
Figure 5.7 Spherical shells around the solid nanoparticle (NP) to plot density distribution
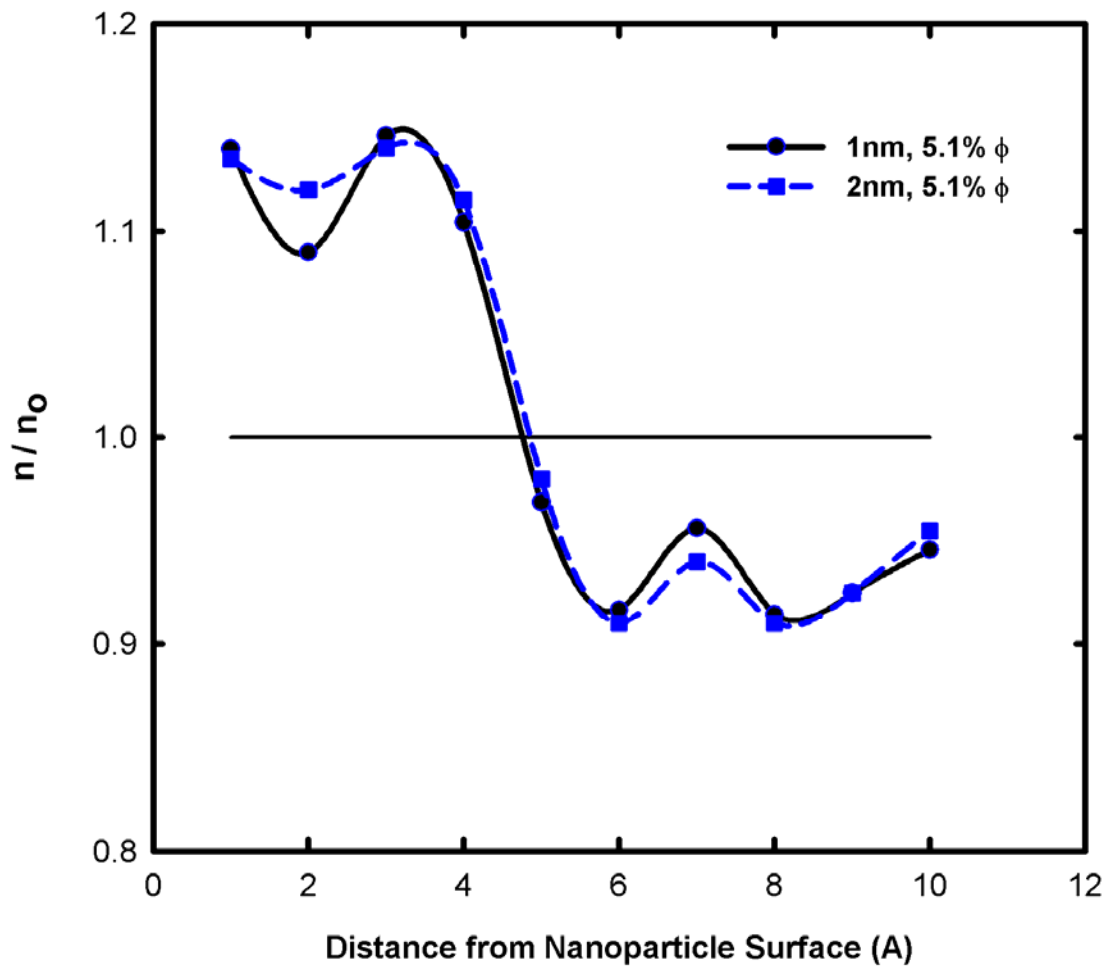
[Teng et al, 2008]

Figure 5.8: Relative number density distribution around the nanoparticle as a function of distance from the nanoparticle surface

5.5.2. Mean Square Displacement (MSD)

In this section another mechanism causing the thermal conductivity enhancement in nanofluids is discussed. As stated in previous section movement of all the liquid and solid atoms in the simulation domain can be easily tracked in molecular dynamics simulation. The movement and interaction of these atoms and molecules at atomic scale is the cause of all macro-scale properties of any material, including the enhanced thermal conductivity of nanofluids. By using the atomic position data at various time steps the mean square displacement (MSD) can be calculated for the liquid and solid molecules. Comparison of the MSD of liquid molecules in the base fluid and in the nanofluid at varying volume concentration can give an insight into the thermal transport mechanism in nanofluids. The MSD is a measure of the distance travelled by an atom or a molecule. It is defined as:

$$MSD(t) = \left\langle \Delta \vec{r_i}(t)^2 \right\rangle = \left\langle \left(\vec{r_i}(t) - \vec{r_i}(0) \right)^2 \right\rangle \qquad (5.3)$$

Here, $\vec{r_i}(t)$ is the position of atom i at time t, and $\left(\vec{r_i}(t) - \vec{r_i}(0) \right)$ is the vector distance traveled by an atom i, over a time interval t. The angular brackets $\langle \ \rangle$ mean average over all atoms. The square of the displacement undergone by all N atoms is averaged to give the mean value. So the above equation gives the mean square displacement of all the molecules in the fluid over a time period t. The angular bracket is also known as 'ensemble average'. To get the MSD of liquid molecules in the nanofluid only the displacement of liquid molecules is considered in the above equation.

Each molecular dynamics simulation is started with a set of initial velocities and positions for all the atoms or molecules involved in the simulation. As the simulation evolves these atoms and molecules "collide" or interact with each other and move around in the simulation domain. The MSD gives an estimate of the "collisions" suffered by atoms in the simulation.

In this study MSD of liquid atoms in nanofluid at various concentrations was calculated and compared with the MSD of the base fluid. MSD of base fluid, water and of liquid atoms in 1%, 3.5% and 5.1% nanofluids is shown in Figure 5.9. MSD of liquid molecules in the 1% nanofluid was approximately 1.1 times higher compared to the MSD of the base fluid. MSD of liquid atoms in nanofluid at various volume concentrations is consistently higher compared to the base fluid. It is observed from Figure 5.9, that the MSD increase is higher for the nanofluid with larger particle volume concentration.
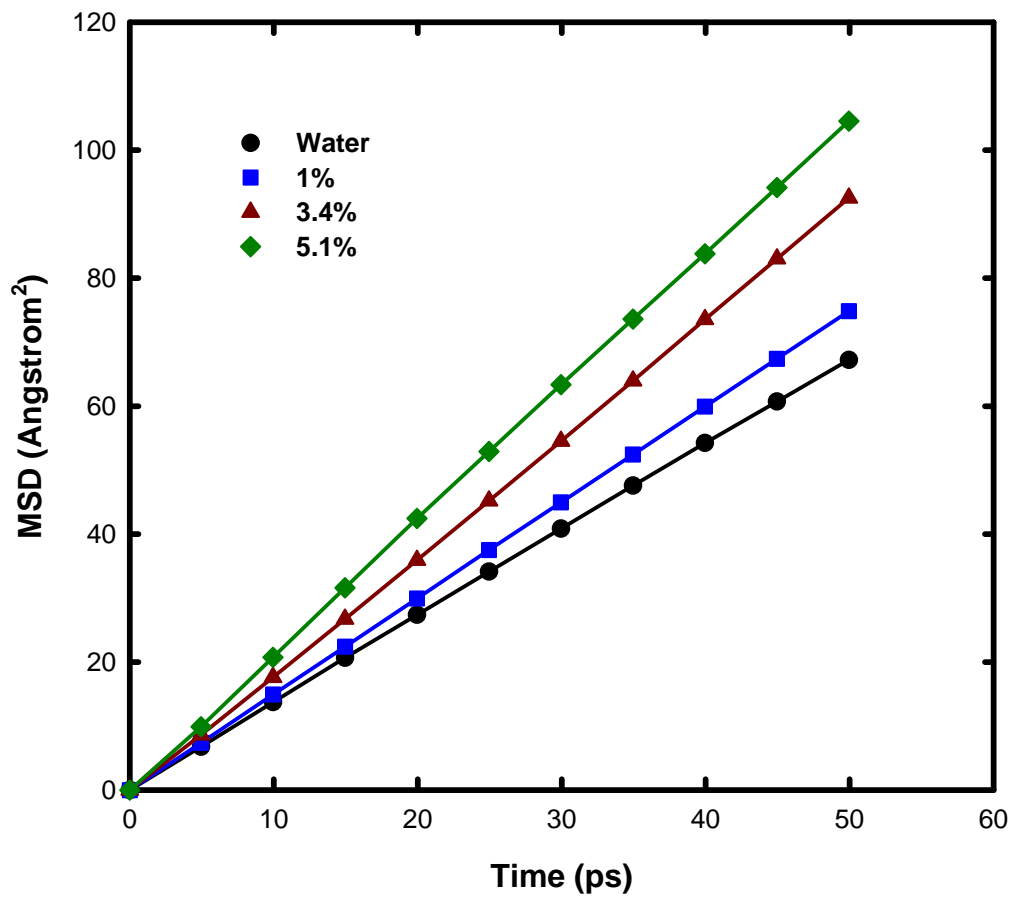
Figure 5.9: Mean square displacement at various volume concentrations for 1 nm
nanofluid

In dilute gases, the intermolecular forces play no role and the mean free path is larger, so the molecules spend most of their time in free flight between brief collisions when their direction and speed changes. Thus, random molecular motions are responsible for the gaseous transport process. In liquids, however, mean free path is smaller and the molecules are closely packed and are in a collision state. These frequent collisions between liquid molecules are responsible for thermal transport in liquids. The comparison of MSD for various nanofluids as observed in Figure 5.9, shows that there is significant increase in the movement and hence the displacement of the liquid molecules due to the presence of solid nanoparticles. This enhanced movement will eventually mean that the liquid molecules undergo more frequent "collisions" and hence transport more energy. This is accentuated by the fact that there are additional liquid molecules close to the nanoparticle in the form of hydration layer. Since these liquid molecules are more closely packed than other liquid molecules away from the particle, the attraction or cohesive potential between the liquid molecules are dominant. The increased movement of liquid molecules in the hydration layer close to the nanoparticle, as well as away from the nanoparticle is due to the interatomic interaction between the solid and liquid atoms, which is much stronger compared to the interatomic potential between the liquid atoms. This enhanced motion of water molecules combined with the hydration layer around the nanoparticle can significantly enhance the thermal conductivity of nanofluids.

5.5.3. Diffusion Coefficient

Various transport coefficients can be calculated using the equilibrium correlations on the position, velocity and force data generated from molecular dynamics simulations. The Einstein's relation [Rapaport, 2004] can be used to calculate the diffusion coefficient (D) from the MSD data. The self-diffusion coefficient is given as:

$$\lim_{t \to \infty} \frac{\left\langle \Delta \vec{r_i}(t)^2 \right\rangle}{3t} = 2D \tag{5.4}$$

The limiting slope of MSD for large time gives the self-diffusion coefficient from above expression. Using equation 5.4 the diffusion coefficient of the base fluid, and liquid molecules in nanofluid is calculated for various volume concentrations. The diffusion coefficient of water was found to be $0.224 \, \overset{o}{\mathrm{A}}^2/ps$. The experimental value of the diffusion coefficient of water is $0.24 \, \overset{o}{\mathrm{A}}^2/ps$. So our molecular dynamic simulation reasonably predicts the diffusion coefficient of pure water. The diffusion coefficient of 1%, 3.4% and 5.1% volume concentration nanofluid cases were also calculated and compared with the diffusion coefficient of pure water. The diffusion coefficient results for various cases considered are presented in Table 5.7. Figure 5.10 shows the ratio of the diffusion coefficient of liquid in nanofluid (D_{eff}) to the diffusion coefficient of pure water (D) for various volume concentrations of nanofluids. It is observed that diffusion coefficient of nanofluid increases almost linearly with increasing particle concentration. This finding is consistent with the results reported by Sarkar and Selvam [2007] for a model Ar-Cu nanofluid system. Comparing Figure 5.10 diffusion coefficient with thermal

conductivity, it is seen that both diffusion coefficient and thermal conductivity increase almost linearly with increasing volume fraction of nanofluid. This shows a strong correlation between the thermal conductivity and diffusion coefficient enhancement. The diffusion coefficient in nanofluid is calculated from the MSD, which shows that the increase in diffusion coefficient with increasing volume concentration is because of the enhanced motion of liquid molecules due to the presence of solid nanoparticle. So this enhanced motion of liquid molecules in the hydration layer is responsible for the enhanced thermal conductivity of nanofluids.

Figure 5.10: Relative diffusion coefficient at various concentrations for 1 nm nanofluid

Table 5.7: Diffusion coefficient at various concentrations for 1 nm nanofluid

Volume Concentration (%)	Diffusion Coefficient (*Angstrom2/ps*)	$D_{nanofluid}/D_{water}$
0.0	0.224	1.00
1.0	0.249	1.11
3.4	0.308	1.38
5.1	0.348	1.55

5.5.4. Heat Current Autocorrelation Function (HCAF) Decomposition

The thermal conductivity of nanofluids in this work is calculated using the Green-Kubo correlation of the heat current. In the linear response region, various transport properties e.g. thermal conductivity, viscosity and diffusion coefficient etc can be calculated using the time correlation. The thermal conductivity is calculated using the time integral of the HCAF as given by equation 3.21. $\vec{q}$ is the instantaneous heat flux vector as given by equation 3.24. Eapen et al [2007] while studying the dominating heat conduction mechanisms in nanofluids decomposed the heat flux vector in its three constituents, namely (1) kinetic, (2) potential, and (3) collision. The total heat flux can be written as sum of 3 terms as given below:

$$\vec{q} = \vec{q}_K + \vec{q}_P + \vec{q}_C \tag{5.5}$$

This decomposition can also be looked at as sum of convective and inter-atomic terms as proposed by Teng et al [2008]. First two terms in equation 5.5 denote the energy transported due to the convective effect and the third term is the energy transport due to the inter-atomic collisions of atoms and molecules in the system. Thermal conductivity for various volume concentrations of 1 nm particle were calculated using this decomposed form of the heat flux vector to compare the contributions to the thermal conductivity of nanofluid from kinetic, potential and collisions mechanisms.

Figure 5.11 shows the variation of overall nanofluid thermal conductivity and the contribution to overall conductivity from each of these modes. It is observed that most of the thermal conductivity comes from the collision mode in pure water. The collision

mode which arises from the inter-atomic interactions between the atoms and molecules is also dominant in the thermal conductivity of the nanofluid. This observation is consistent with the observations made by Eapen et al [2007] in their molecular dynamics study of the Xe-Pt model nanofluid. Another important observation from Figure 5.11 is that the increase in thermal conductivity with increasing volume fraction of the nanoparticle mainly comes from the same collision mode. This observation is in contrast to what was observed by Eapen et al [2007] that the increase in thermal conductivity with increasing volume fraction comes from the potential mode as opposed to the collision mode. Their work did not include any hydration layer around the particle. Their MD simulation consisted of nanoparticles that had 10 atoms and were less than 1 nm in size. In the decomposition analysis of the heat current, they reported that the potential energy increase due to the solid-liquid interaction caused the nanofluid thermal conductivity enhancement. They said the solid-liquid interaction caused the exchange of energy between the solid and liquid atoms, however it was not clear how this exchange was taking place. Sarkar & Selvam [2007] reported an increase in MSD and diffusion coefficient due to the presence of the nanoparticle. But they too did not consider the hydration layer formation.
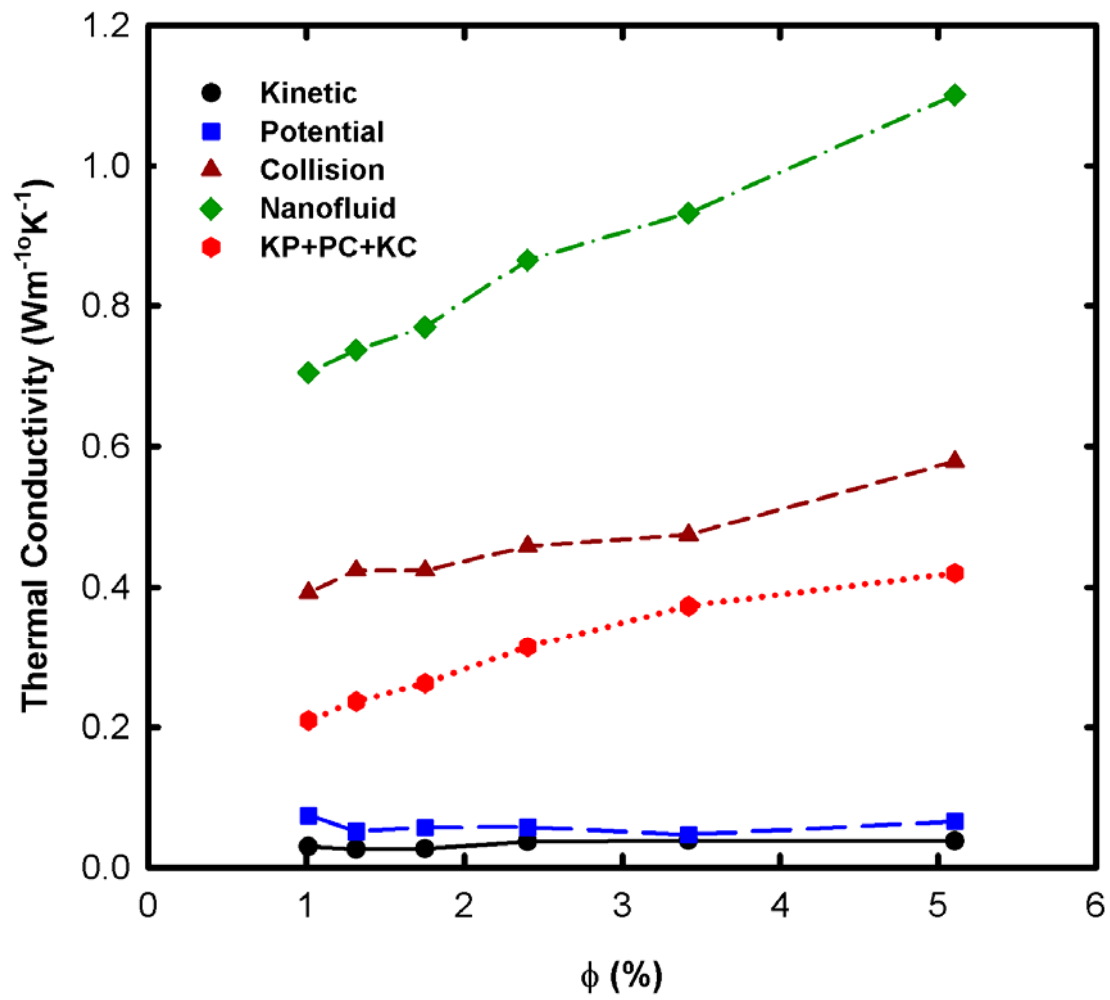
Figure 5.11: Thermal conductivity contribution by various heat current modes

5.5.5. Strong Particle-Fluid Interaction

In the previous sections, it was shown that the presence of nanoparticles in water affects the motion of the water molecules and a hydration layer of water molecules is formed around the nanoparticle. These two phenomena occur due to the strong particle-fluid interaction present in the nanofluid. The effect of the strength of this particle-fluid interaction on the thermal conductivity of nanofluid was shown in section 5.4. The strength of solid-liquid interaction was modified by using an interaction coefficient "c" in the modified Lennard-Jones potential. It was observed that the thermal conductivity of the nanofluid increases with increasing the value of the interaction coefficient "c", which translates to increasing the attractive force between the solid-liquid atoms. It has been shown by Vladkov and Barrat [2008] that a low value of this interaction coefficient means a higher interfacial resistance, also called Kapitza resistance. So our results show that a lower value of interfacial resistance would lead to higher thermal conductivity in nanofluids.

These results show that if functionalized nanoparticles can be produced that are hydrophilic in nature, this could further enhance the thermal conductivity of nanofluids compared to normal nanoparticles. This fact also brings to light the importance of stabilizers used in nanofluids. Various surfactants are used to stabilize these nanofluids and other methods like modifying the pH of the suspension are also used to improve the stability of the nanofluids. The surfactants are long chain like molecules that attach themselves to the surface of the nanoparticle and deter them from agglomerating with each other and settling down with time. So these surfactants molecules cause the

nanoparticle to repel each other. If a surfactant used to stabilize the nanoparticles in a nanofluid causes the nanoparticles to have weaker interaction with the fluid atoms, it can lead to a lower thermal conductivity of the nanofluid. This means that a water-alumina nanofluid of same volume concentration and same original nanoparticle size can have different transport properties if the surfactant used in these suspensions affect the particle-fluid interaction in different ways. Some of the surfactants used by companies that manufacture nanofluids are proprietary and details of these surfactants are not disclosed to the buyer. So what effect these unknown surfactants might have on the transport properties of nanofluids is debatable.

CHAPTER SIX: SUMMARY & FUTURE WORK

In the development of energy efficient heat transfer fluids, required for the cooling applications in many industries, the low thermal conductivity of conventional fluids is a primary limitation. Nanofluids consisting of nanometer size solid particles dispersed in base fluids, have demonstrated great potential in improving the heat transfer characteristics of liquids. Even though research has been done in the area of nanofluids in the past decade, it is still an immature research field. The limitation hindering the use of nanofluids in mainstream cooling applications is the lack of understanding of thermal enhancement of nanofluids in single-phase stationary or flowing situations or in two-phase boiling condition. Before these nanofluids could be used in engineering applications, it is of paramount importance to reliably measure and/or predict the thermal conductivity and viscosity of various nanofluid systems as a function of particle volume fraction, size and system temperature. Significant research work has been conducted in measuring thermal conductivity of nanofluids, with inconclusive results. Although the potential for the use of nanofluids in heat transfer applications is promising, a major stumbling block hindering the development of this field is that, a detailed atomic-level understanding of the mechanisms responsible for the thermal transport enhancement remains elusive.

A systematic study using computer simulation is required to determine the cause of thermal conductivity enhancement and explore these mechanisms at nanoscale. Due to the length scale involved in nanofluids conventional macroscale computational techniques like CFD and FED can not be used here. We believe that modeling of

nanofluids at atomic scale using molecular dynamics (MD) simulation can provide valuable insights in understanding the origins of enhancement of various transport properties in nanofluids. With molecular dynamic simulation we can examine the interplay between solid and liquid atoms occurring at molecular level, which determines the macroscale transport properties.

In this work a molecular dynamic simulation tool is developed to study possible mechanisms causing the thermal conductivity enhancement in water based nanofluids. Previous studies involving MD simulation of nanofluids have considered simplistic Lennard-Jones (LJ) potential to model the interactions between both solid and liquid atoms. In this work, liquid water is modeled as a flexible bipolar molecule using the Flexible 3 Center (F3C) model. Since the complex surface chemical reactions between the solid nanoparticle and fluid atoms have not yet been identified by experiments and expensive quantum-chemistry based simulations are required to identify them, a simple two body LJ potential is used to model the solid nanoparticle. In addition, each atom in the nanoparticle is connected to its first neighbors by finite extensible nonlinear elastic (FENE) bonding potential. The thermal conductivity is calculated by combining the linear response theory with molecular dynamic simulation (Green-Kubo formulation). The molecular dynamic tool is validated for liquid argon and water only systems and an excellent match is found between thermal conductivity calculated from this tool and between the experimental measurements. To date this work is the first to use a realistic potential to model the liquid (water) molecules using molecular dynamic simulation.

A systematic investigation involving particle volume fraction, size, wettability and system temperature is undertaken using molecular dynamic simulation and the effect

141

of these parameters on the thermal conductivity of nanofluids is studied. The various atomic interactions show that there exist two regimes of thermal conductivity enhancement with particle volume fraction, which has also been previously observed in the literature. It is also found that increasing particle size decreases thermal conductivity enhancement, which is consistent with the previous studies. In contrast to previous studies, it is observed that increasing system temperature does not enhance the system thermal conductivity significantly. The temperature dependence in the nanofluid arises mostly from the temperature dependence of the base fluid. It is also seen that increasing the wettability of nanoparticle causes an increase in thermal conductivity enhancement. These findings show that the surface interactions between solid-liquid atoms are very important and functional nanoparticles which are hydrophilic in nature would show higher enhancement in thermal conductivity compared to regular nanoparticles.

By tracking the motion of solid and liquid molecules we show that a hydration layer is formed at the particle-fluid interface. It is also observed that the motion of liquid molecules is enhanced due to the presence of solid particles, which was captured by comparing the mean square displacement (MSD) of liquid molecules in nanofluid to that of the MSD of base fluid. The microscopic heat flux vector is decomposed into three modes, namely kinetic, potential and collision. It is observed that the significant enhancement comes from the collision mode, which arises from the enhanced motion of the liquid molecules. The dense hydration layer at the solid-liquid interface and the enhanced motion of the liquid molecules also create a possibility of cooperative or coherent exchange of thermal transport between the solid and liquid molecules, which enhances the nanofluid thermal conductivity.

1.1 Future Work

This thesis advances the atomic level understanding of mechanisms causing thermal conductivity enhancement in nanofluids using molecular dynamics simulation. A realistic flexible bipolar water molecule was used to model the base fluid in this work. However, in complex chemical reactions between the nanoparticle and liquid molecules in the presence of chemical dispersant was not considered in this work. Experimental and quantum molecular dynamic studies are needed to first identify these chemical reactions and to develop appropriate potentials to model them using molecular dynamic simulation. In this work a Lennard-Jones potential with FENE bonding potential was used to model the solid nanoparticle, which would closely mimic the behavior of a non-metallic nanoparticle. A general water based nanofluid system was studied in this work. To predict the thermal conductivity enhancement of a specific nanofluid system, more sophisticated potentials could be used, e.g. to model metallic nanoparticles, embedded atom method (EAM) potential which can also take care of the metallic bonding should be used. To get most quantitatively accurate results for a particular metal, EAM potential with appropriate parameters for that material should be used.

In addition, various experimental studies have cited nanoparticle agglomeration as an important mechanism causing the thermal conductivity enhancement in nanofluids. In future molecular dynamic studies, the effect of nanoparticle agglomeration on thermal conductivity enhancement should be studied. But, in order to model the nanoparticle agglomeration, a reliable particle-particle interaction potential needs to be established. Experimental work involving the surface chemistry of nanoparticles is required to understand the particle-particle interaction in nanofluids.

Although several research articles have appeared on the measurements of various properties of nanofluids in a static environment, not much has been reported on the measurement of heat transfer coefficient of nanofluids in a flowing situation. In any engineering application, the nanofluids would be used in a forced convection situation, so it is important to measure the transport properties of nanofluids in those conditions. It has not been reported how various properties of nanofluids change with time. With time, some of the nanoparticles could agglomerate or settle down in the channel and this could affect the effectiveness of nanofluids. The effect of time and forced flow will remain an active area for future research in nanofluids.

LIST OF REFERENCES

Ahuja A.S., J. Appl. Phys. 46(8), 3408 (1975)

Alder B. J. and Wainwright T. E., J. Chem. Phys. 31 (2), 459 (1959)

Allen M.P. and Tildesley D.J., Computer Simulation of Liquids, Oxford, Oxford Science
Publications (1987)

Assael, M.J., Metaxa I.N., Kakosimos K., and Constantinou D., Intl. J. Thermophysics,
27(4), 999 (2006)

Beck M.P., Sun T. and Teja A., Fluid Phase Equilibria 260(2), 275 (2007)

Beck M.P., Yuan Y., Warrier P. and Teja A., J. Nanopart. Res. 11(5), 1129 (2009)

Berber S., Kwon Y. K.and Tomanek D., Phys. Rev. Lett. 84(20), 4613 (2000)

Berendsen H.J.C., Postma J.P.M, van Gunsteren W.F., and Hermans J., Intermolecular
Forces, Pullman B., Ed., Reidel, Dordrecht, 331, (1981)

Berendsen H.J.C., Grigera J.R. and Straatsma T.P., J. Phy. Chem. 91, 6269 (1987)

Bertolini D. and Tani A., Phys. Rev. E. 56, 4135 (1997)

Bhattacharya P., Saha S.K., Yadav A., Phelan P.E. and Prasher R.S., J. Appl. Phys. 95,
6492 (2004).

Che J., Cagin T., Deng W., and Goddard W.A., J. Chem. Phys. 113(16) 6888 (2000)

Choi S.U.S., Development and Applications of Non-Newtonian Flows, ASME, FED-Vol.
231/MD-Vol. 66, 99-103 (1995)

Choi S.U.S., Zhang Z.G., Yu W., Lockwood F.E., and Grulke E.A., Appl. Phys. Lett.
79(14), 2252 (2001).

Choi S.U.S., Zhang Z.G. and Keblinski P., Nanofluids, Encyclopedia of Nanoscience and Nanotechnology, 6, 757 (2004)

Chon, C.H., K.D. Kihm, S.P. Lee, and S.U.S. Choi, Appl. Phys. Lett. 87(15), 153107 (2005)

Clarke J.H.R., Smith W., and Woodcock L. V., J. Chem. Phys. 84, 2290 (1984).

Das S.K., Putra N., Thiesen P., and Roetzel W., J. Heat Transfer 125, 567 (2003).

Demontis P., Spann S. and Suffritti G.B., J. Chem. Phys. 114, 7980 (2001)

Eapen J., Li J. and Yip S., Phys. Rev. Lett. 98(2), 028302 (2007)

Eastman J.A., Choi S.U.S., Li S., Soyez G., Thompson L.J., and Di Melfi R.J., Mater. Sci. Forum 312-314, 629 (1999)

Eastman J.A., Choi S.U.S., Li S., Yu W., and Thompson L.J., Appl. Phys. Lett. 78, 718 (2001)

Eastman J.A., Philpot S.R., Choi S.U.S. and Keblinski P, Annu. Rev. Mater. Res. 34, 219 (2004)

Eastman J.A., Yang H.S., Thompson L.J. and Bai G.R. http://chemistry.anl.gov/MSDReview/Complex_Oxides/KapitzaYSZ.pdf (2006)

Evans W., Fish J. and Keblinski P., Appl. Phys. Lett. 88, 093116 (2006)

Evjen H.M., Phys. Rev. 39, 675 (1932)

Florain M., J. Chem. Phys. 106, 6082 (1997)

Gupta A., and Kumar R., Appl. Phys. Lett. 91, 223102 (2007)

Haile J. M., Molecular Dynamics Simulation, New York, John Wiley & Sons (1997)

Hamilton R.L. and Crosser O.K., I&EC Fundamentals 1(3), 187 (1962)

Hoheisel C., Theoretical Treatment of Liquids and Mixtures, Elsevier Publishing
Company (1987)

Hong T., Yang H. and Choi C.J., J. Appl. Phys. 97(6), 064311 (2005)

Hwang, Y.J., Ahn Y.C., Shin H.S., Lee C.G., Kim G.T., Park H.S., and Lee J.K., Curr.
Appl. Phys. 6(6), 1068 (2006)

Hwang, Y., Lee J.K., Lee C.H., Jung Y.M., Cheong S.I., Lee C.G., Ku B.C., and Jang
S.P., Thermochimica Acta, 455(1), 70 (2007)

Jana, S., Salehi-Khojin A., and Zhong W.H., Thermochimica Acta, 462(1), 45 (2007)

Jang S.P. and Choi S.U.S., Appl. Phys. Lett. 84, 4316 (2004)

Kaburaki H., Li J., and Yip S., Mater. Res. Soc. Symp. Proc. 538, 503 (1999)

Kang, H.U., Kim S.H., and Oh J.M., Expt. Heat Transfer, 19(3), 181 (2006)

Kapitza P.L., J. Phys. USSR 4:181, Zh. Eksp. Teor. Fiz. 11, 1 (1941)

Keblinski P., Philpot S.R., Choi S.U.S. and Eastman J.A., Int. J. Heat & Mass Transfer
45, 855 (2002)

Keblinski P., Prasher R. and Eapen J., J. Nanopart. Res., 10(7), 1089 (2008)

Kim P., Shi L., Majumdar A. and McEuen P.L., Phys. Rev. Lett. 87, 215502 (2001)

Kim, S.H., Choi S.R., and Kim D., J. Heat Transfer 129(3), 298 (2007)

Kumar, D.H., Patel H.E., Kumar V.R.R., Sundararajan T., Pradeep T., and Das S.K.,
Phys. Rev. Lett. 93(14), 144301 (2004)

Lee S., Choi S.U.S, Li S. and. Eastman J.A, Trans. ASME J. Heat Transfer 121, 280,
(1999)

Lennard-Jones J.E., Proceedings of the Royal Society (London) 106A, 441 (1924)

Leong K.C, Yang C. and Murshed S.M.S., J. Nanopart. Res. 8(2), 245 (2006)

Levitt M., Hirshberg M., Sharon R., Laidig K.E. and Daggett V., J. Phys. Chem. B 101 (25), 5051 (1997)

Li, C.H. and G.P. Peterson, J. Appl. Phys. 101(4), 044312 (2007)

Li L., Zhang Y., Ma H. and Yang M., Phys. Lett. A 372, 4541 (2008)

Liu K.V., Choi S.U.S. and Kasza K.E., Argonne National Laboratory Report, ANL-88-15, (1988)

Liu, M.S., Lin M.C.C., Tsai C.Y., and Wang C.C., Intl. J. of Heat Mass Transfer, 49(17), 3028 (2006)

Lu W. and Fan Q., Engineering Analysis with Boundary Elements, 32(4), 288 (2008)

Masuda H., Ebata A., Teramae K., and Hishinuma N., Netsu Bussei (Japan) 4, 227 (1993)

Maxwell J.C., A treatise on electricity and magnetism, II ed., Vol. 1, Clarendon press, Oxford, U.K., 435, (1881)

McGaughey A.J.H. and Kaviany M., Int. J. Heat and Mass Transfer 47, 1799 (2004)

McQuarrie, D.A., Statistical Mechanics, 2nd ed., University Science Books, California, (2000)

Murshed S.M.S., Leong K.C. and Yang C., Int. J. Therm. Sci. 44(4), 367, (2005)

Murshed S.M.S., Leong K.C. and Yang C., J. Phys. D: Appl. Phys. 39(24), 5316, (2006)

Murshed S.M.S., Leong K.C. and Yang C., Int. J. Therm. Sci. 47(5), 560, (2008)

Müller-Plathe, F. J. Chem. Phys. 106, 6082 (1997)

Patel H.E., Das S.K., Sundarajan T., Nair A.S., George B. and Pradeep T., Appl. Phys. Lett. 83 (14), 2931 (2003)

Prasher R., Bhattacharya P. and Phelan P.E., Phys. Rev. Lett. 94(2), 025901 (2005)

Putnam, S.A., Cahill D.G., Braun P.V., Ge Z.B., and Shimmin R.G., J. Appl. Phys. 99(8), 084308 (2006)

Rahman A., Phys, Rev. Lett. 136, A405, (1964)

Rapaport D. C., The Art of Molecular Dynamics Simulation – 2nd ed., Cambridge, UK, Cambridge University Press (2004)

Ren Y., Xie H. and Cai A., J. Phys. D: Appl. Phys. 38, 3958 (2005)

Sarkar S. and Selvam R.P., J. Appl. Phys. 102, 074302 (2007)

Smith G.D., http://www.mse.utah.edu/~gdsmith/tutorials/tutorial1.ppt (1999)

Teng K.L., Hsiao P.Y., Hung S.W., Chieng C.C., Liu M.S. and Lu M.C., J. Nanosci. Nanotechnol. 8(7), 3710 (2008)

Timofeeva, E.V., Gavrilov A.N., McCloskey J.M., Tolmachev Y.V., Sprunt S., Lopatina L.M., and Selinger J.V. Phys. Rev. E 76(6), 16 (2007)

Tretiakov K.V. and Scandolo S., J. Chem. Phys. 120(8), 3765 (2004)

Venerus, D.C., Kabadi M.S., Lee S., and Perez-Luna V., J. Appl. Phys. 100(9), 094310 (2006)

Verlet L., Phys. Rev. 159, 98 (1967)

Verlet L., Phys. Rev. 165, 201 (1968)

Vladkov M. and Barrat J.-L., Nano Lett. 6, 1224 (2006)

Vogelsang R., Hoheisel C., and Ciccotti G. J. Chem. Phys. 86(11), 6371 (1987)

Volz S.G. and Chen G., Appl. Phys. Lett. 75(14), 2056 (1999)

Wang X., Xu X.F., and Choi S.U.S., J. Thermophysics Heat Transfer 13(4), 474 (1999)

WangY., Fisher T.S., Davidson J.L., Jiang L., Proceedings of 8th AIAA/ASME Joint Thermophysics and Heat Transfer Conference, USA, AIAA, 2002-3345 (2002)

Wang, Z.L., Tang D.W., Liu S., Zheng X.H., and Araki N., International Journal of
Thermophysics, 28(4), 1255 (2007)

Wen-Qiang L.U. and Qing-Mei F.A.N., Engr. Anal. Boundary Elements 32(4), 73 (2008)

Wolf D., Phys. Rev. Lett 68, 3315 (1992)

Wolf D., Keblinski P., Phillpot S.R., and Eggebrecht J., J. Chem. Phys 110, 8254 (1999).

Woodcock L.V., Advances in Molten Salt Chemistry, edited by J. Braunstein, G.
Mamantov, and G. P. Smith (Plenum, New York), 3, 1 (1975)

Wu X. and Kumar R., Keynote Lecture and Invited Paper, Proc. Nanomaterials:
Synthesis, Characterization and Application, Calcutta, India, 182, Nov. 2004
(2004)

Xie, H.Q., J.C. Wang, T.G. Xi, Y. Liu, F. Ai, and Q.R. Wu, J. Appl. Phys. 91(7), 4568
(2002)

Xie H., Lee H., Youn W., and Choi M., J. Appl. Phys. 94(8), 4967 (2003)

Xie H., Fujii M. and Zhang X., Int. J. Heat & Mass Transfer 48(14), 2926 (2005)

Xuan Y. and Li Q., Int. J. Heat Fluid Flow 21, 158 (2000)

Xue L, Keblinski P., Philpot S.R., Choi S.U.S. and Eastman J.A., J. Chem. Phys. 118(1),
337 (2003)

Yang, Y., Grulke E.A., Zhang Z.G., and Wu G.F., J. Appl. Phys. 99(11), 114307 (2006)

Young H.L., Biswas R., Soukoulis C.M., Wang C.Z., Chan C.T., and Ho K.M., Phys.
Rev. B 43, 6573 (1991)

Yu C. J., Richter A.G., Datta A., Durbin M.K. and Dutta P., Phys. B 283,27 (2000)

Yu A. and Amar J.G., Phys. Rev. Lett. 89, 286103 (2002)

Yu W. and Choi S.U.S., J. Nanoparticle Res. 5, 167 (2003)

Zhang, X., Gu H., and Fujii M., Expt. Thermal Fluid Sci. 31(6), 593 (2007)

Zhu H., Zhang C., Liu S., Tang Y. and Yin Y., Appl. Phys. Lett. 89(2), 023123 (2006)